

**An Investigation into Vibratory Grinding Of Difficult to
Machine Aerospace Materials**

Elsiddig Eldaw Ibrahim

*A thesis Submitted in Partial Fulfilment of the Requirement of Liverpool
John Moores University Faculty of Engineering and Technology for the
Degree of Doctor of Philosophy*

November 2017

ABSTRACT

There is an increased demand for high surface finishes and tight tolerances, especially in high value manufacturing processes. However, progress in materials science has led to the development of new materials especially in the aerospace industry, where high heat resistance materials are preferred such as Ti-6Al-4V. These new materials have different mechanical properties from conventional ones. This makes their machinability very unusual when compared to that of conventional materials. Consequently machining these materials poses a significant challenge to industry. Since this alloy has got low density, high strength to weight ratio and also high temperature strength, it is used for aerospace, civil and military aircraft turbine engine compressor blades manufacturing.

This research programme sets up an investigation into vibration assisted grinding in a range of frequencies and amplitudes combined with various process parameters in the attempt to grind advanced aerospace materials. Such a novel approach called "Resonance machining" also depends on the Taguchi experimental design method, with the aim of improving the grinding quality and efficiency. The novelty of this new approach is that the vibration assisted resonance was implemented in the axial direction of the grinding feed rate, using an aluminium oxide grinding wheel, with the application of coolant fluid to enhance grinding difficult to machine aerospace materials, this approach is considered to be an alternative to the usage of super abrasive wheels such as CBN and diamond wheels currently been used, with negative effect where damage to the workpiece surface and subsurface crack have been reported. However, the advantages of vibration assisted grinding as a new technique are the reduction of wheel wear and cutting forces. Through over this study it has been proven that vibration assisted grinding allows the wheel to cut in two directions and that will increase the material removal rate reduce the wheel wear, cutting forces and also the power consumption.

The purpose of this research is to achieve an optimum performance of vibration assisted grinding processes using difficult-to-machine advanced aerospace materials. The first step in this investigation is to identify the material under investigation.

Therefore, the above mentioned aerospace materials have been tested. Initial hardness testing was carried out on two types of materials involved this study, namely Nickel alloy (Inconel 718) and Ti-6Al-4V. This was followed by a chemical element content analysis undertaken on the scanning electron microscope with X-Ray setup.

However, this work investigates the grinding performance of titanium and nickel alloys using aluminium oxide (Al_2O_3) grinding wheel. Hence, experiments were carried out in wet conditions with/without vibration grinding and the results are provided to confirm the effectiveness of this approach.

Through this study the surface roughness, cutting forces, actual depth of cut, material removal rate and grinding power consumption were obtained. The results of this study showed that the depth of cut and the wheel speed have significant effects on the surface roughness, while the feed rate has lower influence on it. Also it has been observed that vibration assisted grinding reduces cutting forces by about 45%, increases the material removal rate and improves the surface roughness in wet condition. However, vibration assisted grinding also proved to decrease the wheel wear and increases the G-ratio.

In addition to that, as contribution to science, it has been demonstrated mathematically how vibration assisted reduces cutting forces when applied to grinding. The explanation for that is when the superimposed oscillation applied to the workpiece, at a certain point in the process a zero time situation will occur where the cutting tool has no full cutting force, because of the resonance effect which acts in intermittent or lapping side effect. At this moment the force dropped to its lowest values, as the workpiece displacement generated in this case allows the cutting tool to cut into two directions, as that help to reduce the cutting forces and extends the cutting tool life.

However, from this study there are many important findings were reached, such as that and for the first time an aluminium oxide grinding wheel was used with the enhance of vibration assisted to grind difficult to machine aerospace materials, where several benefits of vibration assisted grinding were proved including the reduction of wheel wear and extending wheel life. The obtained results support and validate that employing supper abrasive grinding wheels such as CBN and diamond wheel has negative effect on workpiece surface quality. whilst, the improved surface roughness that obtained, occurred as the result of the application of low vibration frequency which was introduced on the perpendicular direction of the feed rate into the workpiece to secure suitable displacement to allows for cooling fluid to penetrate between the grinding wheel and the workpiece and at the same time to secure suitable displacement that match a low excitation that required to reduce the power consumption.

Table of Contents

ABSTRACT.....	1
Table of Contents.....	3
ACKNOWLEDGEMENTS.....	7
NOMENCLATURE.....	8
LIST OF FIGURES.....	11
LIST OF TABLES.....	14
1. INTRODUCTION.....	16
1.1 Introduction.....	16
1.2 Background.....	17
1.3 Problem Outline.....	19
1.4 Project Aim and Objectives.....	20
1.4.1 Aim.....	20
1.4.2 Objectives.....	20
1.5 Methodology (The Scope of the Investigation).....	21
1.6 Novel Grinding Method.....	22
1.7 Thesis Layout.....	24
2. LITERATURE REVIEW ON VIBRATION ASSISTED MACHINING.....	28
2.1 Introduction.....	28
2.2 Overview of Vibration Assisted Machining.....	28
2.3 Vibration assisted machining (VAM) features.....	31
2.3.1 Extended tool life.....	31
2.3.2 Tool life extension for brittle materials and non-diamond tools.....	32
2.3.3 Improved surface finish and form accuracy.....	32
2.3.4 Ductile regime machining of brittle materials.....	32
2.3.5 Advantages of Grinding With Vibration Assisted:.....	32
2.4 Application of Vibration Assisted to Grinding.....	33
2.5 Summary.....	33
3. FUNDAMENTALS OF GRINDING WITH VIBRATION ASSISTANCE.....	37

3.1 Introduction	37
3.2 Types of Grinding	37
3.4 Grinding Wheel Specifications	39
3.5 The coolant delivery system	41
3.6 Cutting Forces and Power	41
3.7 Chip Formation in Grinding.....	44
3.8 Equivalent Chip Thickness.....	46
3.9 Grinding of Aerospace Materials	47
3.9.1 Titanium.....	47
3.9.2 Nickel Alloy	49
3.10 Summary.....	49
4. KINEMATICS OF VIBRATION ASSISTED-GRINDING.....	52
4.1 Introduction	52
4.2 Dynamic Behaviour of Vibro-Impact System	52
4.3 Principle of Vibration-Assisted Machining Process.....	54
4.4 Designs of Vibration Assisted Machining.....	57
4.5 New Approach (perpendicular direction)	57
4.6 Chip Formation in Vibration Assisted Mode	59
4.7 How did Vibration Assisted Reduce Cutting Forces?	60
4.8 Summary.....	66
5. EQUIPMENT & PRELIMINARY EXPERIMENT	69
5.1 Intoduction.....	69
5.2 Grinding Machine (ABWOOD 5025).....	69
5.3 Grinding wheel.....	70
5.4 Workpiece materials.....	70
5.5 Data Acquisition System (DAQ).....	70
5.6 Piezoelectric Actuator	71
5.7 Power Amplifier	72
5.8 Dynamometer	72
5.9 Accelerometer:	72
5.10 Preliminary Experiment	73

5.10.1 Material Characterization	73
5.11 Experiment Setup Configuration	75
5.12 LABVIEW (VI _s) Software	76
5.13 Dynamometer Calibration	76
5.14 Amplitude-Frequency Response of the oscillating stage.....	79
5.15 Optimization of Vibration Assisted Grinding	81
5.16 Taguchi Method	81
5.17 Preliminary Experiment	82
5.17.1 Experimental Procedure	82
5.17.2 Aim and Objectives	82
5.17.3 Work-piece Materials Preparation	82
5.18 Experimental results	86
5.18.1 Effect of Wheel Speed on Surface Roughness.....	87
5.18.2 Effect of Table Speed on Actual Depth of Cut	87
5.18.3 Effect of Wheel Speed on Cutting Forces	88
5.18.4 Effect of Table Speed on Cutting Forces.....	89
5.19 Effect of Depth of Cut on Grinding Forces	90
5.20 Effect of Depth of Cut on Surface Roughness.....	92
5.21 Actual Depth of Cut (a_e)	94
5.22 Summary	96
6. GRINDING OF Ti-6Al-4V	98
6.1 Introduction	98
6.2 Experimental Methodology	99
6.2.1 Materials.....	99
6.3 Actual Depth of Cut and Material Removal Rate.....	100
6.4. Grinding Force for Ti-6Al-4V	101
6.5 Surface Roughness.....	104
6.6 Grinding Energy.....	106
6.7 Power Consumption	108
6.8 Specific Grinding Energy	108
6.9 Boundaries identification.....	110

6.9.1 Workpiece surface quality	111
6.10 Summary.....	111
7. GRINDING OF NICKEL Alloy (INCONEL 718)	114
7.1 Introduction	114
7.2 Experiment Objectives:.....	114
7.3 The Effect of Applied Depth of Cut on Forces.....	116
7.4 Material Removal Rate (MRR) Results.....	118
7.5 Process Power and Specific Grinding Energy.....	119
7.6 Conclusion.....	121
8. PROCESS PERFORMANCE IN GRINDING ADVANCE AEROSPACE MATERIALS	123
8.1. Introduction	123
8.2 The choice of Aluminium Oxide Wheel.....	123
8.3 Process performance in Titanium and Nickel alloys	124
8.4. Power and Specific Grinding Energy	127
8.5 Material Removal Rate	130
8.6. Surface roughness (Ra)	132
8.7 Wheel Wear	133
8.8 Wear Observation and Testing	134
8.9 Material Removed	137
8.10 G-Ratio	138
8.11 Concluding Remarks.....	140
9. DISCUSSION, CONCLUSION & RECOMMENDATIONS	142
9.1 Discussion	142
9.1.1 Single grit Cutting dynamics-chip length.....	144
9.2 Conclusions	147
9.3 Recommendation for future work.....	150
REFERENCES	152
APPENDICES	165

ACKNOWLEDGEMENTS

In the name of Allah, Most Gracious, Most Merciful.

I would like to express sincere thanks to my Director of Study Dr. Andre Batako for his wise supervision, inspiration, motivation and support during the entire period of the project. So many thanks for him for his efforts and patience. I hope peace and blessing will be with him for the rest of his life.

I would like also to express sincere gratitude to Professor, Xun Chen for his support, help and advice during the entire period of this project, his unlimited help is highly acknowledged and appreciated; I am very thankful to him for his massive input in the entire project.

Compliments are also conveyed to Mr Peter Moran senior technical staff member, who devoted his time, to share his experience for the benefit of the project; without his efforts and support this work would not have been done.

I would like also to express my sincere gratitude to my patient lovely wife Samia Abdelaziz, for her support and help during the whole period of my study in Liverpool. I'm very greatfull to her and to my cute children/ Sarah, Suzan, Ahmed and Ibrahim for sacrificing their time to enable me accomplish this journey.

Compliments are also conveyed to my family members especially my parents: My father, my mother, my brothers and sisters without their love and support I wouldn't have been able to make this achievement.

Finally, I would like to extend my greetings to the dignified people of my home country Sudan for their sacrifices and long struggle for the sake of dignity, equality and freedom as they suffered to establish a democratic governing system for a better future for many generations to come.

I would like to extend my gratitude to all members of the Faculty of Engineering and Technology, the staff, the technician, the secretaries and my fellow students, all of whom are highly acknowledged.

Finally, I will not forget to send sincere gratitude to my support manager Mrs Sarah Singleton for her help and support during my entire period in Liverpool.

NOMENCLATURE

SYMBOL	MEANING	UNITS
a	Applied depth of cut	μm
a_e	Real depth of cut	μm
a_p	Grinding depth of cut for single grit	μm
A_0	Amplitude	μm
A_m	Average chip cross section area	m^2
b_w	Work piece contact width	m
DOC	Depth of cut	μm
d_s	Wheel diameter For single grit	μm
e_c	Specific energy	J/mm^3
F_n	Normal grinding force	N
F_t	Tangential grinding force	N
F_{tot}	Cutting force	N
F'_n	Specific normal force	N/mm
F'_t	Specific tangential force	N/mm
F_v	Vertical component	N
F_{cutting}	Cutting force	N
F_H	Horizontal component	N
$F_{\text{ploughing}}$	Ploughing force	N
F_{sliding}	Sliding force	N
h_{eq}	Equivalent Chip thickness	μm
K_0	Constant	-
L_c	Contact Length	mm
L_g	Geometric contact length	mm
P	Grinding power	W
Q	Material removal rate	m^3/s

Q'	Specific material removal rate	m ³ /s
Ra	Surface roughness	m
Vs	Wheel speed	m/s
V _w	Work speed	mm/s
Vc	Average chip volume	mm ³
x(t)	Velocity	m/s
X(t)	Acceleration	m ² /s
Greek Symbols	Meaning	Unit
τ	Shear stress (Pa)	(Pa)
θ	Temperature (°C)	(°C)
κ	Thermal conductivity (W/m.K)	(W/m.K)
ρ	Density (N/m ³)	ρ Density (N/m ³)
λ	Cutting edge density	N/μm
c	Specific heat (J/Kg.K)	(J/Kg.K)
W	Work equivalent of heat (J)	(J)

LIST OF ABBREVIATIONS

CBN	Cubic Boron Nitride
DAQ	Data Acquisition
FEA	Finite Element Analysis
GERI	General Engineering Research Institute
HEDG	High Efficiency Deep Grinding
HRB	Hardness Rockwell C (Cone Tip)
MQL	Minimum Quantity Lubricant
NI	National instrument
PZT	Piezoelectric lead Zirconate Titanate
RPM	Revolutions Per Minute
UAG	Ultrasonic Assisted Grinding
VI	Virtual Instruments

LIST OF FIGURES

Figure 2.1: Design of Micro-Vibration Device (Z.W.Zhong &H.B. Yang, 2004)	34
Figure 3.1: Surface grinding (Book of Modern Grinding Technology/ Second Edition, Rawe.W.B)38	
Figure 3.2: Internal grinding http://www.HJMTC 26/02/201	38
Figure 3.3: Grinding Wheel Marking System (Modern Grinding Technology, Second Edition)	41
Figure 3.4: Grinding force, (Vaios, 2011)	42
Figure 3.5: Chip formation (Barczak L. (2010). Application of Minimum Quantity Lubrication (MQL) in Plane Surface Grinding, PhD Thesis, (Ref, 19).....	44
Figure 3.6: stage of chip formation, where: rubbing, ploughing & cutting (Ref, [31]. 1996).....	46
Figure 3.7: The different materials used in a Rolls- Royce jet engine. In blue titanium alloy and in red nickel based super alloy. [31], (D. Rugg, 2003), Hamburg, Germany	48
Figure 4.1: Oscillator with linear single Impact & Its motion with time (Babitsky, 1998).	52
Figure 4.2: Dynamic of Vibratory System (Babitsky, 1998).....	54
Figure 4.3: Vibration Assisted Machining (Shamoto, 2004).....	55
Figure 4.4: Vibration Assisted Machining (Dow, 2007).....	55
Figure 4.5: 2D Vibration Assisted Mechanism (Shamoto & Moriwaki, 2004).....	56
Figure 4.6: Picture of the Oscillating Jig, a- Model, b- actual oscillating jig	58
Figure 4.7: Schematic Drawing of Grit Motion in both cases/ when grinding with vibration assisted and without vibration assisted (conventional), Ewad, 2013).....	59
Figure 4.8: Schematic Drawing of Chip formation for single grain cutting;	60
Figure 4.9: Chip formation	64
Figure 4.10: Chip formation with vibration assisted grinding (SEM Images)/ 200 µm scale at 100x-resolution	64
Figure 4.11: Chip formation without vibration assisted grinding (SEM Images)/ 200 µm scale, at 100x- resolution	65
Figure 4.12: Chip formation without vibration assisted grinding (Measurements)	65
Figure 5.1: Equipment – ABWOOD 5025 machine.....	69
Figure 5.2: Grinding Wheel	70
Figure 5.3: DAQ system; a): input- NI 9215, NI 9233 and output – NI9263; b) configured in chassis	70
Figure 5.4: Piezoelectric Actuator	71
Figure 5.5: 3-axis Kistler 9257A dynamometer & Kistler charge amplifier type 5073	72
Figure 5.6: Function Generators	73
Figure 5.7: Oscilloscope	73
Figure 5.8: Workpiece Jig (Self Containing Vibration System)	73
Figure 5.9: Closed loop Control System	75
Figure 5.10: Actual Configuration for the Experimental Work (Ewad, 2013)	75
Figure 5.11: LabVIEW Data Acquisition Software –Block Diagram (Ewad, 2013)	76
Figure 5.12: Dynamometer calibration process.....	77

Figure 5.13: Normal Component of Force Calibration Results.	77
Figure 5.14: Tangential Component of Force Calibration Results.	78
Figure 5.15: Axial Component of Force Calibration Results.....	78
Figure 5.25: Tangential force Ft versus depth of cut/ Vibration/ No vibration	91
Figure 6.1: Actual Depth of Cut Versus Applied Depth of Cut	100
Figure 6.2: Material Removal Rate Versus Depth of Cut	101
Figure 6.3: Normal force Vs depth of Cut	102
Figure 6.4: Tangential Force Vs Depth of Cut	102
Figure 6.5: Normal and Tangential forces for Ti-6Al-4V as a function of depth of cut when grinding with vibration at 20m/s wheel speed & 250mm/s feed rate.	103
Figure 6.6: Normal & Tangential Forces Versus Depth of Cut at 17m/s Vs	103
Figure 6.7: Surface roughness Ra for (Ti-6Al-4V) when grinding at 17m/s wheel speed.....	105
Figure 6.8: Surface roughness Ra for (Ti-6Al-4V) when grinding at 20m/s wheel speed.....	105
Figure 6.9: Power Consumption VS Applied Depth of Cut.....	107
Figure 6.10: Specific Grinding Energy (J/mm ³) VS Material removal Rate	109
Figure 6.11: The effect of wheel speed on specific normal forces.	109
Figure 6.12: The effect of Wheel Speed on Specific tangential Forces.....	110
Figure 7.1: Normal force (Inconel 718) as a function of depth of cut when grinding with / without vibration at 17m/s wheel speed, 250mm/s table speed.	116
Figure 7.2: Tangential force (Inconel 718) as a function of depth of cut when grinding with/without vibration at 17m/s wheel speed, 250mm/s table speed.....	117
Figure 7.3: Normal & Tangential forces (Inconel 718) as a function of depth of cut when grinding with/without vibration at 17m/s wheel speed, 250mm/s table speed.....	117
Figure 7.4: The Effect of Applied Depth of Cut on Actual Depth of Cut.....	118
Figure 7.5: The Effect of Applied Depth of Cut on Material Removal Rate	118
Figure 7.6: The Effect of Applied Depth of Cut on Surface roughness.....	119
Figure 7.7: Grinding Power Consumption Vs Applied Depth of Cut	120
Figure 7.8: Specific Grinding Energy VS Material Removal Rate.....	120
Figure 8.1: Image of the wheel surface after series of test grinding showing no clogging.....	124
Figure 8.2: Normal Force Versus Applied Depth of Cut for Titanium and Nickel alloys	125
Figure 8.3: Normal Force for titanium and Nickel alloys (15 m)	125
Figure 8.4: Normal Force for Titanium and Nickel alloys (30µm)	126
Figure 8.5: Tangential Force Versus Applied Depth of Cut for Titanium and Nickel alloys.....	126
Figure 8.6: Tangential Force Titanium and Nickel alloys (15 µm)	127
Figure 8.7: Tangential Force for Titanium and Nickel Alloys.....	127
Figure 8.8: Power Consumption Versus Applied Depth of Cut for Two Materials (15 µm)	128
Figure 8.9: Power Consumption Versus Applied Depth of Cut for Two Materials (30 µm)	128
Figure 8.10: Specific Grinding Energy for Titanium and Nickel.....	129
Figure 8.11: Specific Grinding Energy Versus Material Removal Rate	129
Figure 8.12: Specific Grinding Energy Versus Material. Removal Rate.....	130
Figure 8.13: Material Removal Rate Titanium and Nickel alloys (15µm).....	131

Figure 8.14: Material Removal Rate Titanium and Nickel Alloys (30 μ m)	131
Figure 8.15: Material Removal Rate for Nickel Alloy & Ti-6Al-4V, Without / With Vibration.....	132

LIST OF TABLES

Table 5.1: Materials Rockwell hardness Tests Results	74
Table 7.1: Grinding Parameters (Set-up Parameters).....	114
Table 7.2: Experimental Results/ With the Application of Vibration Assisted.....	115
Table 7.3: Experimental Results/ Without the Application of Vibration Assisted	115
Table 8-1: Surface roughness Measurement	Error! Bookmark not defined.

CHAPTER-1

INTRODUCTION

1. INTRODUCTION

1.1 Introduction

Current manufacturing processes make ever-increasing demands for higher machining removal rate as well as better quality of the final product, this is particularly true in cars and aircraft production but also for cutting tools. A number of researchers (Shamoto et al, 1991) around the world are trying to develop new techniques that accelerate any machining process without sacrificing the quality of the work-pieces. One of these new techniques is to introduce vibration to grinding (Shamoto et al, 1991), where vibration could be used in various technological processes to improve the performance of the machines by intelligently exploiting the synergy of the oscillations. However, the use of vibration on the workpiece, on the tool or on the tool-bed during a machining process and especially in grinding can bring positive results in terms of wheel loading, temperature, grinding forces reduction and better surface quality.

Classic examples of utilising vibration are vibration conveyers, ultrasonic assisted turning of aerospace materials, as well as ultrasonic grinding and vibro-impact drilling in offshore technology. Vibration provides several benefits for various technologies, such as manufacturing, medical, communications, transport industries, etc. Vibration assisted machining techniques have recently become an attraction for many engineering applications. In machining processes, vibration can lead to improvements when applied in a controlled manner. Vibration assisted machining is a technique in which a certain frequency of vibration is applied to the cutting tool or the work-piece (besides the original relative motion between these two) to achieve better cutting performance (Shamoto et al, 1991). There are a number of different experimental setups to simplify the process, but the tendency is to give a wide range of machining processes to machine hard and brittle materials (Matsumura, 2005). However, grinding technology does not generally exploit the positive aspects of superimposed vibration. The avoidance of vibration (chatter) is a main concern due to its effect on accuracy. However, chatter is a persisting problem, regardless of the measures taken

to mitigate against it and a list of techniques is provided in (Marinescu, 2005), to reduce vibration. A self-excited vibration that leads to an undulation of the cutting force, with subsequent uneven wear or fracture of the tool, causes the so called regenerative chatter, which is an unfavourable dynamic phenomenon encountered in various machining processes. In grinding, which is often the finishing machining operation, the occurrence of chatter is particularly critical because it adversely affects the two main objectives of grinding: geometrical form accuracy and surface finish of the grinding work-pieces. In order to avoid additional costs due to rework or even disposal of chatter-damaged work-pieces, early and reliable detection of chatter is necessary. A possible solution to this type of chatter is to apply a periodic disengagement of the tool from the workpiece; and periodic variation of the work speed, which has been reported to increase the productivity by up to 300%, (Gallemaers, 1986).

Regardless of its cause, chatter in grinding usually manifests itself as large amplitude, nearly harmonic vibrations of the grinding wheel and the workpiece. These vibrations distort the round form of the wheel and/or the workpiece. (Inasaki, Karuschewski, Lee, (2001).

1.2 Background

The basic element of vibration assisted machining is the oscillation that can be generated using a series of methods; however, piezo-actuators are most commonly used. Different designs of actuators have been developed for various applications, such as vibration assisted turning, milling, drilling, grinding, and, recently, the combination of electric discharge micro-milling with vibration assisted machining has been reported (Brehl, 2008).

The fundamental feature of vibration assisted machining is that the tool face is repeatedly separated from the workpiece. This technique was first employed in the precision drilling of wood and low carbon steel (Cerniway, 2005).

There are a number of processes with vibration devices for cutting purposes using diamond tools. However, the existing vibration machining process does not effectively cut in hard and brittle materials because of excessive wear of the diamond tool due to high chemical activity with iron (Bonifacio et al. 1994).

Chern et al, (2006), applied vibration in ultra-precision micro drilling at higher frequencies and observed a direct effect on tool life with the amplitude having the highest influence on the interaction between the cutting tool and work-piece.

In vibration assisted machining, the intermittent gap during cutting and was identified as an important mechanism in vibrational cutting. Increasing the vibration amplitude means an enlargement of the gap that allows cutting fluid to extract the heat from the cutting process. This enhances the tool's life and reduces the production cost.

Tsiakoumis, (2011), showed that the application of vibration to grinding improved the surface finish quality due to the lapping effect; a reduction of cutting force and a reduction of grinding power. Here the interrupted contact allowed for better coolant delivery over the entire contact zone with trapped coolant between successive oscillations which is impossible in continuous grinding, and involved a self-sharpening process because grains operate cutting in two directions securing longer wheel life.

In vibration assisted machining, a number of advantages were reported in processing hard-to-machine material. Considerable extended tool life was observed in diamond machining, (Shamoto and Moriwaki, 1992 and 1999). Weber (1984) showed that 2D vibration provided longer tool life for the same machining configuration.

Using superimposed vibration it is possible to machine brittle materials as if they were ductile, (Xiao, Sato and Karube, 2003; Zhou, Eow, Ngoi and Lim, 2003) where in precision machining small depth in order of $1\mu\text{m}$ was used. Parts machined with vibration assistance were burr free.

Surface roughness in vibratory machining is better than the quality achieved by conventional machining and can reach the nano-meter range depending on process configuration. In large part machining, the superimposed vibration secures a degree of precision with limited tool wear and provides surface roughness about $10\mu\text{m}$ RMS with 1mm depth of cut, (Shamoto, Suzuki, Tsuchikya and Hori, 2005). In precision diamond turning, Robenach, (2003) achieved surface finishes in the range of 10-30 nm RMS, where Brehl and Dow, (2006) reported some economical machining distances of hundreds to several thousand metres in hardened steels.

However, it has been reported by Xian, Sato, Karube, (2003) that machining brittle and ductile materials and super alloy is possible if depth of cut is kept to its smaller value and the frequency carefully controlled. Moreover, in practice ductile-regime machining frequency remains uneconomical since the critical depth of cut is very small.

In the past, several attempts have been made at machining these new materials; however the results are not satisfactory. Therefore, this is a key challenge for this project. If the outcomes of this investigation were positive, then this would lead to a

major breakthrough in machining these new advanced aerospace materials. The approach planned to be used in this study has never been attempted before; however, a breakthrough is anticipated with some advantages such as a better finished surface, chip-breaking effects, reduced wheel wear, a lapping effect, improved cutting efficiency, reduced load per grit and hence low cutting forces and low power consumption.

1.3 Problem Outline

Recent advances in material research have led to the development of a range of new materials that have different machining properties from classical well-studied materials. Thus, these new materials pose several challenges in their machining. The materials under investigation in this project involve new advanced aerospace materials, which are hard to machine.

This includes two groups of materials: namely brittle and gummy types.

Brittle group

- The CMC (Ceramic Matrix Composite) materials based on (SiC-SiC) which are abrasive and brittle, thus very hard-to-machine
- The titanium aluminide (Ti6Al4V), with high percentage of alumina oxide inclusion, hence this material is brittle and hard-to-machine

Gummy group

- The High - grade titanium aluminide – a gummy material with peculiar behaviour in machining
- The nickel alloy (Inconel 718) – a gummy material that is hard to machine, however it has been well explored in conventional machining

The above mentioned materials are heavily used to manufacture turbine blades for jet engines. Conventional cutting processes have been used to machine these materials with relatively low success. However, with the increased demand on high productivity and high precision, conventional machining seems to be lagging behind current machining demands for new materials. Moreover, the aerospace industry heavily depends on these materials and progress in the aforementioned industry indicates that the materials in the brittle group will be more and more used in the future for turbine blade manufacturing.

Therefore, there is an imperative need for new radical solutions to support industrial demand. This project sets out to explore one potential avenue that could potentially provide a solution to this problem. Any successful outcome from this project would provide the manufacturing industry and the aerospace industry with the much-needed

new method of machining these types of new materials. The novelty, here lies in an intelligent use of vibration to machine these materials in resonance grinding. However, the newly introduced technique of vibration assisted machining with the implementation of conventional grinding wheel namely aluminium oxide grinding wheel seems to be the state of arts so far.

1.4 Project Aim and Objectives

1.4.1 Aim

This research project will focus on the optimization of the performance of vibration assisted grinding processes using difficult-to-machine advanced aerospace materials, such as Ceramic Matrix Composites and titanium alloys. A comparison with other hard, brittle materials, in this case titanium aluminide (Ti6Al-4V), will be performed. This study also aimed to find out what are the benefits of the superimposed vibration assisted in the perpendicular direction of the grinding wheel, however, this superimposed vibration could be controlled by using a closed loop control system which, also aimed to keep the whole grinding process parameters consistent with the imposed vibration.

The purpose in general is to provide understanding of the process output measures (grinding forces, temperatures, surface finish and integrity, consumable life/wear patterns, material removal rates, etc.) in relation to the process inputs varied at different levels (grinding wheel specification, coolant parameters, cut strategy, grinding and dressing parameters, vibration frequency and amplitude, etc.). However, since the feature of vibration assisted machining is that the tool face is repeatedly separated from the work-piece, this will create a gap or lapping effect during cutting process through which the coolant could be delivered. This will lead to a reduction in cutting forces, power consumption and the production cost as well.

1.4.2 Objectives

To achieve an optimum performance of vibration assisted grinding processes using difficult-to-machine advanced aerospace materials, it is very necessary to carry out state –of-the-art grinding process experiments, which could avoid all the previous grinding boundaries. However, this work will be done throughout an investigation that will progress through a series of tasks and objectives designed to facilitate an effective delivery of the project. The key objectives of this study are as follows:

-
- ❖ Comprehensive literature review on vibration assisted machining and its application in surface grinding.
 - ❖ A combination of low frequency and large amplitude to secure suitable displacement for the workpiece which could match a low excitation that required to reduce the power consumption and the specific grinding energy.
 - ❖ Providing a novel oscillating system which could vibrates the workpiece in the perpendicular direction to the feed rate, to achieve specific displacement.
 - ❖ Proving the feasibility of vibration- assisted grinding through experiments as an effective beneficial technique.
 - ❖ Identifying the relationship between input parameters and grinding results using factorial experimental methods (Taguchi DOE).
 - ❖ Process optimization within LABVIEW & MATLAB, (MINITAB), to improve the grinding process efficiency by reducing the numbers of trials and to validate that experimentally using SEM and Taylor Hobson machine.
 - ❖ Carry out preliminary experiments to find out the boundary conditions for grinding these aerospace materials on surface grinding machine using aluminium oxide wheel with the enhance of coolant and vibration assisted technique.
 - ❖ Carry out full experiments conventionally using the same parameters and conditions for these aerospace materials and with the implementation of vibration assisted to investigate a comparative procedure in both cases for the obtained cutting forces, amount of materials removal, surface roughness, power consumption, specific energy, wheel wear and grinding efficiency.
 - ❖ Write up a guideline for vibration assisted grinding for the aforementioned new materials; especially high-grade titanium (Ti-6Al-4V), and (Inconel 718) should be observed.
 - ❖ Draw conclusions and recommendations.
 - ❖ Writ up Thesis and submission.

1.5 Methodology (The Scope of the Investigation)

To achieve the aim of this project a literature review will first be undertaken to identify existing practice in machining the materials involved this study. A full factorial design of the experiments will be elaborated using various methods including the well-known Taguchi factorial method. An experimental work programme will be performed using a range of materials in both the gummy and brittle groups. The main focus will be on Ceramic Matrix Composite materials (SiC-SiC), Titanium aluminide Ti6Al4V and nickel alloys. Faculty of Engineering and Technology

laboratory (GERI) at Liverpool John Moores University has a range of grinding machine tools including the newly designed high-speed grinding machine tool, which will be used in this investigation. Resonance grinding will be achieved using piezo-actuators. Additional vibratory process will be undertaken using the high-speed machine tool. Three types of wheels will be employed, including variation of conventional alumina wheels, metal bonded and diamond wheels. For process characterisation, the cutting forces will be measured using a 3-axis dynamometer, and temperatures will be measured using optic fibre sensors. The signals from the sensors will be recorded using existing data acquisition systems driven by LabView software. The surface texture will be measured using the Bruker contour GTK and the Taylor Hobson systems available in GERI. Metallographic characterisation and sub-surface damage will be investigated using scanning electron microscopy.

1.6 Novel Grinding Method

Current manufacturing processes required high prescience, especially in the automotive and aerospace industry. Many researchers around the globe have tried to find suitable and less costly methods to grind aerospace materials without sacrificing the quality of the work-pieces. However, Asppinwall in 2001 from the University of Birmingham research centre found that the use of electric discharge machine (EDM) can be a promising solution to this problem. In this study, an advanced approach called vibration assisted resonance was implemented using an aluminium oxide grinding wheel (Al_2O_3 (OVU33 A602HH 10VB)) with the application of coolant fluid to enhance the grinding process of hard aerospace materials. However, in this experiments vibration assisted meant to be introduced in the perpendicular direction of the feed rate to vibrate the workpiece to an specific displacement that could allow the coolant to enter the contact zone between the grinding wheel and the workpiece, to extract the heat flux generated by the cutting forces of the grinding process.

However, this attempt is meant to find an alternative to the usage of super abrasive grinding wheels, such as CBN and diamond wheels which have currently been used to grind these advanced aerospace materials such as titanium aluminide, alfa-beta-titanium alloys such as Ti 6Al-4V and nickel alloy (Inconel 718). In addition to that, since these materials are gummy, brittle and difficult to machine, usage of super abrasive cutting tools through over the years, caused massive damage and cracks on the work-piece surfaces.

In this approach four samples of each of these hard materials will be ground with vibration assisted and without vibration assisted to investigate the following:

- Cutting forces & specific grinding energy

-
- How vibration assisted grinding reduces cutting forces & wheel wear
 - How vibration improves the material removal rate and surface roughness
 - Microscopic results

Procedure: Two conditions can be set up for experiment such as:

- Cracking checking plus explanation of the material damage and how it occurs
- Aching can be done to check material dissolvent (Acid engine).

Grinding Condition A:

A comparison procedure between materials' grinding results in terms of grinding with/without vibration should be done to give a general explanation about what are the differences in both cases from the mechanical point of view and to observe the following measurements:

Forces measurement, this will be checked by comparing with literature review studies and recalibration.

Material removal rate

Surface roughness measurement, this need to be checked by stylus method using the (TAYLOR HOBSON) machine.

Grinding Condition B:

Finishing

Smearing checking

Test 10 pictures of the material under the micro-scope to test:

- 1 Chip thickness
2. Chip length

Experiments were conducted using an existing surface grinding machine '**ABWOOD 5025**'. The implementation of vibration assisted in the axial direction of the machine spindle, led to wheel load reduction, consequently the cutting forces were reduced and the wheel wear also reduced as well, this led to wheel life extension by about 30%. Whilst, the chip length and thickness in both cases grinding conventionally and grinding with vibration assisted were measured using SEM. The results show that chip length in case of vibration assisted grinding was longer by about 1.5%, while the chip thickness is smaller. However, these results are also in accordance with the mathematical validation, which proved that the cutting forces were reduced by the implementation of vibration assisted grinding. In addition to that, the results also proved that the choice for low frequency and high displacement is a suitable choice which led to avoid the high frequency choice that proved to be through over the years as risky to damage the surface roughness of workpiece, increase the

tool wear and the harm the machine and the operator as well. While the choice for high amplitude proved that the application of low amplitude that been used in the past was not efficient enough to allow for sufficient coolant fluid to be trapped between the cutting tool and the workpiece in the grinding contact zone.

1.7 Thesis Layout

This research project forms this PhD thesis which consists of 9 chapters, each of them presents a specific topic, starting with chapter 2 which gives a general overview about grinding with vibration assisted, especially the previous work that been done in the past by other researchers including state-of-the-art applications of grinding with vibration assisted.

Chapter 3 gives a comprehensive background on the conventional grinding process where the most concepts related to grinding have been studied and analysed to gain fundamental knowledge and experience practises.

Chapter 4 describes how vibro-impact systems and vibratory devices that produce and also maintain vibration, work. Furthermore, different models of previous and current design of grinding with vibration assisted has been investigated using empirical and mathematical procedure. However, state-of-the-art model design has been extensively studied, in order to improve and develop a new model that combines the previous and the latest advantages

Chapter 5 initially describes all the equipment that was employed during the experiments such as a traditional surface grinding machine, grinding wheel, sensors, vibration amplifier, piezo actuator and the work-piece materials. Moreover, in this chapter the whole experimental system configuration is presented by a camera picture. However, materials characterization and preparation process are illustrated in chapter 5. This chapter also gives a brief description of control system devices which were introduced to help control the grinding process and to obtain accurate results. Then preliminary experiments were undertaken in order to give initial results about the materials' behaviour, the input design parameters; the output results were obtained including Taguchi design of experiment method. This method shows how some of the input parameters such as grinding wheel speed, feed rate, and depth of cut affect the output results.

Chapter 6 presents the actual experimental work after fewer preliminary tests were carried out as mentioned in chapter 5. Mainly titanium work-piece bars with the following dimensions: 60 mm length x 8 mm width x 20 mm height are used in the

Experiment, where, a surface grinding machine was used to grinding them with application of vibration assisted and with enhance of coolant fluid as well. Then the machinability of the materials was tested in terms of four factors such as tool life, cutting forces, power requirements and surface finish. However, a crack underneath the workpiece was tested using SEM, and also a method of aching the workpiece surface after grinding with Acids to identify the depths & width of the internal crack was also used. Whilst, cutting forces, power, material removal and wheel wear were also been measured.

However, in chapter 6 the behaviour of a difficult-to-machine aerospace material known as Ti6Al4V has been investigated, the investigations include grinding forces analysis, material removal rate, surface quality and grinding wheel (Tool) wear. All these tests were carried out twice, once with the implementation of vibration assisted grinding and once conventionally.

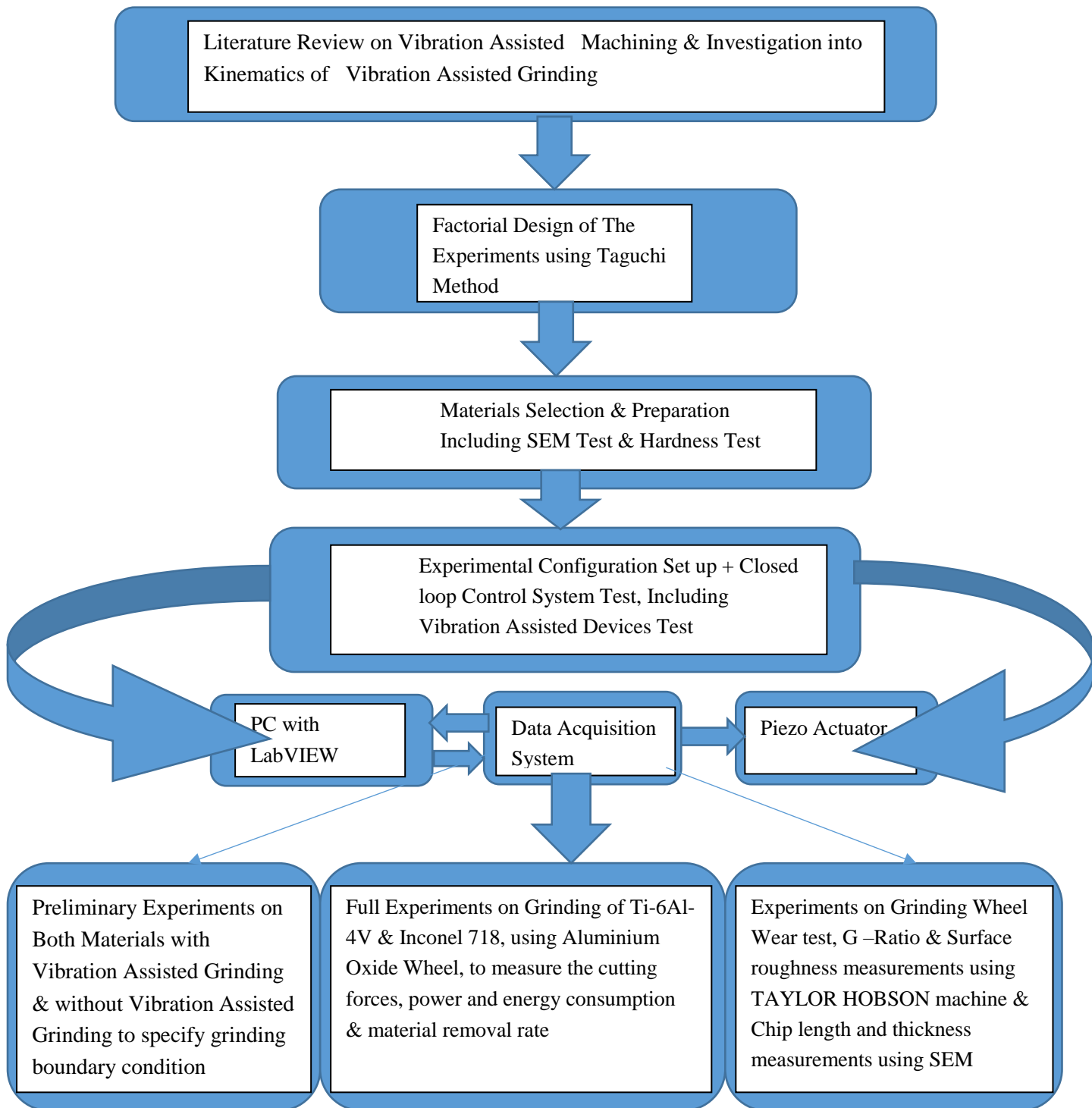
In chapter 7 the grinding output parameters for another aerospace hard material known as nickel Inconel 718 were also investigated. The grinding results in both cases with the application of vibration and without the application of vibration, were compared to each other especially the grinding forces, the material removal rate and the surface roughness.

Chapter 8 illustrates the variations of the grinding output parameters' results for both aerospace hard-to-machine materials. However, a comparative method was undertaken to characterise grinding with superimposed vibration. The grinding wheel wear was also investigated under both cases - conventional and vibratory grinding.

Chapter 9 presents a comprehensive discussion of all the theoretical and experimental work including the newly developed model hypothesis and calculation. Hence, summary of the results is given in detailed key points to form the conclusion. Then a few suggestions are given as future recommendations.

In the next page below a flow chart diagram represents the methodology of this study in terms of chapters. The chart has been drawn to explain the chapter's sequences and also to explain how the entire project has been developed and managed from the literature review stage up to the final results and conclusion.

METHODOLOGY FLOW CHART DIAGRAM



CHAPTER-2

**LITERATURE REVIEW ON VIBRATION
ASSISTED MACHINING**

2. LITERATURE REVIEW ON VIBRATION ASSISTED MACHINING

2.1 Introduction

Metal cutting precision with high surface roughness accuracy tends to sub micro and up to nanometres, enhanced the production of mechanical and electrical components over the years (Brehl, 2008). This was motivated by the huge demands from the manufacturing sector in the mid 1960s in the United States of America. However, this demand was mainly from the aerospace industry, namely the defence and civil sectors.

Vibration assisted machining is a cutting technique that uses imposed periodic oscillating cycles on the cutting tool or the work-piece to improve the cutting performance and efficiency. In addition to that, this basic idea of vibration assisted can be explained by a relative motion between the tool and the work-piece. However, the fundamental theory of vibration assisted machining is that the tool face is separated repeatedly from the work-piece. Cerniway, (2005), has implemented this technique in the drilling of wood.

Moreover, it has also been explained that the basic element of vibration assisted machining is the imposed oscillation that can be generated using many methods; such as piezoelectric actuators which have commonly been developed and used for various applications such as drilling, grinding, milling and recently the electric discharge micro-milling (Brehl, 2008).

2.2 Overview of Vibration Assisted Machining

Shamoto et al, (1991) claimed through his sufficient results, that vibration assisted improves the performance of the machine by adding extra energy via oscillation. Likewise he also clarified how vibration assisted can be used as a useful tool for the industrial applications depending upon the usage of low or high frequency. Major examples of that are vibration conveyers, ultrasonic assisted turning of aerospace materials, ultrasonic grinding. Since then the technique was under investigation, then the idea of vibration assisted machining theory with certain frequency and low amplitude came out. Since the new idea had been built upon the variation of frequency and amplitude, it became a very widely required process in the engineering applications such as surface finish, material removal rate and wheel wear.

Shamoto et al, (1990) also claimed that vibration assisted grinding can lead to improvement in cutting performance if applied to the cutting tool or the workpiece in a correct way.

(Zhang & Meng, 2003) found that reduction in grinding normal forces was achieved with the implementation of vibration assisted. However, the reduction in normal forces basically led to surface integrity improvement and at the same time secured workpiece subsurface damage reduction and median cracks prevention.

Moreover, the variation in frequency and amplitude help to generate a vibro-motion upon which vibration assisted machining is based. This vibro-motion can be generated by employing a piezoelectric actuator to impose vibration into milling, drilling, grinding and electric discharge machining (EDM) as well (Endo et al.2008).

Shortly after Shamoto's findings, Adachi and Arai (1997) claimed that low frequency vibration assisted helps to reduce burr and to extend tool life. However, the frequency used is 1000 Hz which is much lower than the usually used frequency in the ultrasonic application (20 KHz). A few years later (2007) Brehl and Dow demonstrated the benefit of vibration assisted when this method was implemented with the variation of high, low frequency and low amplitude also varied between 3um and 100um. They claimed that this method could improve the process quality especially by introducing the idea of periodic separation between the workpiece and the tool rake face. However, this separation process will influence the chip formation by reducing the chip thickness and therefore reducing cutting forces that led to improvement in surface finish quality.

In (2006) Chen et al implemented high level of frequency and amplitude to influence the interaction between the rake face of the cutting tool and the workpiece, this led to enlarging the intermittent gap during cutting when applying vibration assisted machining. However, the bigger the gap the bigger the chance of improving the fluid extraction in between the cutting tool and the workpiece. This process of gap enlargement between the cutting tool and the workpiece called disengagement can be controlled in order to achieve periodic disengagement motion that leads to precise and stable vibration assisted machining process. However, a control system program is the only way to secure this task and also to enhance controlling work speed variation and the periodic disengagement (imposed oscillation in grinding) which by definition explains the concept of vibration assisted machining in grinding. Nevertheless, for the benefit of the industry, the process needs to be controlled via a close loop control system to ensure that the imposed oscillation that is generated by several vibration devices is measurable and under control. However, the vibro- devices such as

piezoelectric actuator, signal generator, data acquisition system can also be controlled via a feedback loop to a PC machine that is connected to the machine's spindle and other components. Nevertheless, in vibration assisted machining, vibration amplitude (usually sine wave form) could lead to large intermittent gaps during cutting, this is in accordance with the findings of Chern et al., (2006) the amplitude in vibration assisted has the highest influence on the interaction between the work-piece and the cutting tool due to high vibration frequency. This high vibration frequency has a negative effect on tool life.

Over the years many researchers tried to investigate the process of machining hard and brittle materials such as ceramics nickel and titanium, by employing diamond and CBN wheels to achieve better surface finish and to improve material removal rate. Although, researchers knew that these hard materials are difficult to be machined by diamond cutting tools because of wear to the cutting tools due to the chemical reaction between the tool and the work-piece (Bonifacio et al., 1994).

Several studies throughout the years have been done to investigate the possibility of introducing vibration assisted machining in turning, milling, and drilling. For example, Chen and Lee (2005) implemented vibration assisted machining depending on vibration frequency to improve surface roughness in drilling, while Adachi and Arai in 1997 were able to prove that extended tool life help to reduce the burr phenomenon in the drilling of aluminium by employing 1 kHz vibro-electronic system for this task. A couples of years later Wang and Zhou (2002) presented experimentally how they were able to machine hard and brittle materials using ultrasonic diamond cutting tool at 3um amplitude and 40 KHz frequency.

Brehl (2008) also mentioned in his article that applying vibration assisted machining that was based on the piezoelectric actuator method, won't be able to produce a complex shape unless polishing and grinding process were done in advance prior to employing a diamond cutting tool to improve surface roughness and to extend tool life.

In 2003 Babitsky and Kalanishikov proved experimentally the possibility of cutting aerospace material by employing a turning machine with the implementation of an ultrasonic vibration process with the combination of load bar applied to the cutting tool at 20 kHz frequency and maximum amplitude of 3 um to secure the required displacement for the experiment.

The high frequency interaction between the work-piece and the tool, resulted in a decrease of cutting forces and noise by about 50% and improved surface roughness by about 50% as well.

Cerniway (2005) carried out a simulation study to investigate vibration assisted machining. This was done by employing a computer system technique which was able to simulate the effect of horizontal speed ration (HSR) that was produced from kinematic tool tip surfaces. Cerniway also attempted the evolvement of the implementation of oscillation assessment technique to study how the frequency and the amplitude of the machining tool tip location compared to simulation validation results.

Vibration assisted machining 1D and 2D in comparison.

Ultrasonically assisted turning, with high frequency vibration ($f \approx 20$ kHz) with amplitude equal to around $10 \mu\text{m}$ being imposed on the movement of the cutting tool, proposed by Mitrofanov

allows significant improvements in machining. Ultrasonic turning demonstrates many advantages like: a significant decrease in cutting forces, better surface roughness (improvement in surface finish by up to 50%. Compared to conventional technology, increase in tool life up to 20 times. This difference is mostly caused by the fact that the tool remains in contact with the chip for only about 40% of the cutting time, which improves cooling and simplifies chip removal.

Zhong & Yang, (2004) generated a micro-vibration motion out of a vibro-device to support a work-piece in a grinding process. This vibro-device consists of two mechanical systems that aimed to generate micro vibration in two directions horizontal and vertical.

Batako (2005) employed several thermal methods analysis including the thermocouple techniques method during high efficiency deep grinding (HEDG) to measure the grinding temperature. Some of his measurement methods proved to be very accurate.

2.3 Vibration assisted machining (VAM) features

Vibration was proved to be an effective solution in manufacturing in most of the chip removal processes, however it is a new concept and still under development.

Moreover, it has been reported by a number of publications that machining with vibration assistance has positive effects on the machining performance as a whole (Moriwaki, 1999). These positive effects include:

2.3.1 Extended tool life

VAM can extend tool life significantly, compared to conventional machining methods: this improvement is seen when diamond tools are used to machine ferrous, CBN, and carbide tools (Shamoto et al., 1999). Different wear mechanisms appear to be operative depending on the combination of tool and work materials. 2D VAM generally provides longer tool life than 1D VAM for the same depth of cut, tool geometry, and tool-work-piece material combinations (Weber, 1984).

2.3.2 Tool life extension for brittle materials and non-diamond tools

VAM improves diamond tool life when machining brittle materials. In an early test, Moriwaki and Shamoto found negligible flank wear after a 59m cutting distance using a diamond tool to machine soda-lime glass with 1D VAM (Moriwaki et al., 1992).

2.3.3 Improved surface finish and form accuracy

Improved surface finish compared to conventional machining is characteristic of VAM regardless of the material machined or the depth of cut required, and the level of roughness is only a few nanometres RMS. For making large parts, where VAM is used to achieve a degree of precision while limiting tool wear (Shamoto et al., 2005), the depth of cut may be as large as 1mm and an acceptable surface finish may be on the order of 10 μm RMS. When used with precision diamond-turning machines (Rubenach, 2003), VAM can achieve surface finishes in the range of 10-30 μm RMS for hardened steels at economical machining distances of hundreds to several thousand metres (Brehl et al., 2006).

2.3.4 Ductile regime machining of brittle materials

When the depth of cut is carefully controlled to a small value many brittle materials machine as if they were ductile, producing chips by means of plastic flow and with minimal sub surface cracking (Xiao et al., 2003). In practice, ductile-regime machining frequently remains uneconomical since the critical depth of cut is on the order of 1 μm , resulting in small material removal rates, (Zhou et al., 2003).

2.3.5 Advantages of Grinding With Vibration Assisted:

There are many advantages of Grinding with vibration assisted, which can be summarised as follows (Tsiakoumis, 2011):

- Reduced cutting forces
- Increased cutting efficiency
- Increased material removal
- Improved surface finish
- Extended wheel life (low wheel wear)
- Help to reduce wheel loading
- Improves coolant entry into the contact zone

2.4 Application of Vibration Assisted to Grinding

Ahmed (2007) claimed in his investigation that any increase in the vibration amplitude will lead to more than 50% reduction in cutting force, because of the increase of the dis-contact movement between the chip and the tool.

Furthermore, Wu and Fan, (2003) in their study claimed that one dimensional vibration assisted machining can extend tool life, and improve surface roughness compared to conventional machining. On the other hand they also claimed that two dimensional vibration assisted machining is more effective, beneficial and reliable to cutting forces than one dimensional vibration assisted. In this context Skelton and Wang, (2002) also found that two dimensional vibration assisted machining reduces tool forces by around 20% and a few percentage points more compared to one dimensional vibration assisted even with the same tool geometry and machining conditions.

Brehl and Dow (2007) mentioned that the application of vibration assisted machining is meant to reach precision machining with small-amplitude tool vibration to improve the production of metal cutting. However, the imposed periodic separation between the tool rake face angle and the work-piece was related to the reduction of chip thickness due to reduction in machine cutting forces which led to surface finish improvement and tool life extension, where the vibration was applied to the cutting tool. Hence, the vibration frequency varies from zero Hz to 40 KHz and the amplitude varies from 2 μm to 100 μm

Tsiakoumis.I.Vaios (2010) designed a system to produce periodic oscillation on the work-piece by employing piezoelectric actuators. However, the imposed oscillation (vibration) was applied horizontally on the direction of the cutting force to enhance to create slots lead to accommodate the cooling fluids and reduces the temperature in the grinding zone as well.

It has been reported by Tsiakoumis, (2011) that a possible design of devices that can produce micro-vibration is supposed to be under the following assumptions:

- The dimensions of the devices are based on the maximum distance between the machine grinding wheel and the work table.
- The vibrations are produced by piezoelectric actuators.
- There is no displacement in vertical axis.
- Damping in the system is neglected.
- The flat springs are weightless.

For the above assumed assumption the system considered to be a single degree of freedom system.

Figure 2.1 shows a similar system designed by Zhang and Yang (2004) to produce a micro-vibration oscillation to the work-piece in the vertical and horizontal directions with the enhancement of three piezoelectric actuators acting vertically and one piezoelectric actuator acting in the horizontal direction. All of these piezoelectric actuators were fixed to a sample plate and moving platform under the influence of linear motion guides to enable them to vibrate easily.

Or otherwise to apply vibration assisted grinding which was used to prevent wheel loading and sliding friction and also to enhance coolant delivery.

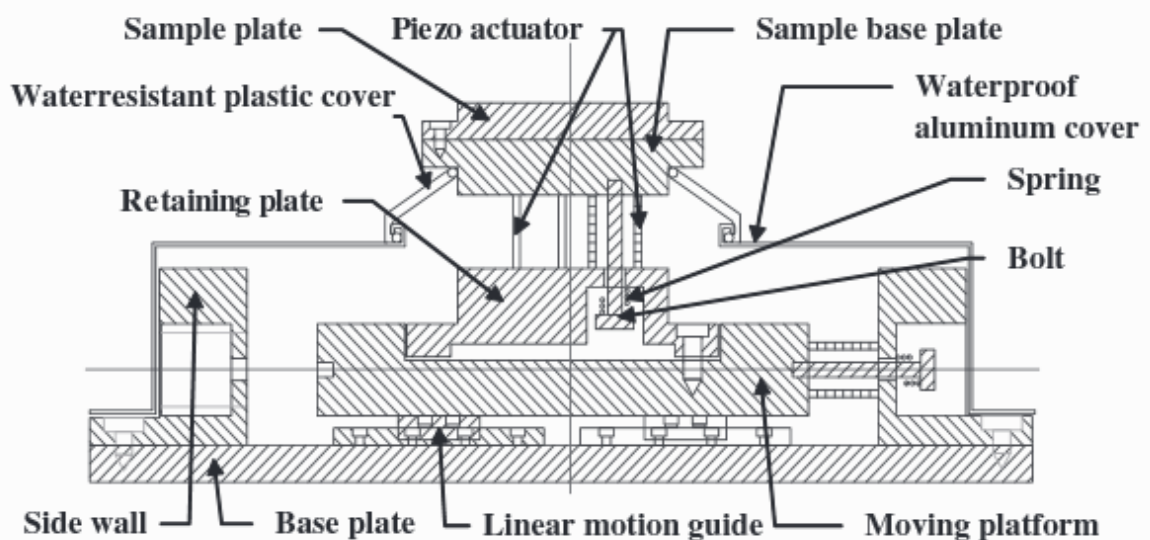


Figure 2.1: Design of Micro-Vibration Device (Z.W.Zhong &H.B. Yang, 2004)

2.5 Summary

To achieve the aim and the objectives of this project a literature review on vibration assisted machining first has been undertaken to identify existing practice in machining the materials involved this study and also to identify the state of the arts technology in the field of grinding with vibration assisted.

Hence, the huge demand from the manufacturing sector in the mid 1960s, mainly from the aerospace industry was the main motive behind metal cutting precision.

Vibration assisted machining is a cutting technique that uses imposed periodic oscillating cycles on the cutting tool or the work-piece to improve the cutting performance and efficiency. In 1991, Shamoto claimed that the implementation of

vibration assisted improves the cutting performance of the machine. His findings were under investigation since then, especially in the field of frequency and amplitude variation to achieve good surface finish, high materials removal and low wheel wear.

In 2003 Zhang found that the implementation of vibration assisted led to normal forces reduction, as the result of that workpiece subsurface damage was reduced and median cracks also prevented. Through over the years, many researchers have tried to investigate the process of machining hard and brittle materials such as ceramics nickel alloy and titanium alloy, by employing diamond and CBN wheels to achieve better surface roughness and to improve material removal rate.

In 2007 Ahmed claimed that any increase in vibration amplitude will lead to reduction in cutting forces. Meanwhile, in 2011 Tsiakoumis designed a system in which oscillation were introduced into the workpiece in the direction of the feed rate. He claim that if low frequency applied to the system, there will be many advantages of vibration assisted grinding beside reduction of cutting forces such as increase cutting efficiency, increased material removal and extended wheel life.

All previous and current studies were focused on vibration applied in the direction of grinding to create slots lead to ease the cooling system, while this study investigated the possibility of vibration imposed in the axial direction of the grinding wheel (perpendicular) which has not been done before. This new system allowed to vibrates the workpiece in a direction that perpendicular to the grinding direction by employing a piezo electric- actuator, where 100 Hz vibration frequency was applied to the system to secure 130 μm displacement and to match low excitation of (4volts) to secure lower power consumption. This will met the proposed objectives such as reduction in cutting forces, power consumption, wheel wear and also improvement in material removal and surface roughness.

CHAPTER-3

**FUNDAMENTALS OF GRINDING WITH
VIBRATION ASSISTANCE**

3. FUNDAMENTALS OF GRINDING WITH VIBRATION ASSISTANCE

3.1 Introduction

Grinding is the process of removing metal in the form of minute chips by the action of irregularly shaped abrasive particles, the so called a chip removal process that uses an individual abrasive grain as a cutting tool. As the grain passes over the work-piece it cuts away a small chip, leaving a smooth, accurate surface, thus grinding wheels by definition are bonded abrasives in which the abrasive grains are distributed, Kalpakjian and Schmid, (2010). Hence, grinding is the most important abrasive machining process that was developed as a metal manufacturing process in the nineteenth century, where grinding played an important role in the development of tools and in the production of steam engines, internal combustion engines, bearings, transmissions and ultimately jet engines, astronomical instruments and microelectronic devices. However, grinding also is a term used in modern manufacturing practice to describe machining with high-speed abrasive wheels, pads and belts.

3.2 Types of Grinding

They are many types of grinding depending on the wheel and the workpiece shape as well as the motion of the workpiece and the spindle unit, some of them listed below here, but the first two are the most major used types in the industry nowadays:

- 1- **Surface grinding:** is one of the most common operations that uses a rotating abrasive wheel to smooth the flat surface of the materials to attain the desired surface finishing. Rowe (2014).
- 2- **Cylindrical grinding:** used for external cylindrical surfaces and shoulders of work pieces such as; crank shaft, bearings rings, spindles and pins-etc.
- 3- **Internal and external grinding** (in which a grinding wheel is used to grind the inner & outer diameter of the parts such as in bushings, bearing races and a rotating stock piece such as shafts. (<http://www.HJMTC> 26/02/201).
- 4- **High efficiency deep grinding (HEDG):** is an advance grinding method which combines very large depths of cut with extremely fast work speeds and high removal rates. Tawakoli (1990).

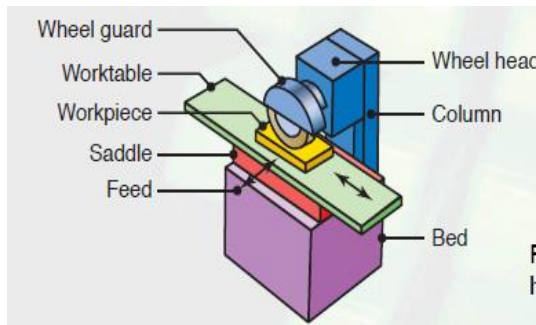
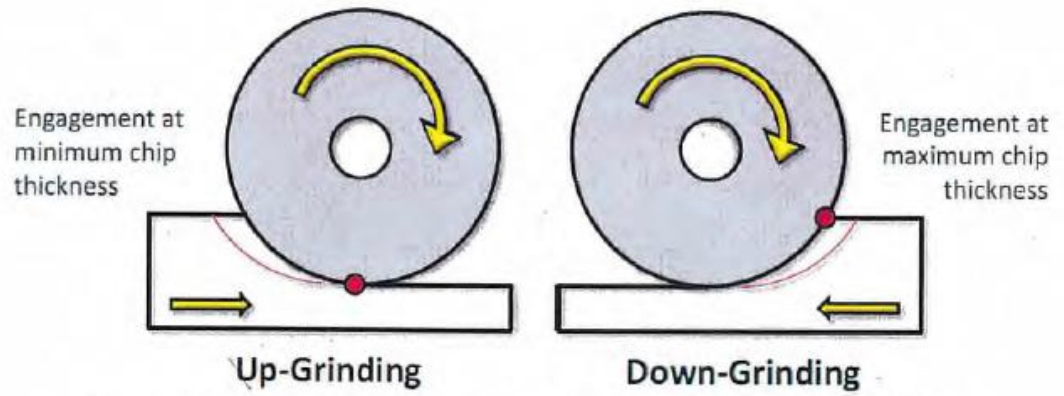


Figure 3.1: Surface grinding (Book of Modern Grinding Technology/ Second Edition, Rawe.W.B (2014)



Figure 3.2: Internal grinding <http://www.HJMTC> 26/02/201

3.4 Grinding Wheel Specifications

Grinding wheel manufacturers have agreed to a standardization system to describe wheel composition as well as wheel shapes and faces.

However, the basic component materials of grinding wheels are abrasive mineral grains and bonding material. The abrasive mineral or synthetic mineral grains must be selected with respect to the material that needed to be cut or finished. The abrasive grains can be made from diamond, silicon carbide or aluminium oxide. The bonding materials in which the abrasive grains are fixed is usually made either from organic materials (rubber, resin), or inorganic materials (clay). The inorganic materials allow medium to fine sizes of grains, while the organic material allows large sizes of grains. Grinding wheels are composed of thousands of small abrasive grains held together by a bonding material. Each abrasive grain is a cutting edge. As the grain passes over the work piece it cuts small chip, leaving a smooth, accurate surface, thus grinding wheels by definition are bonded abrasives in which the abrasive grains are distributed. Also grinding wheels used to sharpen knives and tools, as well as using sandpaper to smoothen surfaces and remove sharp corner.

Grinding wheels are generally made from a matrix of coarse particles pressed and bonded together to form a solid, circular shape. Various profiles and cross sections are available depending on the intended usage for the wheel. They may also be made from a solid steel or aluminium disc with particles bonded to the surface.

Characteristics

There are five characteristics of a cutting wheel: material, grain size, wheel grade, grain spacing, and bond type. They will be indicated by codes on the wheel's label.

Abrasive Grain, the actual abrasive, is selected according to the hardness of the material being cut.

- Aluminium Oxide (A)
- Silicon Carbide (S)
- Ceramic (C)
- Diamond (D, MD, SD)
- Cubic Boron Nitride (B)

Grinding wheels with diamond or Cubic Boron Nitride (CBN) grains are called super-abrasives.

Grinding wheels with Aluminium Oxide (corundum), Silicon Carbide or Ceramic grains are called conventional abrasives.

Grain size, from 8 (coarsest) 1200 (finest), determines the physical size of the abrasive grains in the wheel. A larger grain will cut freely, allowing fast cutting but poor surface finish. Ultra-fine grain sizes are for precision finish work.

Wheel grade, from A (soft) to Z (hard), determines how tightly the bond holds the abrasive. Grade affects almost all considerations of grinding, such as wheel speed, coolant flow, maximum and minimum feed rates, and grinding depth.

Grain spacing /or structure, from 1 (densest) to 16 (least dense). Density is the ratio of bond and abrasive to air space. A less-dense wheel will cut freely, and has a large effect on surface finish. It is also able to take a deeper or wider cut with less coolant, as the chip clearance on the wheel is greater.

Wheel bond; are described to be by how the wheel holds the abrasives, affects finish, coolant, and minimum/maximum wheel speed.

Vitrified(V), Resinoid(B), Silicate(S), Shellac(E), Rubber(R), Metal(M), Oxychloride (O).

Materials:

- 1- Consideration of;
 - Wheels materials
 - Work piece
 - Quality of the surface produced
 - Surface finish, surface integrity
 - Cycle time
 - Overall economics of the operation
- 2- Proper selection of process parameters:
 - Grinding wheels, grinding fluids
 - Using the appropriate machine characteristics

Specific recommendations for selecting wheels and appropriate process parameters for metals are given especially aerospace materials composites. However, wheels selection involves not only the shape of the wheel and the shape of the part to be produced, but the characteristics of the work piece material as well. Nevertheless, they are two types of abrasives are used in grinding wheels: natural and manufactured, Except for diamonds, manufactured abrasives have almost entirely replaced natural abrasive materials. Even natural diamonds have been replaced in some instances by synthetic diamonds.

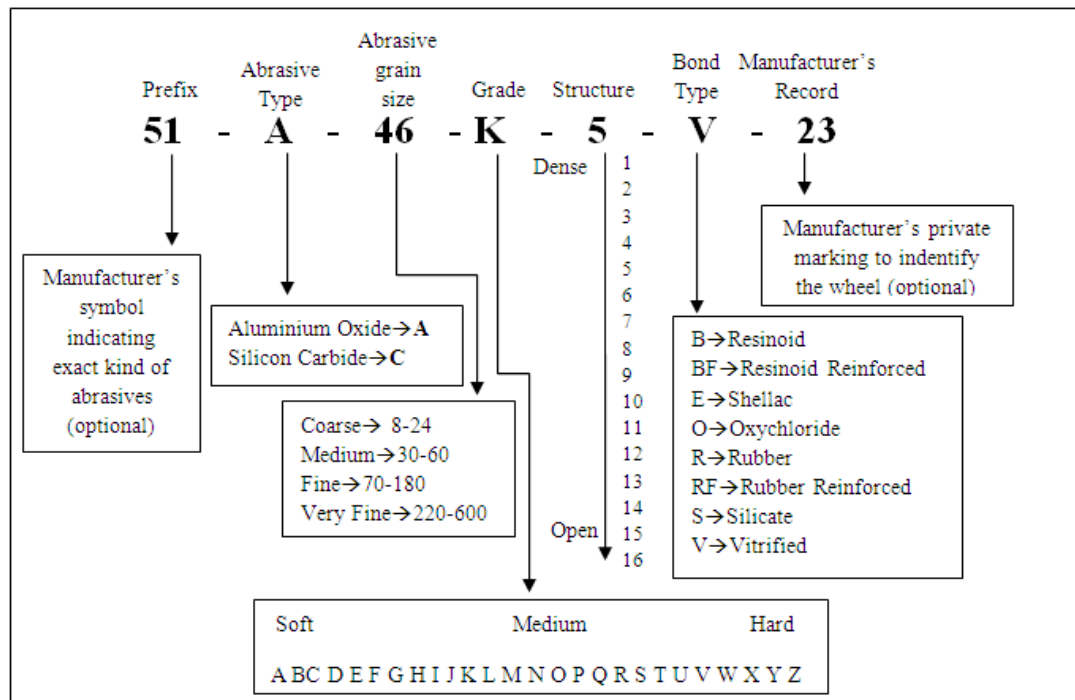


Figure 3.3: Grinding Wheel Marking System (Modern Grinding Technology, Second Edition)

3.5 The coolant delivery system

Coolant application is an important factor to reduce the excessive heat that developed in the grinding zone. This heat leads to poor surface quality, low material removal rate, high wheel wear and thermal damage of the workpiece. However, the main aim of the coolant is to cool and lubricate the work piece and the grinding wheel during grinding. The coolant used for grinding was an emulsion, HYSOL-X. HYSOL_X is a semi-synthetic cutting and grinding fluid that was employed with a dilution ratio of 10:1 in water to reduce the wheel loading, the pressure of the coolant system was increased to 4 bar. However, the coolant supply was also employed for wheel cleaning, grinding process debris cleaning and cooling the grinding process as well. By using this coolant arrangement for coolant delivery, the stability of the grinding wheel performance was improved.

3.6 Cutting Forces and Power

Knowledge of cutting forces and power involved in machining operations is important for the following reasons:

- 1- Data on cutting forces is essential so that:

Machine tools can be properly controlled to minimize distortion of the machine components, maintain the desired dimensional accuracy of the machined part, and help select appropriate tool holders and work holding devices.

The workpiece is capable of withstanding these forces without excessive distortion.

2- Power requirements must be known in order to enable the selection of a machine tool with adequate electric power.

Power is the product of force and velocity. Thus, the power input in cutting can be shown as Power is:

$$P = F_c V$$

Where F_c is cutting force and V is the cutting velocity (Kalpakjian, Schmid, 2010).

There are two main components of a cutting force in grinding: normal and tangential. Values of each of them strongly depend on ploughing and cutting phase during cutting and depth of cut as well.

In addition to that, many theoretical models have been developed to represent the grinding forces on work-piece. These models were based on the fact that chip formation during grinding process that consists of three stages: sliding, ploughing and cutting. The total grinding force vector F exerted by the wheel on the work-piece could be analysed into a horizontal force (Tangential force F_t) and a vertical force (Normal force F_n) where the normal force has an influence on the surface deformation and the tangential force affects the power consumption and service life of the wheel.

See Figure 3.4. below

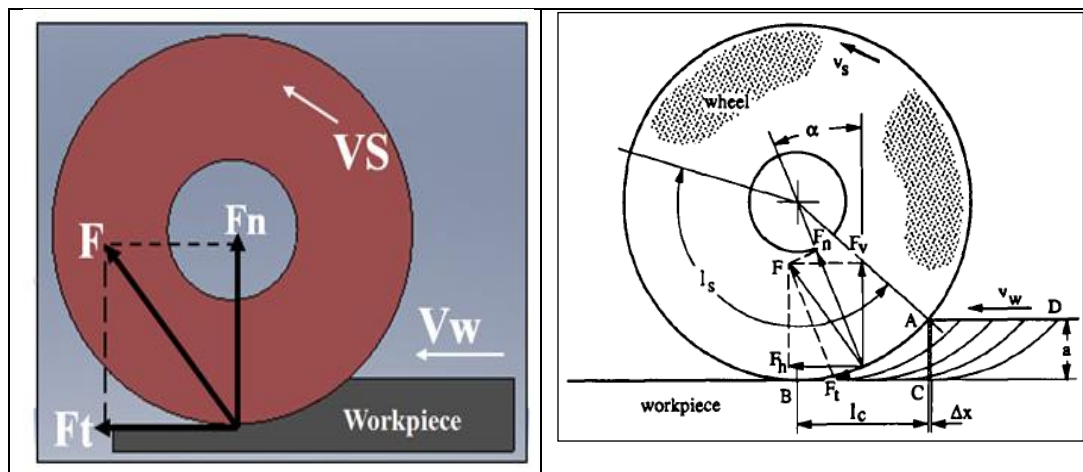


Figure 3.4: Grinding force, (Vaios, 2011)

Where:

V_w : Workpiece Velocity,

V_s : Wheel Velocity,

F_t : Tangential Force,

F_n : Normal Force,
 F : Total Force

$$F_t = K_c A_m \quad 3.1$$

$$K_c = K_0 A_m^{-\eta} \quad 3.2$$

Where F_t is the cutting force of single grit, A_m is the average chip cross section area, K_0 is a constant depending on materials and grit shape.

The total grinding cutting force is the sum of the cutting force of individual grain engaged in grinding.

$$F_t = b l_c \lambda f_t = b l_c \lambda K_c A_m = K_0 b l_c \lambda A_m^{1-\eta} \quad 3.3$$

Where F_t is tangential grinding force, b is grinding width, λ is cutting edge density, η is a constant.

However, the grinding cutting efficiency can be described by the specific grinding energy, which is the energy consumption with a unit volume of material removal.

$$e_c = \frac{P}{Q_w} = \frac{F_t V_s}{a_p v_w b} \quad 3.4$$

Thus the grinding force model in equation (1) can be expressed in the following form

$$F_t = \left[\lambda k_0 b \sqrt{d_e a_p} \right]^\eta \left[k_0 b \left(\frac{a_p v_w}{v_s} \right) \right]^{1-\eta} \quad 3.5$$

Therefore

$$e_c = k_0 \left[\lambda \sqrt{d_e a_p} \right]^\eta \left[\left(\frac{a_p v_w}{v_s} \right) \right]^{-\eta} = K_0 (l_c \lambda)^\eta h_{eq}^{-\eta} \quad 3.6$$

Hence, this equation can also be written in a similar form to equation (3) where the coefficient of a single grit cutting force $K_c = K_0 A_m^{-\eta}$, can be substituted in equation (13) to give grinding force between two boundary conditions; $\eta = 0$ and $\eta = 1$, as η value represents the grinding cutting efficiency.

$$\text{At } \eta=0, F_t = k_0 b \left(\frac{a_p v_w}{v_s} \right) = K_0 b h_{eq} \quad 3.7$$

In this case the grinding force is directly related to the equivalent chip thickness while the specific grinding energy remains constant with the increase in depth of cut. In fact this means that the grinding force is generated mainly by chip formation.

$$At \eta=1, Ft = \lambda k_0 b \sqrt{d_e a_p} = \lambda K_0 b l_c. \quad 3.8$$

In this case the grinding force is directly related to the contact area (bl_c) and the cutting edge density λ . Since there is a contact situation involves, this gives the indication that the grinding force is generated by friction and also indicate that at $\lambda = 1$ the grinding doesn't remove materials.

Therefore, The smaller the η the more efficient the cutting process, ((In practice $0.1 < \eta < 0.7$)).

The η value also represents the size effect of grinding. Furthermore, grinding size effect is a phenomenon that grinding specific energy decreases with the increase of grinding removal rate (see figures 7.10b & 7.9c)

However, any increase in cutting edge density λ will increase the specific grinding energy where energy consumption will be high. That means high density of cutting edges leads to smaller chips and more energy consumption.

3.7 Chip Formation in Grinding

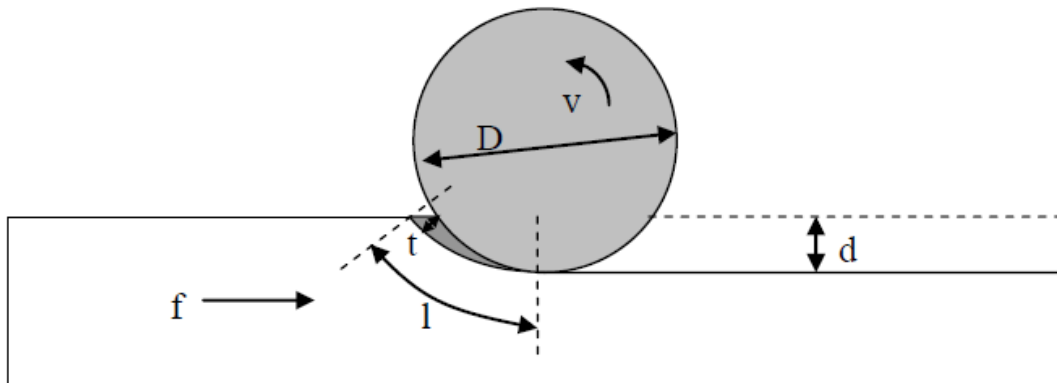


Figure 3.5: Chip formation (Barczak L. (2010). Application of Minimum Quantity Lubrication (MQL) in Plane Surface Grinding, PhD Thesis, (Ref, 32)

Metal cutting process in which material removal occurred to form a certain shape with new size, new dimensions and surfaces finish. However, all cutting process such as milling, drilling, turning and boring produce chips in similar fashion. Therefore, studying chip formation is the only way to understand the mechanics of alloys machining process.

Chip formations are given by three different types such as; continuous chip, discontinuous and shear-localized chip it depends on the work material type, and its metallurgical conditions and the proposed cutting conditions.

However, this analysis can be focused on continuous chip, because it is stable for analysis with uniform strain and it cause no damage to the system, such as the machine or cutting tool.

Aerospace materials especially titanium alloys are extremely difficult to machine at high cutting speeds due to their physical properties. However, chip formation has been influence by the thermos-mechanical behaviour of the alloys at the workpiece tool contact zone. In machining of aerospace materials the chip is segmented especially in case of machining titanium where a segmented chip with ununiform strain distributed can be generated likewise the deformation in continuous chip is uniform. However, high temperatures in the chip were attributed to high flow stress of the alloys and also to its lower density. Komanduri and Turkovich (11) explained that in their experiment at low speed machining of Ti6Al-4V a segmented chip formation was observed (inside the scanning electron microscope).furthermore, the mechanism of chip formation was also been described in a different way from continuous chip formation. The science behind each of the two mentioned case of chip formation is that:

- Segmented chip involve plastic instability and strain localization in a narrow band in the primary shear zone led to shear failure.
- Where continuous chip formation involve gradual build-up of segment with negligible deformation.

In addition to that, due to negative rake angle of cutting edge in grinding, chip formation is different than in milling or turning. Material is mostly removed due to compression of workpiece, that is why, very high stresses can be observed. For brittle materials it is possible to observe stresses greater than value of elasticity module, what consequently leads to unexpected breaks in workpiece structure. It is the main reason why grinding is more complex process for hard and brittle materials and difficult to simulate. There are three stages of chip formation in grinding: rubbing, ploughing, cutting [31]. All are presented in figure (4.11).

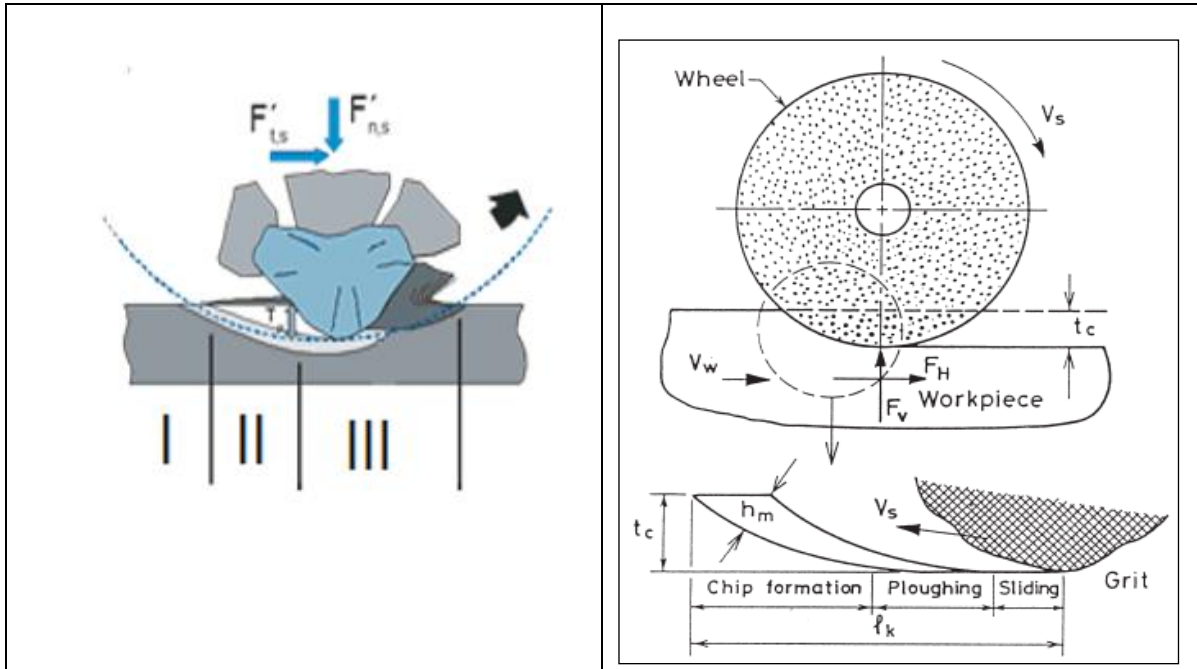


Figure 3.6: stage of chip formation, where: rubbing, ploughing & cutting (Ref, [31]. 1996)

During the first stage (I) rubbing or sliding phase, friction and elastic deformation between the grain and work-piece material occur. In the second stage (II) ploughing, the grain moves inside the work-piece what causes plastic deformation and internal friction in the work-piece material. The third stage (III) cutting or chip formation begins, with the material being moved from the work-piece .

3.8 Equivalent Chip Thickness

The equivalent chip thickness (h_{eq}) by definition is the thickness of the chip after grinding, in other word it is the thickness of the chip that has been produced by the grinding wheel after a cutting trial to the work-piece. However, the value of this chip thickness is proportional to the actual depth of cut (a_e), table speed and inversely-proportional to the grinding wheel speed and it can be given by the following equation:

$$h_{eq} = a_e \frac{V_w}{V_s} \quad 3.9$$

However, Marinescu et al (2007) challenged this finding of chip thickness calculation without considering the space between the grinding wheel grains at the surface of the wheel. Therefore he claimed that the best way to specify the material removed during grinding is by studying the uncut chip thickness (h_{cu}) because the uncut chip

thickness calculation depends on material removed in the grinding process as general and it can be defined by this equation:

$$h_{cu} = \sqrt{\frac{V_w}{V_s} \frac{1}{C r}} \sqrt{\frac{a_e}{d_e}} h_{cu} \ll a_e \quad 3.10$$

Where C is the active grit density; r is the grit cutting point factor; d_e is the equivalent wheel diameter and a_e is the actual depth of cut.

Hence, r is also given by the ratio of chip width to chip thickness.

3.9 Grinding of Aerospace Materials

Machinability by definition means is to ease the difficulties in order to enable the material to be machine under certain conditions such as feed rate, cutting speed and depth of cut. However, machinability index of any material is accessed in terms of four factors; such as tool life, cutting forces, power requirements and surface finish. Hence, machinability index of titanium aluminide alloys is about 3 times difficult than free machining low carbon steel.

Aerospace materials are categorised in two different groups; brittle such as titanium alloys and hard such as nickel alloys. In this chapter literature review about the machinability of these materials was given.

Conventional titanium alloys such as Ti-6Al-4V, which contribute by 50-60% to the total production of titanium alloy, are characterised by high tensile strength $\sim 1100\text{Mpa}$ at 20°C combined with low density ($\sim 4\text{g/cm}^3$) and good corrosion resistance. These properties explain why titanium used in the manufacturing of commercial aircraft engine (33% of engine weight), [1].

3.9.1 Titanium

It is a chemical element with the symbol Ti and atomic number is 22. It is a lustrous transition metal with a silver colour, it appearances is silvery grey-white metallic shape with low density and high strength. It is highly resistant to corrosion in sea water, aquilegia and chlorine.

Recent trends in the aerospace industry increase the use of titanium alloys because of its outstanding mechanical properties that can be provided at critical load carrying locations in many military and commercial aircraft, however, weight saving is also the main driving factor as gamma titanium alloy -TiAl , have the ability to operate at temperatures of up to 800°C . These high temperatures resistance properties of the

material provide an indication of its adaptability for the manufacturing of aero-engine components such as HP compressor and LP turbine blade. However, from an aero-engine point of view, greater fuel economy and hence a market advantage, can be provided through the use of a lighter materials with low density such as gamma titanium, and these are the main reasons for the current interest by aerospace companies such as Rolls-Royce, GE, SNECMA, (Ramulu, Branson, Kim, 2001).

However, since the initial development of gas turbine in 1940s there are two most commonly used alloys in aerospace industry: titanium and nickel based alloys. Figure 3.7 presents that both of these alloys were used in different parts of the jet engine. Titanium based alloy is ideal for its strength and density in the first part of the turbine, where only air compression takes place, at high temperatures it is replaced by nickel-based super alloy, which is much more resistant to the high temperatures.

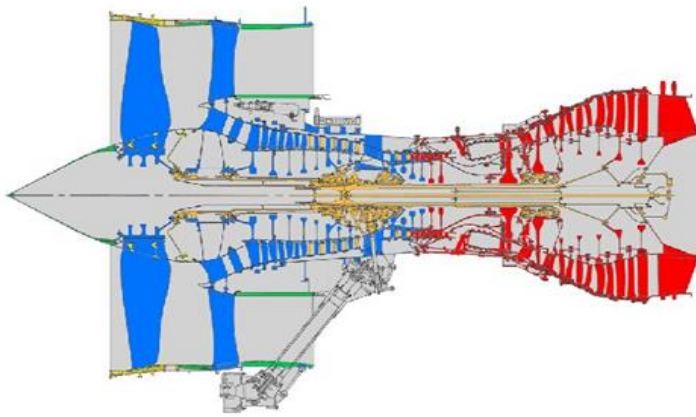


Figure 3.7: The different materials used in a Rolls- Royce jet engine. In blue titanium alloy and in red nickel based super alloy. [31], (D. Rugg, 2003), Hamburg, Germany

Due to high strength to weight ratio, titanium is used in the compressor stages in gas turbines. Titanium content has increased from around 3% in 1940s to around 35% nowadays of the aero-engine weight. High temperature titanium alloy like Ti-6Al-4V is used for static and rotating components in gas turbine engines (Muktinutalpati, 2011).

Nevertheless, grinding of titanium differs significantly from that of other metallic materials, primarily due to its poor machinability. In addition to this fact, machining of titanium on conventional equipment is possible, but is a ‘black art’ restricted to a small body of highly experienced operators and considered by them as being no more difficult than the machining of austenitic stainless steel. However, titanium and titanium alloys are among the most difficult-to machine materials, because of their low thermal conductivity and high chemical reactivity, which causes heat generation during machining and strong adhesion between the tool and the workpiece material.

That is also the cause of poor surface quality, as titanium and titanium alloys are easily disrupted during grinding. Nevertheless, in grinding, the difference between titanium and other metals is the activity of titanium at higher temperatures (Emsley, 2011). At the localized point of the wheel contact, titanium can react chemically with the wheel materials. The important factors to consider in preventing this are:

1. Correct wheel speeds - A good general rule is, use a half to one third of conventional operating wheel speeds to get the best results with titanium
2. Grinding wheel selection - Silicon carbide wheel can be used at 20-30 m/s to give optimum surface finish and minimum wheel wear. The high speeds essential with these wheels produce intense sparking which can cause a fire hazard. The work-piece should be flooded with coolant to reduced sparking.

Moreover, to understand the impact of process conditions on the surface quality of titanium during the grinding process, the input parameters of the experiment should be correctly selected, such as cutting depth, feed rate and diameter of the grinding wheel. Roughing operations presented in literature employed the following process parameters:

Grinding wheel type: 99A90J9V; Wheel diameter: 200 mm at 2500 rpm; Depth of cut: 0.01, 0.02, 0.03, 0.04 mm and Feed rate: 8, 12, 16, 24 m/min

3.9.2 Nickel Alloy

It is a chemical element with symbol Ni and atomic number is 28. It is a transitional metal with silver colour, versatile element and will alloy with most metals such as molybdenum, niobium, tantalum, aluminium and titanium, it gives exceptionally high yield, and good corrosion resistance, tensile and creep rupture properties at temperature up to 700 °C.

Nickel Alloy (Inconel 718) bar is a precipitation-hardening nickel-chromium alloy containing significant amounts of iron, columbium, and molybdenum, alloy with lesser amounts of aluminium and titanium. 718 nickel bar maintains high strength and good ductility up to 1300 F (704 °C). This nickel bar alloy has relatively good weldability, formability, and excellent cryogenic properties compared to other precipitation hardening nickel alloys. The sluggish precipitation hardening response of this alloy allows it to be readily welded without hardening or cracking.

Nickel Alloys 718 bar indicates material stocked in the heat treated condition to have high strength and meet the maximum hardness (40 Rockwell C) requirements of the NACE, MR0175, MR0103, ISO 15156-3 specifications.

3.9.3 Features of Nickel Alloy (Inconel 718)

The key features of nickel alloy (inconel718) include:

- Highly resistant to chloride and sulphide stress corrosion cracking
- High strength in the aged condition
- Good corrosion resistance

Nickel and nickel alloys are used for a wide variety of applications, the majority of which involve corrosion resistance and/ or heat resistance. Some of these include:

1. Aircraft gas turbines
2. Steam turbine power plants
3. Medical applications
4. Nuclear power systems
5. Chemical and petrochemical industries. (www.totalmateria.com)

3.10 Summary

Grinding with vibration assistance is a process in which an oscillations were introduce to the tool or the workpiece to enhance the cutting process. Whilst, a suitable grinding wheel with certain specification is also required to grind aerospace materials such as nickel alloy and titanium alloy. These materials are used for a wide variety of applications, the majority of which involve corrosion resistance and/ or heat resistance especially in the manufacturing of air craft compressors and turbines blades. However, machinability index of any material is accessed in terms of four factors; such as tool life, cutting forces, power requirements and surface finish. Hence, machinability index of titanium aluminide alloys is about 3 times difficult than free machining low carbon steel.

Aerospace materials are categorised in two different groups; brittle such as titanium alloys and hard such as nickel alloys. To grind these materials a grinding wheel selection procedure should take place to specify the correct wheel speeds. A good general rule is; use a half to one third of conventional operating wheel speeds to get the best results with titanium. Also to secure good surface finish the input parameters of the experiment should be correctly selected, such as cutting depth, feed rate and diameter of the grinding wheel.

Hence, for the task of grinding aerospace materials a surface grinding machine was chosen to match the application of vibration assisted in the axial direction of the machine spindle, at the same time an aluminium oxide grinding wheel has also been selected together with cooling system to tackle the problem of the excessive heat flux that has been generated in the contact zone during the grinding process.

CHAPTER-4

**KINEMATICS OF VIBRATION ASSISTED
GRINDING**

4. KINEMATICS OF VIBRATION ASSISTED-GRINDING

4.1 Introduction

Forced vibration- impact concept is been defined as a single collision between two bodies one of them must be in motion whilst the other might be at rest or movement, Harris, (1988).

In addition to that, Babtisky (1978 defined a vibro- impact process by a mechanical system with systematic impact interactions of its elements. However, the Kinematic of Vibro- impact interaction of a tool with a medium can be described in a single degree of freedom model where the system consists of a mass M suspended on spring on a total stiffness k , and the mass represent the vibrating body with external excitation

4.2 Dynamic Behaviour of Vibro-Impact System

Vibro-impact systems dynamic behaviour has been studied through over the years via oscillator system's motion and its amplitude-frequency response when it collides with rigid body. Such an oscillator system consists of mass M placed at a distance delta from rigid body the dynamics of can portray single impact as illustrated in Figure 4.1 or multiple impacts per period.

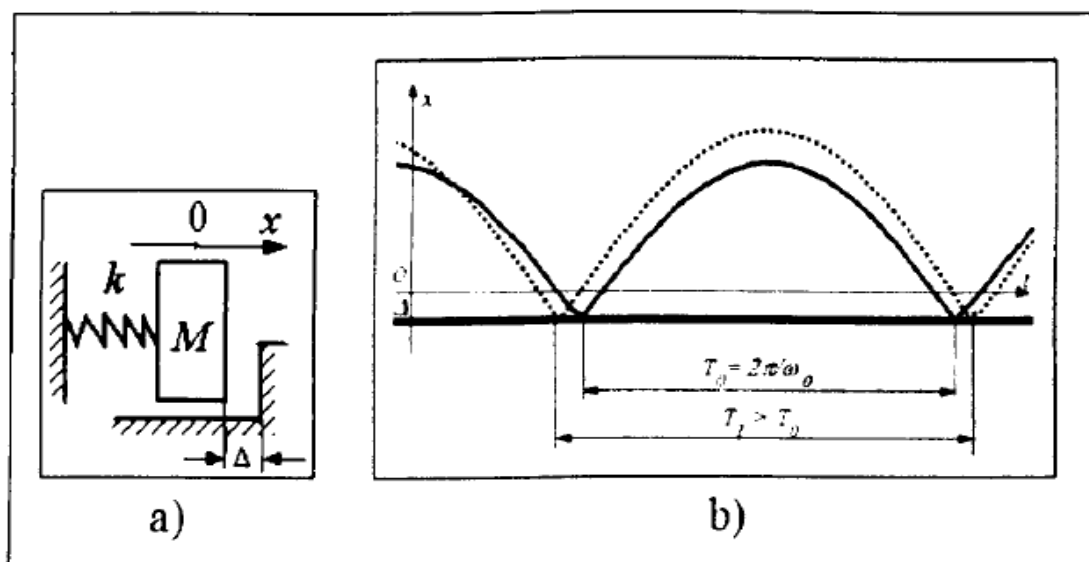


Figure 4.1: Oscillator with linear single Impact & Its motion with time (Babitsky, 1998).

Assuming the impact Collision of two bodies with mass m_1, m_2 and velocities \dot{x}_1, \dot{x}_2 ; ($\dot{x}_1 > \dot{x}_2$), and using the law of conservation of momentum the coefficient of restitution R can be given by the following equation, Babitsky et al, (1998):

$$R = \frac{\dot{x}_2 - \dot{x}_1}{\dot{x}_{11} + \dot{x}_{22}} \quad 4.1$$

Where \dot{x}_1, \dot{x}_2 are velocities of bodies before a collision; $\dot{x}_{22}, \dot{x}_{11}$ are the velocities of bodies after collision. Babitsky et al (1998), investigated the evolution of collision by considering two bodies lumped with mass m and visco-elastic bumper mounted on a wall similar to Figure 4.1, Where the bumper (spring and dashpot with viscous damping c) is mounted in parallel to an accelerometer that is attached to the mass in order to record the acceleration during the collision. The equation of system motion is written for time τ , to obtain the duration of impact as follows Babitsky et al, (1998):

$$\tau = - \frac{1}{\Omega n \sqrt{1-2\xi^2}} \arctan \left(\frac{2\xi\sqrt{1-\xi^2}}{1-2\xi} \right) \quad 4.2$$

Where, $\xi = \frac{c}{2m\Omega n}$ is the damping loss factor; and Ωn is the natural frequency of the system.

This means that the impact duration depends on system natural frequency and the damping loss factor. Therefore, the max impact force (peak acceleration) during the evolution at a time τ_1 is derived as follows Babitsky et al, (1998):

$$\tau_1 = - \frac{1}{\Omega n \sqrt{1-2\xi^2}} \arctan \left(- \frac{(4\xi - 1)\sqrt{1-\xi^2}}{\xi(3-4\xi^2)} \right) \quad 4.3$$

Substituting the velocity, the peak acceleration, the duration of the impact and the velocity at the end of impact in the equation of the impact duration, the equation of coefficient of restitution can be derived as follows Babitsky et al, (1998):

$$R = \frac{x(\tau)}{v} = \exp \left[- \frac{1}{\sqrt{1-2\xi^2}} \arctan \left(- \frac{2\xi\sqrt{1-\xi^2}}{1-2\xi} \right) \right] \sin \left[\arctan \left(- \frac{2\xi\sqrt{1-\xi^2}}{1-2\xi} \right) \right] \quad 4.4$$

Where $x(\tau)$ is the velocity at the time of the separation, v is pre-impact velocity;

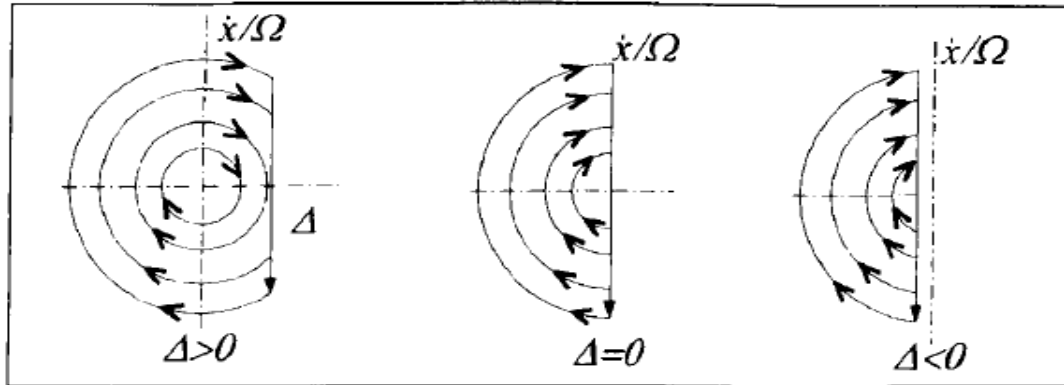


Figure 4.2: Dynamic of Vibratory System (Babitsky, 1998)

However, in Figure 4.2 above it has been noticed that a vibro-impact system can be set with negative, positive or zero clearance., the motion of the system interaction can be determined between a period of time T_1 and T_0 , where, ($T_1 > T_0$) and $T_0 = 2\pi / \omega_0$.

However, the motion of the system can be characterised by its natural vibration where the system is assumed to be a conservative oscillator with elastic impact (coefficient of restitution $R = 1$).

For the system in Fig 4.2 a, at the instant when the system mass M collided with the stop body, at $x = \Delta$, and Δ is a positive value meaning that there is a gap between the system mass and the stop body, but also it can be a negative value if is initial interference.

4.3 Principle of Vibration-Assisted Machining Process

Figure 4.3: Explains the kinematic of 1 D Vibration assisted machining where the cutting tools moves in a parallel direction to the work-piece (Shamoto, 2004)

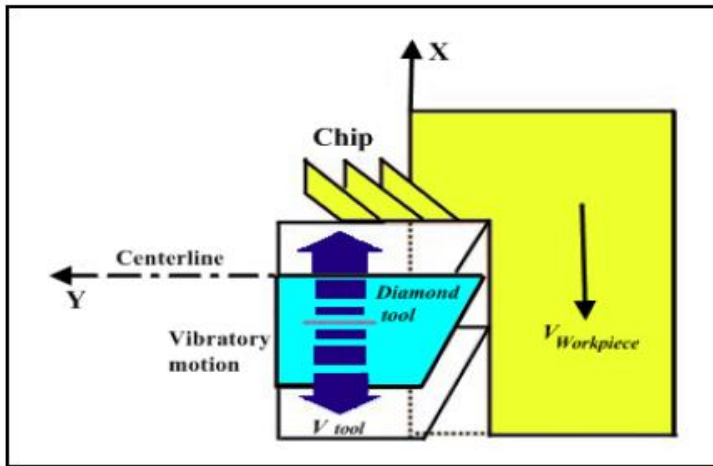


Figure 4.3: Vibration Assisted Machining (Shamoto, 2004)

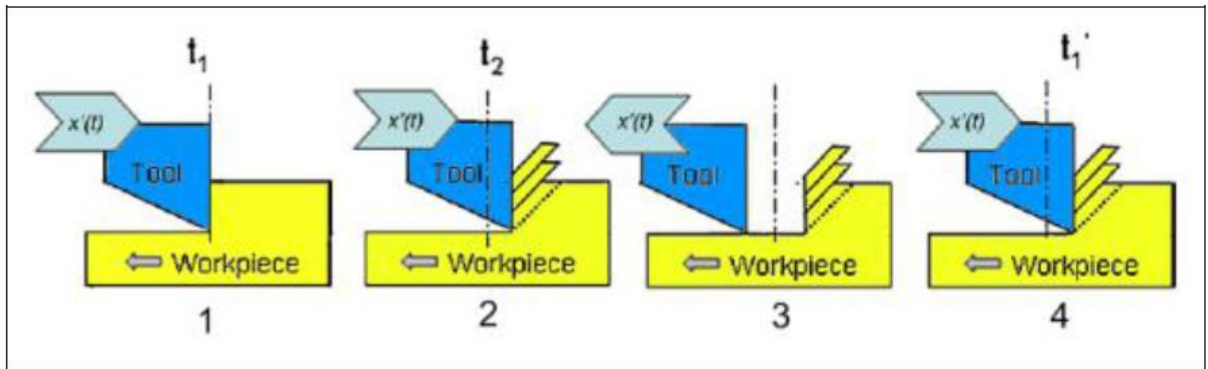


Figure 4.4: Vibration Assisted Machining (Dow, 2007)

Figure 4.4 illustrates the cutting tool linear movement of 1D Vibration assisted machining under certain vibration frequency and amplitude. Hence, the intermittent contact mechanism between the tool and the work-piece is given by the sinusoidal equation of motion as shown in (4.5) & (4.6). Where the tool has been driven harmonically in a linear path parallel to the work-piece feed direction between points 1, 2, 3 and 4.

Equation (4.5) illustrate that the tool is in contact with the work-piece

$$x(t) = A \sin(\omega t) + Vt \quad 4.5$$

$$\dot{x}(t) = A \omega \cos(\omega t) + V \quad 4.6$$

Where; x and \dot{x} are the intermitted position and the velocity respectively, and A is the amplitude, ω is the vibration frequency and t is the time.

Hence, the tool cutting velocity in position 1 and 2 is positive vector towards the positive direction. That means the tool in contact with the work-piece at this moment. Whilst in position 3 and 4 the tool cutting velocity became negative and acted in the opposite direction for fraction of second due to the vibration frequency magnitude (tool separated from the work-piece).

In other words, intermittent cutting in vibration assisted machining creates a gap between the tool and the work-piece.

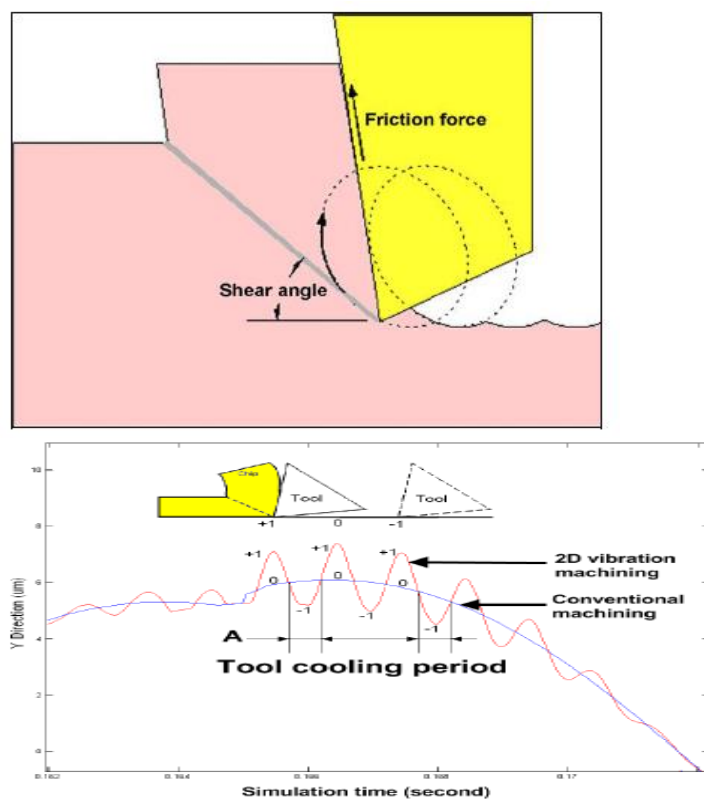


Figure 4.5: 2D Vibration Assisted Mechanism (Shamoto & Moriwaki, 2004)

Figure 4.3: Illustrates how vibration assisted machining reduces cutting force when employing low frequency as much as 6 Hz. Shamoto and Moriwaki [2004] explained in their experimental study how vibration assisted machining reduce cutting forces. They claimed that the reduction in force came at a zero time when the tool has no cutting force partially or completely, this because of the kinematic disengagement (tool separation) between the tool and the work-piece, as there was no contact or less contact between tool edge and the work piece at that particular moment. They also

claimed that this reduction in cutting force reached 40%, in comparison to cutting force in conventional machining.

However, the imposed vibration on the cutting tool had vibration frequency varies from zero Hz to 40 kHz and amplitude varies from 2 μm to 100 μm .

4.4 Designs of Vibration Assisted Machining

Tsiakoumis (2010) designed a system similar to produce periodic oscillation on the work-piece by employing piezo electric actuators. However, the imposed oscillation (vibration) was applied horizontally on the direction of the cutting force to enhance create slots lead to ease intermitted of the cooling system and reduces the temperature in the grinding zone as well.

Zhang et al, (2006) design a piezo-table including a piezo electric actuator for vibration assisted grinding of ceramics to investigate problem caused by wheel loading in rise temperature in the contact grinding zone. He also claimed that the grinding normal force reduced from 50 N to 25 N for a 30 μm depth of cut. Consequently, this reduction in normal grinding force improved surface integrity and reduced subsurface damage to ceramic materials (increase in normal grinding force may initiate and propagate cracks), (Zhang & Meng, 2003).

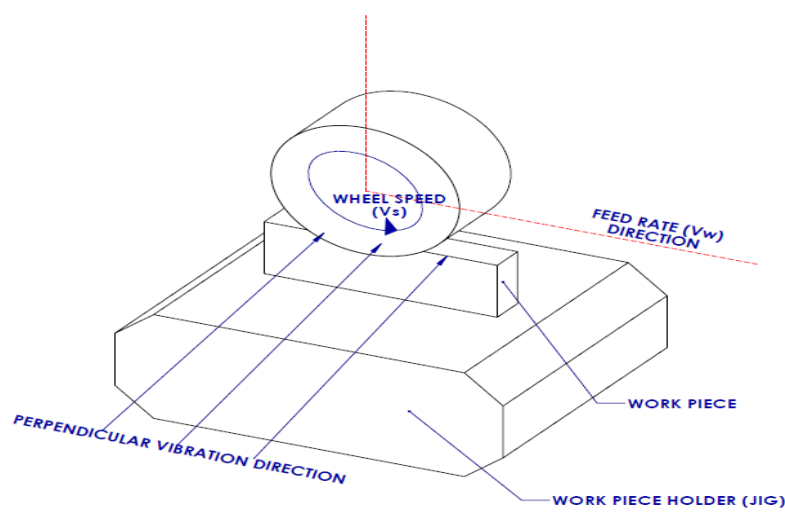
A system designed by Zhang and Yang (2004) to produce a micro-vibration oscillation to the workpiece in the vertical and horizontal directions with the enhancement of three piezoelectric actuators acting vertically and one piezoelectric actuator acting in the horizontal direction. All of these piezoelectric actuators were fixed to a sample plate and moving platform under the influence of linear motion guides to enable them to vibrate easily.

The system achieved improvement in surface finish and surface roughness in feed rate direction by about 33% to 48% in comparison to the conventional grinding system without vibration.

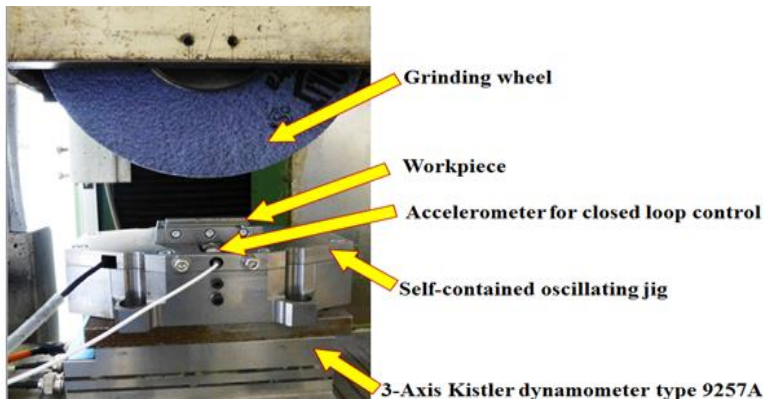
Wang et al, (1996) also claimed that the implementation of higher frequency micro-actuation system in grinding process of ceramic materials in a cross feed direction of the grinding process led to surface roughness improvement in that direction.

4.5 New Approach (perpendicular direction)

Previous and current studies were focused on vibration applied in the direction of grinding (tangential force cutting direction) while this study investigated the possibility of vibration imposed in the axial direction of grinding wheel (perpendicular) which has not been done before. A system was allowed to vibrates the work-piece in a direction that perpendicular to the grinding direction via moving platform (work-piece holder) fixed to the piezo electric-actuator, where a 100 Hz vibration frequency been applied to the system in the perpendicular direction after a calibration proved that this frequency is suitable to match specific voltage that secure less power consumption (4Volts) and at the same time 100Hz frequency was applied to avoid resonance.



a)



b)

Figure 4.6: Picture of the Oscillating Jig, a- Model, b- actual oscillating jig

4.6 Chip Formation in Vibration Assisted Mode

Figure 4.7 demonstrates the grinding process performance in both cases conventional and vibration assisted mode. By considering that the grinding wheel motion path could be represented by a single grit motion path throughout the work-piece material surface, the outcome could be illustrated clearly in the type of motion pattern which could be obtained in conventional grinding (straight line) but in vibration assisted grinding its path is a sinewave. However, it has also been noticed here that the vibration has been applied to the work-piece in the axial direction (perpendicular) to the feed rate, axial to the spindle direction, this allows to generate a sine wave motion over the contact length as shown in Figure 4.7, where the grit performs in an oscillatory motion while the work-piece moves.

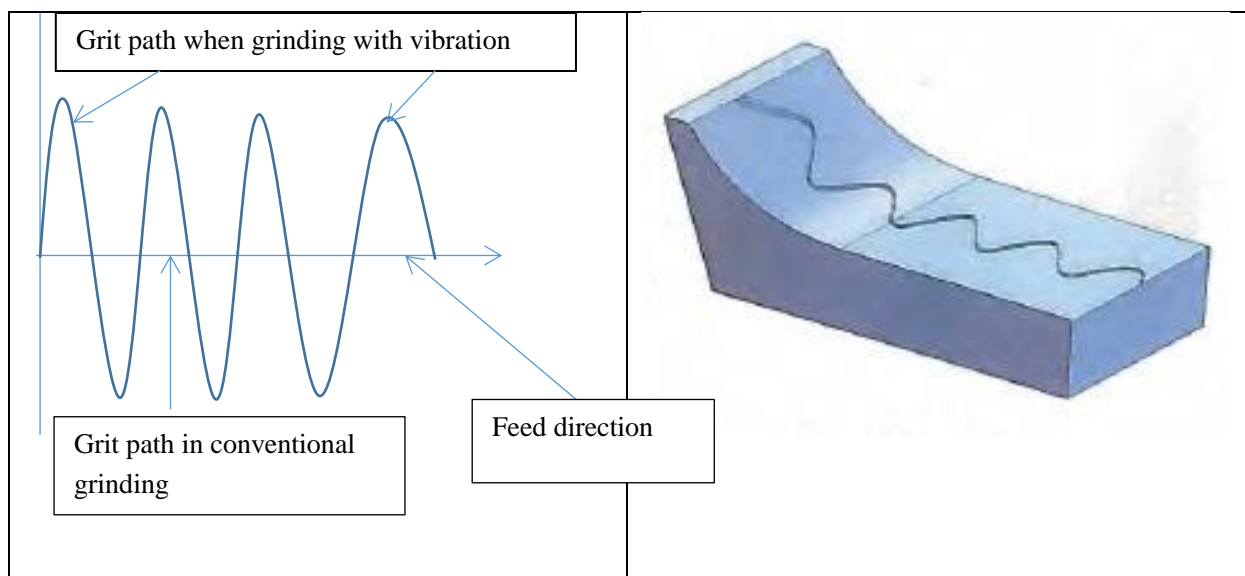


Figure 4.7: Schematic Drawing of Grit Motion in both cases/ when grinding with vibration assisted and without vibration assisted (conventional), Ewad, 2013)

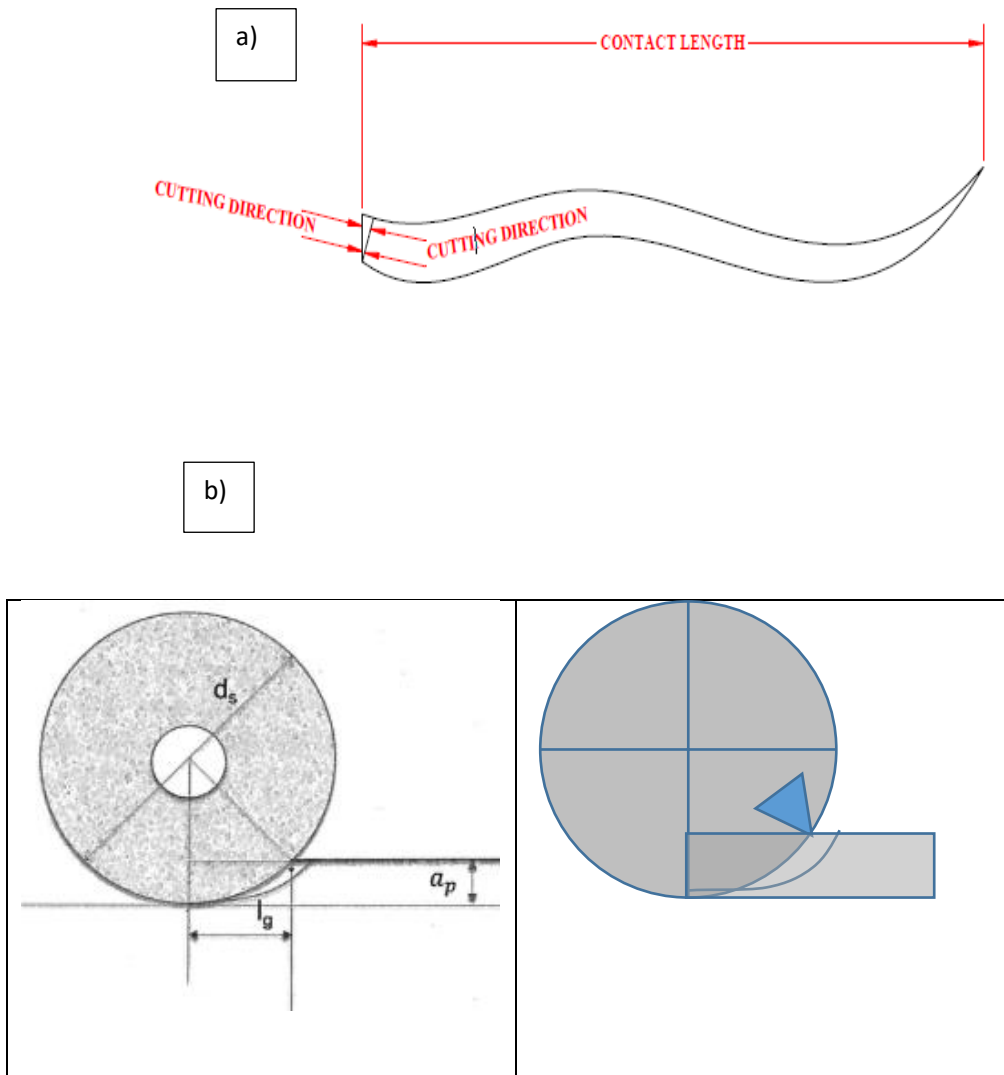


Figure 4.8: Schematic Drawing of Chip formation for single grain cutting; a –vibration assisted Mode, b- Conventional Mode (without vibration assisted)

4.7 How did Vibration Assisted Reduce Cutting Forces?

Considering the sketch in Figure 4.8-b where a single grit grain of a grinding wheel and a work-piece were in contact to produce a single chip as a result of constant material removal rate. Hence, varies cross sectional areas were considered in both cases vibration assisted grinding and conventional grinding for two separated trials.

The following assumptions were taken into account to find out how vibration assisted grinding reduces cutting force:

- ❑ The frequency, the amplitude and the grinding time in vibration assisted grinding) considered to be constant (100Hz, with amplitude of 130um)
- ❑ The grinding wheel speed V_s (17m/s (1300 rpm), table speed V_w (250mm/s) and the depth of cut a_p (20 um) also chosen to be constant during the two trials
- ❑ The cross section area of a single chip removed due to a single grit grinding force on each individual abrasive cutting edge considered to be not similar in both cases conventional grinding and vibration assisted grinding
- ❑ The length of the chip formed will be longer in vibration assisted grinding mode than in the conventional grinding mode because of the sine wave path that chip follows due to the imposed oscillation upon the work-piece. However, longer chip means bigger volume (more material removal)
- ❑ The volume of the chip moved is a function of cross section area of the chip and it's length (Chip length $l_{chip} > l_g$ grinding contact length):
- ❑ Thus, if a constant volume of chip material removal is considered due to that the chip length can be approximately equal to the grinding zone contact length (l_c) in both cases conventional grinding and vibration assisted grinding
- ❑ Since the chip cross section area is considered to be not constant and the length of the chip is assumed to be longer in vibration assisted grinding mode $\{A_m = \frac{Vc}{lc} = \frac{h_{eq}}{\lambda lc}\}$. Hence, F_t is a function of A_m ($F_t \propto A_m : F_t = K_c A_m$).
- ❑ Where, A_m , F_t is the cutting force of single grit, A_m is the average chip cross section area, K_0 is a constant depending on materials and grit shape, Vc is Average chip volume is and h_{eq} is the equivalent chip thickness. Hence, F_t which it supposed to varies reverse proportional to the chip length. By other meaning longer chip will lead to smaller cross sectional area (narrow chip or smaller chip thickness) thus low tangential force and low specific energy ($e_c = kc = K_0 (l_c \lambda)^\eta h_{eq}^{-\eta}$
Where K_c , K_0 and η are constant.
- ❑ The assumptions & the equations here below from (4.5) to (11) support the theory of a single grit model that illustrates how the tangential cutting force could be reduced if vibration assisted grinding is imposed (See SEM images of chips formation on Figures (4.10, 4.11 & appendices A).

The grinding force is considered as the sum of the grinding forces on each individual abrasive cutting edge

The single grit grinding for model established from experiments can be expressed as:

$$F_t = K_c A_m \quad 4.7$$

$$K_c = K_0 A_m^{-\eta} \quad 4.8$$

Where F_t is the cutting force of single grit, A_m is the average chip cross section area, K_0 is a constant depending on materials and grit shape.

The total grinding cutting force is the sum of the cutting force of individual grain engaged in grinding.

$$F_t = bl_c \lambda f_t = bl_c \lambda K_c A_m = K_0 bl_c \lambda A_m^{1-\eta} \quad 4.9$$

Where F_t is tangential grinding force, b is grinding width, λ is cutting edge density, η is a constant.

For simplification, the chip length can be approximately equal to the grinding zone contact length l_c .

$$l_g^2 + \left(\frac{d_s}{2} - a_p\right)^2 = \left(\frac{d_s}{2}\right)^2 \quad 4.10$$

$$\left(\frac{d_s}{2}\right)^2 - \left(\frac{d_s}{2} - a_p\right)^2 = \sqrt{\left(\frac{d_s}{2}\right)^2 - \left(\frac{d_s}{2} - a_p\right)^2} \quad 4.11$$

Where l_g is geometrical contact length, d_s is wheel diameter, a_p is grinding depth of cut.

Hence, considering figure (4.11) where a single grit grinding situation was studied the following equations were derived:

$$l_g^2 - d_s a_p + a_p^2 = 0$$

$$\text{Since } d_s \gg a_p, \text{ thus } l_g = \sqrt{d_s a_p} \quad 4.12$$

However, the grinding speed V_s is much higher than the work speed V_w , the grinding contact length l_c could be considered equal to the geometrical contact length l_g . Average chip volume $V_c = A_m l_c$ should be equal to the material removal in a unit time divided by the number of grains engaged in the unit grinding time, i.e.

$$V_c = \frac{a_p v w b}{\lambda v s b} = \frac{a_p v w}{\lambda v s} = \frac{h_{eq}}{\lambda}$$

$$\text{Where } h_{eq} = \frac{a_p v w}{v s} \quad 4.13$$

Represents the grinding equivalent chip thickness.

Therefore, the average chip cross section area can be expressed as:

$$A_m = \frac{V_c}{l_c} = \frac{h_{eq}}{\lambda l_c} = \frac{h_{eq}}{\lambda \sqrt{d_e a_p}} \quad 4.14$$

Where the material removal chip volume $V_c = A_m l_c$ (F_t is a function of A_m). However, from the expressions in equation (4.14), if the material removal of a chip volume is constant for a non-constant chip cross section area then the grinding contact length should be longer, due to the fact that a the chip length increases because of the vibration effect, which allows to generate a sine wave grinding pattern. Furthermore, since the cross section area A_m is not constant and at the same time it varies inverse proportional with the tangential cutting force F_t , where the contact length l_c increases. Thus, the grinding force is the only parameter that could became smaller to keep the chip cross sectional area varied with the value of the contact length l_c .

This finding led to the outcome which proved that vibration assisted grinding reduces grinding cutting forces and specific grinding energy as well.

The reason why vibration assisted reduced cutting forces is due to the small chips that are formed by the cutting tool which moves with lower average force for larger distance in repetitive passes to remove the same volumetric amount of material that could be moved in conventional grinding in the same period of time, this can be explain as follows:

Average chip volume $V_c = A_m l_c$ should be equal to the material removal in a unit time divided by the number of grains engaged in the unit grinding time (volumetric chip removal V_c is constant) i.e:

$$A_m = \frac{V_c}{l_c} = \left\{ \frac{h_{eq}}{\lambda l_c} \right\}. \text{ Hence, } F_t \text{ is a function of } A_m (F_t \propto A_m : F_t \propto K_c A_m).$$

That means the only other parameter that could be changeable or variable in this equation is the tangential cutting force F_t which it supposed to varies reverse proportional to the chip length.

Therefore $F_t = K_c \frac{V_c}{l_c}$. Where the volumetric chip removal V_c is constant;

Thus $F_t = K_c \frac{\text{Constant}}{l_c}$ Where K_c is also constant

The calculations and the drawing in figure (4.8) give an illustration of the novel hypothesis of how vibration assisted grinding reduce cutting force.

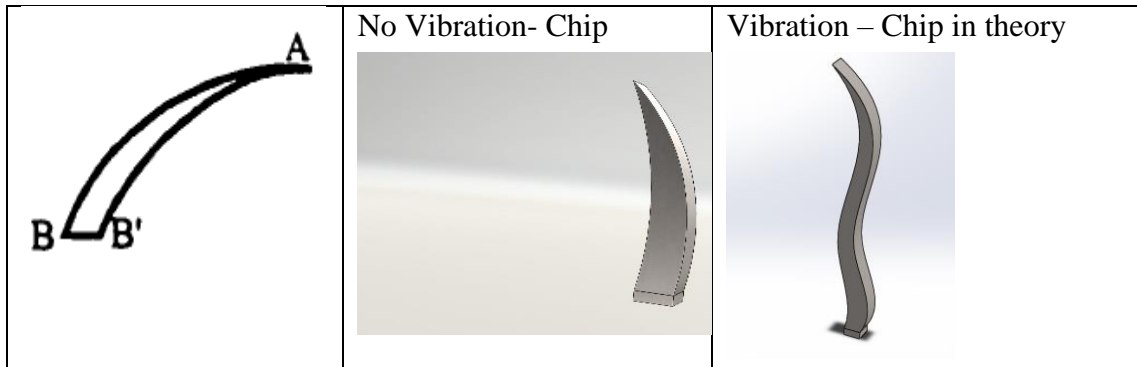


Figure 4.9: Chip formation

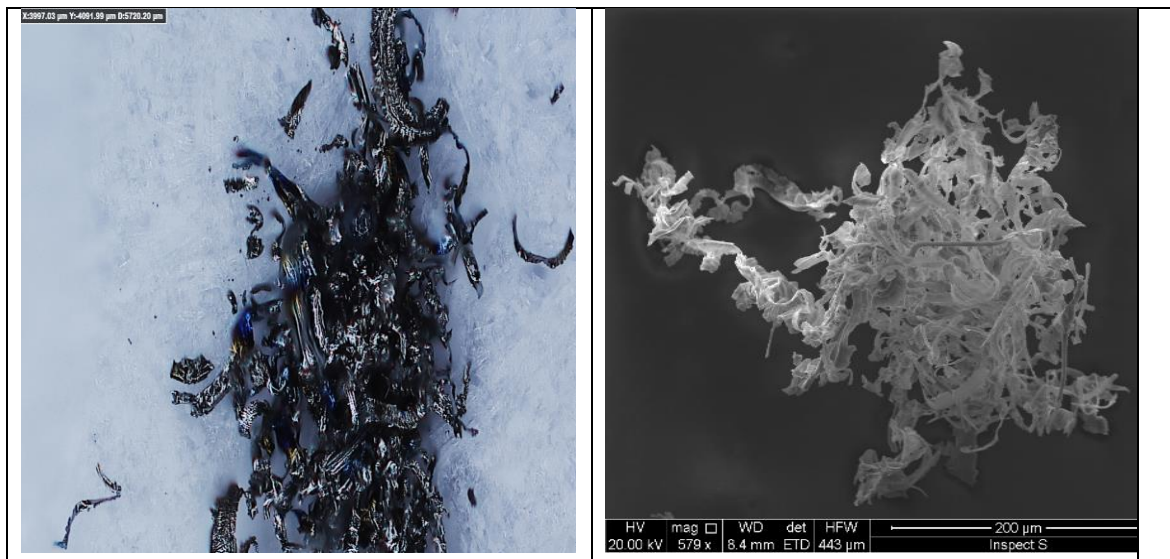


Figure 4.10: Chip formation with vibration assisted grinding (SEM Images)/ 200 μm scale at 100x- resolution



Figure 4.11: Chip formation without vibration assisted grinding (SEM Images)/ 200 μm scale, at 100x- resolution

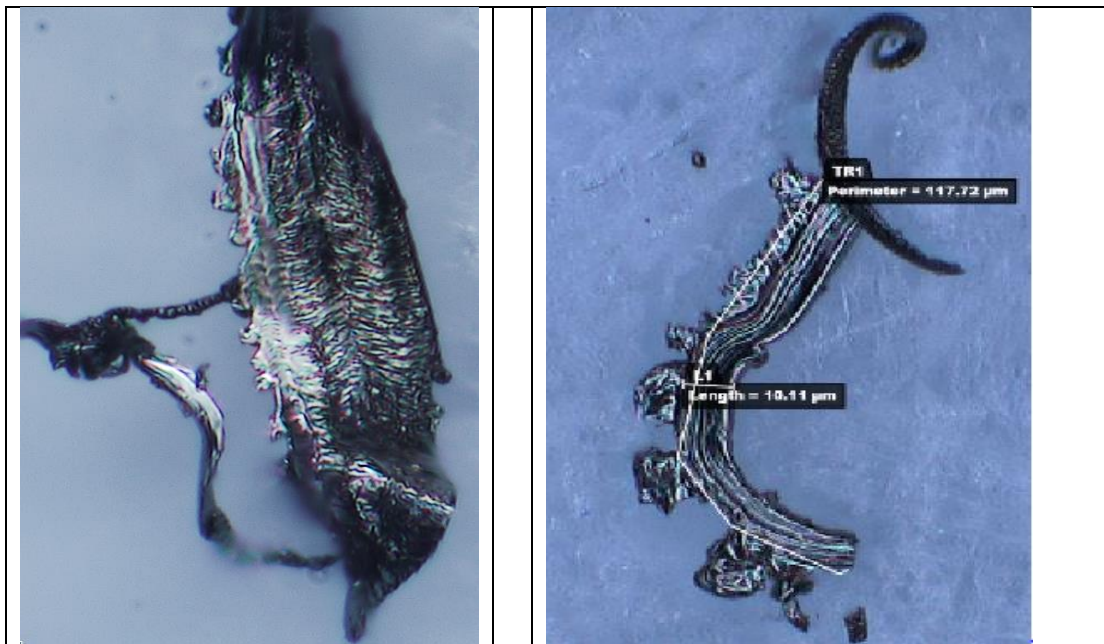


Figure 4.12: Chip formation without vibration assisted grinding (Measurements)

Figure 4.10 shows a picture of chip formation been taken by SEM. However, the chip has been formed and measured after applying vibration assisted grinding. It has been noticed clearly that the chip is taller and thinner and because the chip is so thine and tiny, there was chip segmentation involve as well.

Figures 4.11 and 4.12. Represent an (SEM) pictures for chip formation that been collected and measured in conventional grinding process, the pictures show that the chip is bigger in shape and thickness and also taller than the chip dimensions that have measured in the vibration assisted grinding mode for the same scale and resolution.

	Length (µm)	Perimeter (µm)
Min	10.11	
Max	10.11	
Range	0.00	
Average	10.11	
Total	10.11	
Deviation	0.00	
Count	1	

Name	Item	Result
L1	Length	10.11 µm
TR1	Perimeter	117.72 µm

Table 4.1: SEM Chip length and thickness results/ at scale of 200 µm and 100x resolution

Keynotes:

Table 4.1 shows chip formation that been collected and measured under (SEM) when grinding without vibration assisted, the maximum length found = 10.11 µm, and the maximum perimeter is = 117.72 µm.

However, average chip volume $V_c = A_m l_c$ should be equal to the material removal in a unit time divided by the number of grains engaged in the unit grinding time (volumetric chip removal V_c is constant) i.e:

$$A_m = \frac{V_c}{l_c} = \left\{ \frac{h_{eq}}{\lambda l_c} \right\}. \text{ Hence, } F_t \text{ is a function of } A_m (F_t \propto A_m : F_t = K_c A_m).$$

That means the only other parameter that could be changeable or variable in this equation is the tangential cutting force F_t which it supposed to varies reverse proportional to the chip length.

Therefore $F_t \propto K_c \frac{V_c}{l_c}$. Where the volumetric chip removal V_c is constant;

$$\text{Thus } F_t = K_c \frac{\text{Constant}}{l_c} \quad \text{Where } K_c \text{ is also constant}$$

Then and only then, if the chip length L_c become longer (vibration mode), F_t the tangential force will become smaller that means low force. In the other hand, if the chip length ‘ L_c ’ became smaller in conventional grinding, the tangential force F_t

became bigger. Therefore vibration assisted application reduces force because of the thinner and longer catted chip in vibratory grinding.

4.8 Summary

In this chapter a theoretical concepts from previous study have been demonstrated to explain the kinematics of vibration assisted grinding. Meanwhile, through over the years force vibration system has been defined by a single impact system that could be represented by a single degree of freedom model. Very limited models have been designed in the past to obey the kinematics of vibration assisted machining technique where the imposed oscillations under certain frequency and amplitude, creates an intermittent contact mechanism between the tool and the work-piece. However, few models have been designed in the past to produce oscillation on the workpiece by employing piezo electric actuators horizontally on the grinding direction to secure very small displacement to the workpiece in the range of 2 μm to 100 μm . Through these models an improvement in surface roughness was observed and also cutting forces reduction was also noticed.

All previous and current studies were focused on vibration applied in the direction of grinding to create slots lead to ease the cooling system, while this study investigated the possibility of vibration imposed in the axial direction of the grinding wheel (perpendicular) which has not been done before. This new system allowed to vibrate the workpiece in a direction that perpendicular to the grinding direction by employing a piezo electric- actuator, where 100 Hz vibration frequency was applied to the system to secure 130 μm displacement and to match low excitation of (4volts) to secure lower power consumption.

Mathematical formulations & calculations and SEM measurements for chip formation proved that the cutting forces were reduced practically and scientifically when vibration assisted grinding applied using the new developed system approach.

CHAPTER-5

**EQUIPMENT & PRELIMINARY
EXPERIMENT**

5. EQUIPMENT & PRELIMINARY EXPERIMENT

5.1 Introduction

In order to carry out experimental trials, several equipment have been used. These equipment have been also used to facilitate the data acquisition system to transfer the experiment output data to the PC. In this context LabVIEW software has been used for monitoring and controlling of these devices. Then experimental set-up was tested to make sure that the equipment is assembled accurately in order to meet machining system requirements. In this chapter the features and description of this equipment are given in three subcategories such as; grinding machine, external sensors and devices, and the consumable products.

5.2 Grinding Machine (ABWOOD 5025)

The experimental work was carried out on the Abwood 5025 grinding machine, which is a conventional surface grinder with pneumatic controls for the automatic traverse cycles. It has a 1.5Kw motor for the wheel head ensuring rapid stock removal..



Machine Specification

Spindle motor power	1.5KW
Spindle speed	5000 RPM
▪Cross traverse of head	260 mm
▪Resolution	10 μ m
▪Longitudinal traverse	530 mm
▪Resolution	10 μ m
▪Vertical traverse of head	350 mm
▪Resolution	1 μ m
Automatic feed	Pneumatic control x, y, Z Axis
Maximum wheel size	400mm*25mm

Figure 5.1: Equipment – ABWOOD 5025 machine.

5.3 Grinding wheel

For the experimental study An aluminum oxide grinding wheel was employed with following specifications as follows:

Vitrified bonds (Al_2O_3 (OVU33 A602HH 10VB), 50% porosity- high aspect ratio in the range of 10:1. Its diameter was 208 mm and the maximum operating speed could reach 66 m/s (more details about wheel specifictaion found in (section 3.4.).



Figure 5.2: Grinding Wheel

5.4 Workpiece materials

In this study two types of advance aerospace materials work-pieces were used, namely: Titanium alloy (Ti-6Al-4V) and Nickel alloy (Inconel 718). The first one is brittle and the second one is ductile which is difficult to machine. Hence, hardness for all samples was measured and presented in Table 5.1.

5.5 Data Acquisition System (DAQ)

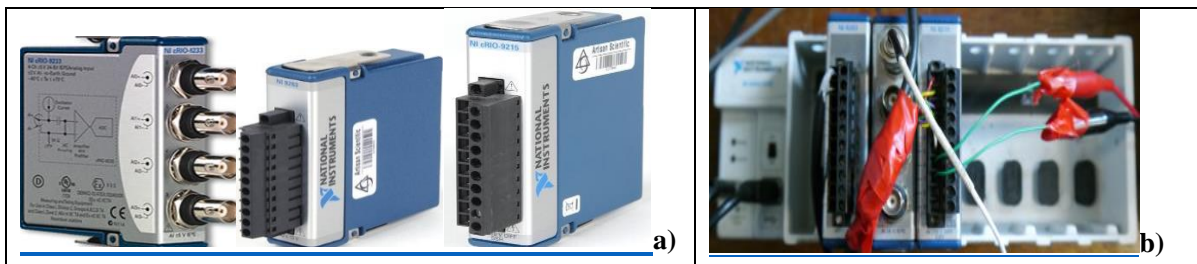


Figure 5.3: DAQ system; a): input- NI 9215, NI 9233 and output – NI9263; b) configured in chassis

The purpose of data acquisition was to to measure an electrical signals such as voltage generated by the sensors. The PC-based data acquisition uses a combination of

modular hardware, application software, and computer to take measurements. While each data acquisition system is defined by its application requirements, every system shares a common goal of acquiring, analyzing, and presenting information. Data acquisition systems incorporate signals, sensors, actuators, signal conditioning, data acquisition devices, and application software.

During this experiment DAQ was used to record the acquired data from the dynamometer, displacement sensor and accelerometer and a filter was used to reduce noise. In addition to that, the NI-9267 data acquisition card had 8 analogue inputs channels. With the combination of DAQ and Lab View 8.5 software package the hardware was controlled, where the required signals were recorded such as: displacement, acceleration normal and tangential forces. The original signal was saved and posted into an excel file to be analysed.

5.6 Piezoelectric Actuator

This device can produce a small displacement at high frequencies with a high force when an alternated voltage is applied to it. The piezo-elements (ceramic discs) inside, can produce oscillations by their expansion and contraction depending on the applied voltage. The actuator was driven by a power amplifier, which amplifies a small sinusoidal input signal from a function generator. The piezoelectric actuator employed for the present study was a high performance P212.8 suitable for static and dynamic applications. It could produce up to 2,000 N peak force with a 120 μm maximum displacement.

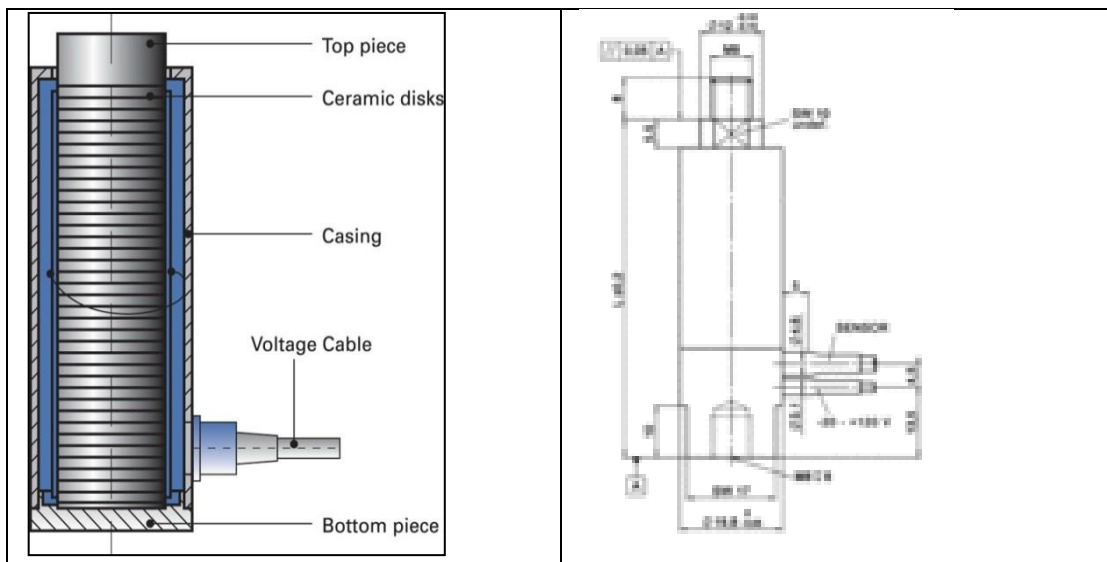


Figure 5.4: Piezoelectric Actuator

5.7 Power Amplifier

The E-472.2 series high power amplifier is a device which is used regularly in the industry to enlarge the signal wave and the E 472.2 was employed in this study specially to drive high capacitance PZT actuators. The output voltage range of the device varied between -3 and 1100 Volts. The DC current has been added by the offset potentiometer to the input, to assure continuous input supply in the range of -10 V to 0V and from 0V to +10V Consequently a close loop system could be designed to generate specific displacement between zero and the design required set point depending on the piezo-actuator.

5.8 Dynamometer

Grinding forces were measured with a 3-axis Kistler dynamometer type 9257A. It allows measurement up to 5000 N in X, Y, and Z coordinates. It has a resolution of <0.01% of full scale great rigidity, high natural frequency and insensitivity to temperature influences.

In order, to assure the experimental accuracy, this device is calibrated before any experiment.



Figure 5.5: 3-axis Kistler 9257A dynamometer & Kistler charge amplifier type 5073

5.9 Accelerometer:

An accelerometer was used in this study to measure acceleration, via Q NI 9233 with four channel Data signal acquisition mounted into DAQ 9172 chassis as illustrated in Figure 5.6.



Figure 5.6: Function Generators

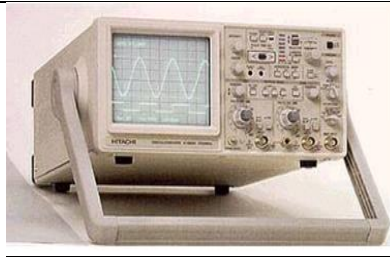


Figure 5.7: Oscilloscope

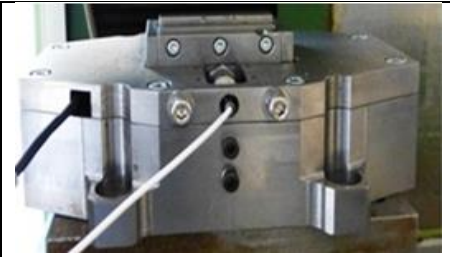


Figure 5.8: Workpiece Jig (Self Containing Vibration System)

5.10 Preliminary Experiment

5.10.1 Material Characterization

Hardness is the property of a material that enables it to resist deformation, usually by penetration. However, the term hardness may also refer to resistance bending, scratching, abrasion or cutting. (www.gordonengland.co.uk/hardness/rockwell.htm).

The hardness tests for the materials under investigation show that their hardness differs slightly depending on the direction of testing. However, only two directions were tested, because the grinding test will be carried in those directions. These tests were repeated including micro-hardness to investigate the effect of grinding and grain flow after grinding. Initial hardness testing was carried out on three types of materials involved in this study, namely Nickel alloy (Inconel 718), High-grade titanium (Ti Al) and Ti6Al4V. This was followed by a chemical element content analysis undertaken on the scanning electron microscope with X-Ray setup.

Material	Average Rockwell C hardness	
	X-direction	Y-direction
Inconel 718	40.3 N	37.3N
Ti 1 (High-grade (TiAl))	30.7N	31.3N
Ti2 (Ti 6Al-4V)	28.6N	25.3N

Table 5.1: Materials Rockwell hardness Tests Results.

Test No	X-direction	Y-direction	
1	40	35	
2	40	38	
3	41	39	
Total	121	112	
Average	40.3	37.3	

Table 5.2: Nickel Alloy (Inconel 718) Rockwell C Hardness (N)

Table 5.1 gives the hardness response of the three materials use in this study, whereas table 5.2 provides a typical hardness profile of Inconel 718, measured in newton (N).

The average hardness according to Rockwell C scale is around 31 for High-grade Ti1, and 40 for Nickel based alloy. Comparing those results and the results of mass spectrometry, investigated materials were defined as Ti-6Al-4V alloy, which is a commonly used alloy in gas turbines, a common aerospace alloy Inconel 718, and high-grade TiAl, which is used for jet engine components.

This helped in searching for information about the best practice of machining these materials. These materials were identified via Scanning Electron Microscope as Nickel alloy Inconel 718, high-grade (TiAl) and Titanium Aluminide Ti-6Al-4V. However,(www.matweb.com accessed 14,15,16,27 June 2014).

However, in order to define the alloys which will be examined in the further analysis, mass spectrometry analysis was carried out on the machined surface of the material in the LJMU laboratory. The obtained images (results) of the mass spectrometry test are in appendices A-5a, A-5b and A5-c.

5.11 Experiment Setup Configuration

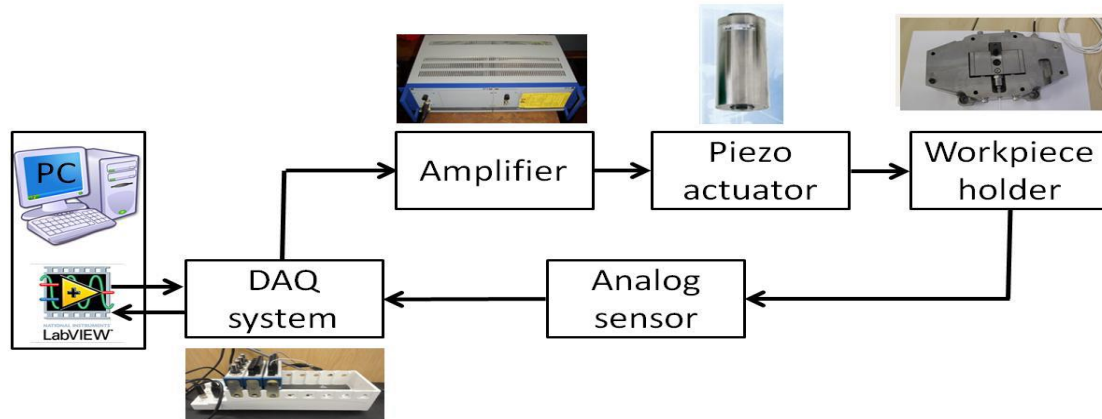


Figure 5.9: Closed loop Control System

Figure 5.9 shows the actual arrangement of the devices during the experimental work. However, during the experiment the frequency and the amplitude of the vibration were specified in the closed-loop system, which determined the performance of the piezoelectric actuator using the signal from the accelerometer. Also all the data signals that been sent out from the accelerometer via a Kistler dynamometer were recorded through the data acquisition system using Labview software, and were stored on a PC for analysis.

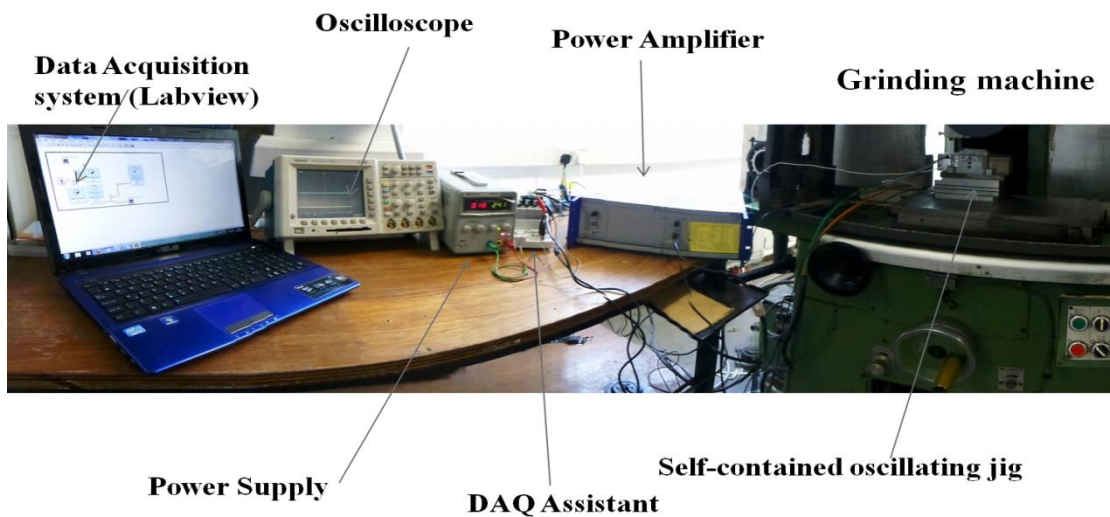


Figure 5.10: Actual Configuration for the Experimental Work (Ewad, 2013)

The experimental setup included a piezo- electric- actuator, power amplifier, an accelerometer and a dynamic signal analyser coupled to a computer through a DAQ system. As shown in figure (5.11) Labview is used to drive the oscillating jig and record the output data in real time during the experiment.

5.12 LABVIEW (VI_s) Software

A vibration control system has been set up in AMTREL. The Labview soft framework is shown in Figure 5.11.

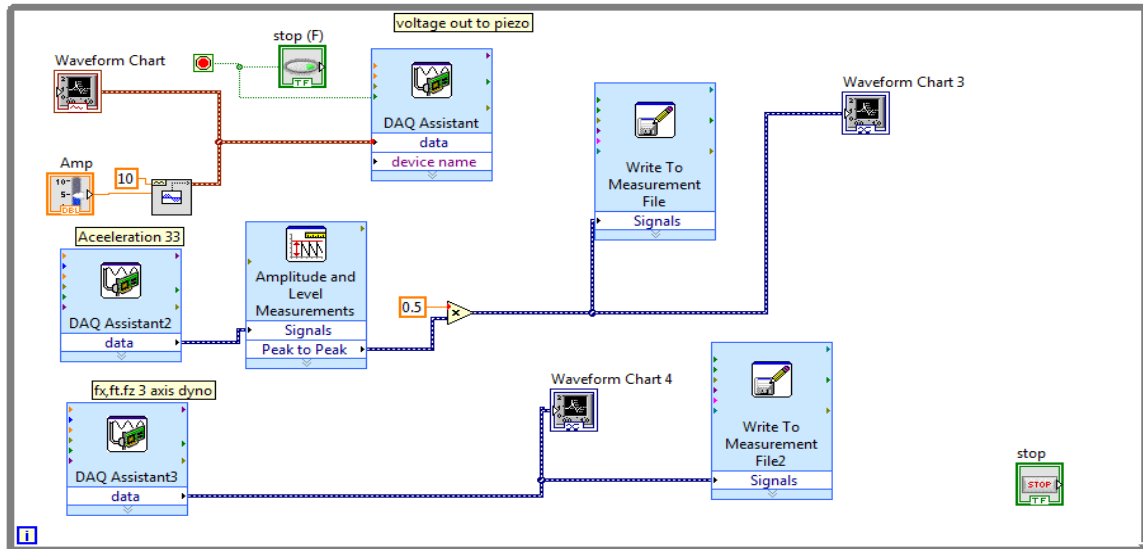


Figure 5.11: LabVIEW Data Acquisition Software –Block Diagram (Ewad, 2013)

5.13 Dynamometer Calibration

In order to assure the accuracy of the experiment all the devices involved should be checked before the start of the trial, or calibrated from time to time to reduce the chances of errors. In this particular case the dynamometer was calibrated, as an initial experiment to pave the way for the grinding trial. So the calibration was conducted employing different loads from 1kg (10N) up to 20kg (200N).

However, the calibration arrangement for the different components, started from DAQ system connected to a PC containing LabVIEW package software, charge Amplifier, Magnetic chunk placed on a measurement table to hold the dynamometer, a Roller Bearing connected to a Mounted pulley and random weights. In addition to that, this arrangement was set to measure axial, normal and tangential forces. The charge Amplifier was set with respective sensitivity of 8.015 pc/N for 100 units per volt for the tangential force (Ft). While for the normal force (Fn) the sensitivity of the amplifier was set at 3.755 pc/N for every 100 units per volt, a similar procedure was applied for the force in axial direction (Fx). The calibration data were captured and

analysed for all the three direction to represent the three forces where a linear approximation supported by equation for each case was derived including the process of converting voltage into force.

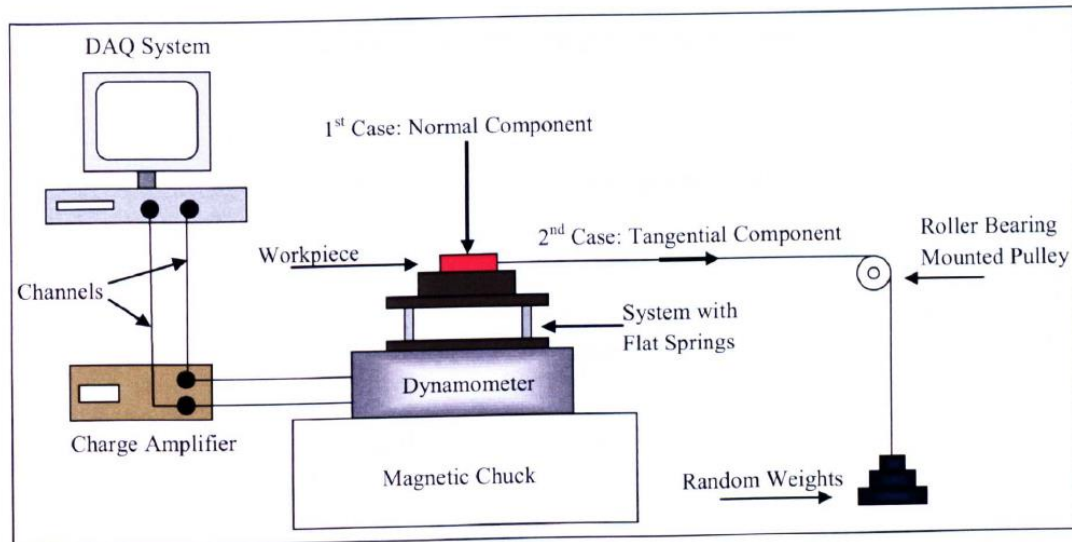


Figure 5.12: Dynamometer calibration process

The results can be seen in Figures (5.13, 5.14, 5.15) below which reflect the results of all three components. (F_x , F_t , F_n). However, the equation of the calibration curve was obtained from the experimental values, where x represents the load in Newton while y represents the output voltages in mill-volt (mV).

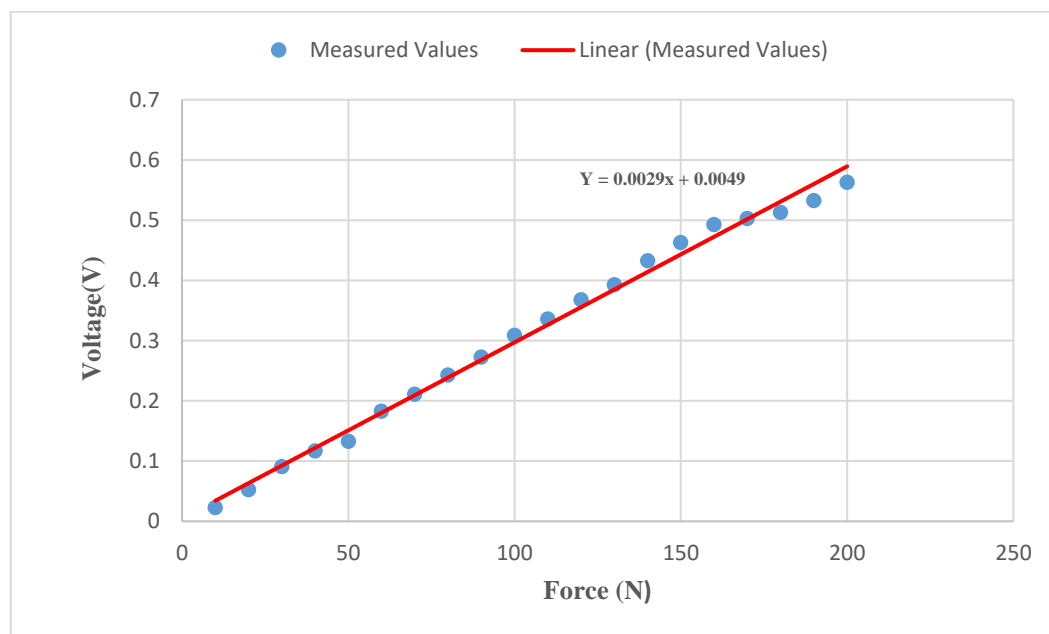


Figure 5.13: Normal Component of Force Calibration Results.

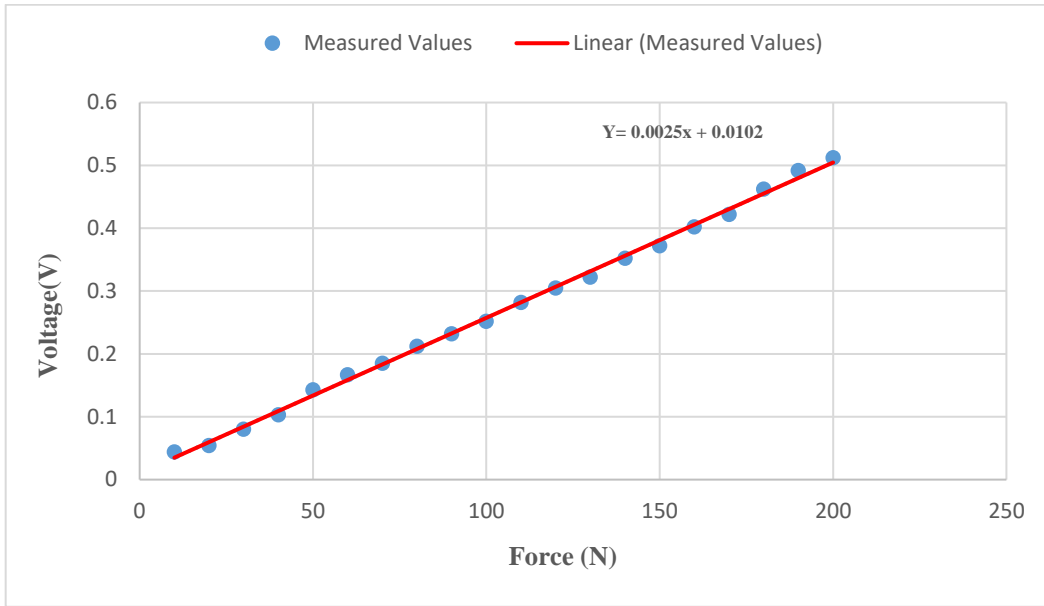


Figure 5.14: Tangential Component of Force Calibration Results.

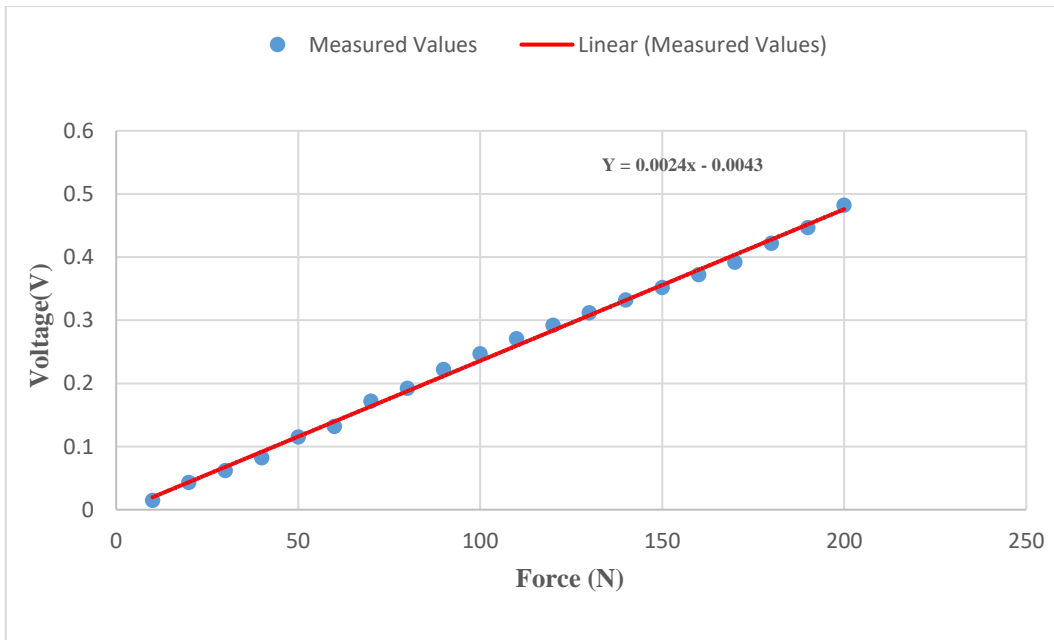


Figure 5.15: Axial Component of Force Calibration Results.

5.14 Amplitude-Frequency Response of the oscillating stage

There are many similar previous design hypothesis to this study enabled vibration assisted machining to gain advantageous upon the conventional machining. One of the main hypothesis to achieve that advantages is to secure work-piece displacement in the range of tens of micrometres. This displacement should be at specific frequency at specific excitation driving voltage. However, the power amplifier can take up 10 volts whilst providing up to 1000 volts to the piezo actuator. Via a calibration test the required displacement at low voltage could be secured. However, the suitable calibration includes a selection of a displacement sensor that could enhance to identify the optimum parameters configuration to achieve the target displacement. The calibration tests results are given in table (5.3) to secure a displacement of 130um, which was achieved when operating at a frequency of 100Hz at excitation voltage of 4 volts. However, there are many closer figures to the targeted displacement (130um) but the only disadvantage here is that these figures could be achieved at high frequency.i.e.150 Hz to 250Hz which is not desired choice. Furthermore, calibration shows that a combination of high excitation voltage and high frequency are not suitable for the oscillating stage and it might harm the equipment and the operator by generating noise.

Consequently, the system has been established upon the obtained displacement and frequency Figures (130um, 100Hz).

		Excitation Voltage									
		1	2	3	4	5	6	7	8	9	10
Frequencies, Hz		Actual Displacement, μm									
50 Hz		1	24	47	80	124	145	152	158	173	194
100Hz		5	48	87	130	174	220	246	261	269	276
150Hz		7	68	122	177	238	276	293	301	279	280
200Hz		6	99	172	259	252	247	243	241	242	241
250Hz		9	137	208	254	213	218	207	204	207	198

Table 5.3: Amplitude Calibration Results

Table 5.3 shows the amplitude calibration for couples of frequencies starting from 50 Hz up to 250Hz. Hence, the target is to identify a suitable excitation that match lower power consumption. The calibration tests results are given in table (5.3) to secure a displacement of 130um, which was achieved when operating at a frequency of 100Hz at excitation voltage of 4 volts. However, there are many closer figures to the targeted

displacement (130 μm) but the only disadvantage here is that these figures could be achieved

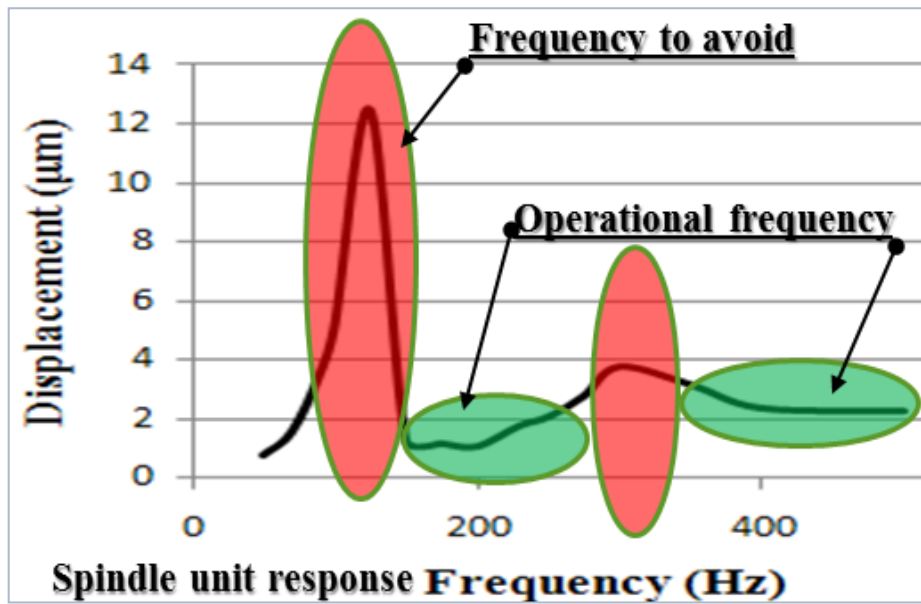


Figure 5.16: Displacement Versus Machine Spindle response frequency (Vios, 2011)

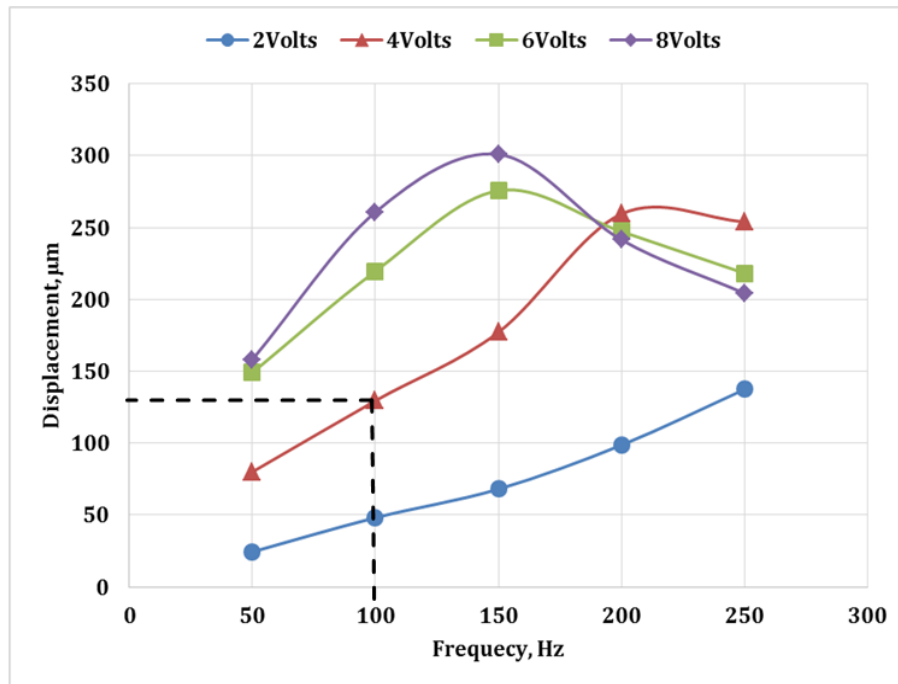


Figure 5.17: Obtained Displacement Versus the Imposed Vibration Frequency

5.15 Optimization of Vibration Assisted Grinding

In this chapter the prediction of aerospace materials machinability will be investigated in depth to determine the optimal values of the grinding process parameters. The well-known Taguchi method is used because this method allows to control the process parameters and production efficiency.

Various operating conditions in grinding process such as wheel speed, work-piece speed, depth of dressing and lead of dressing, area of contact, grinding fluid, are considered in optimal selection for grinding process.

However, in this study the optimization aim is to control four parameters:

1. The cutting forces
2. The material removal rate
3. The surface roughness of the work-piece
4. The grinding wheel wear.

These four parameters have to be controlled, because the selection of the process parameters is very important in terms of the impact that might affect the production, the product quality and costs. However, the quality and the costs are much related to surface roughness, cutting tool life, actual depth of cut, wheel speed, table speed, vibration frequency and displacement and material removal rate as well. Nevertheless, to achieve the optimization objectives, the Taguchi array method was used. The grinding trials were carried out repeatedly several times.

5.16 Taguchi Method

To determine the effect of each of the parameters tested a standard $L_{16} 2^8$ orthogonal array was modified to $L_4 2^3$ and used. This provides the most economical testing plan for evaluating the direct effects of eight parameters. According to Taguchi Grove & Davis1992, the plan may be checked for reliability by running confirmation trials based on the results collected. If the results from the confirmation trials agree with the expected results, then the experimental plan may be considered to be reliable.

Taguchi Design of experiments is a method that concern the process development and performance improvement with the aim to obtain optimum process while reducing effects of uncontrollable factors (noise)” Hence, designed experiments serve two purposes:

1. To determine the important parameters affecting a certain outcome.
2. To optimize the outcome by controlling such parameters.

Moreover, the Taguchi method is a robust method used to improve the quality of the

product and the process. However, depending on Taguchi methods an experimental work will be done with the following considerations:

- Define the problem or determine the objective of the experiment: in the case here studied, the objective is to obtain optimum vibration assisted grinding process for brittle advanced aerospace materials, mainly titanium aluminide, (Ti6Al4V) Titanium and Nickel alloy (Ni, Inconel 718).
- Select the design (Orthogonal Array) that best fits the experimental conditions.

5.17 Preliminary Experiment

This preliminary experiment was undertaken in order to investigate the relationship between the inputs and the outputs parameters of the process. However, the investigations include the experimental system configuration and the possibility of how to test the system configuration setup reliability, accuracy and precision. Then the performance of vibration assisted grinding can be investigated.

5.17.1 Experimental Procedure

This set of experimental work was conducted on the ABWOOD 5025 surface grinding machine in wet condition using Castrol Hysol coolant liquid and aluminium oxide (Al_2O_3) conventional grinding wheel was also used. Table 5.4 gives the overall parameters for the preliminary experimental work where the effect of vibration with different depths of cut during grinding was examined.

5.17.2 Aim and Objectives

The experiment aims to give understanding of the grinding parameters' effects on the work- piece surface roughness, amount of material removal and forces as follows:

1. Defining the grinding parameters such as, wheel speed (V_s), Table speed (V_w) and Depth of Cut (DOC).
2. Observing & measuring Applied grinding forces (The normal & tangential force F_n , F_t) surface roughness (R_a), actual depth of cut and material removal rate during grinding process.

5.17.3 Work-piece Materials Preparation

The materials used for the tests were Titanium aluminide and Inconel 718. These new materials are difficult-to-cut in conventional mode, thus required especial tools. In

preparation for this experimental work it was very obvious from the beginning how difficult it would be to cut these material as illustrated in Figure 5.18 where broken cutting tips and material fracture due to the brittle structure of the material. Hence it took few months to cut the material cost effectively.



Figure 5.18: Materials preparation equipment



Figure 5.19: Failed Cutting Tips and fractured grinding disk

Grinding Trials:

- 4 work-pieces material: TiAl, titanium aluminide alloy and nickel alloy (Inconel 718) were pre-machined and prepared for experiment.
- Workpieces dimensions:
 - 1- Ti6Al4V Alloy; 4 pieces : Length;60mm, Width;20mm, Hight; 7mm
 - 2- Nickel alloy (Inconel718); 4 pieces: Length; 70mm; W;13mm; Height; 7mm
- 4 experiment trials were conducted for each material sample to meet the Taguchi table requirements $\{L_4, (2^3)\}$.
- Table speed V_w was calibrated.
- The following grinding output parameters were measured: Cutting forces actual depth of cut (a_e),] surface roughness (R_a) and wheel speed was calculated.
- The effects of wheel speed and work-piece speed on surface roughness was also observed.
- Each experiment was run without vibration and with vibration in order to compare the obtained results.

- The experiments parameters are shown in Table 5.4.

Grinding parameters	Value			
Grinding Wheel Type	Al ₂ O ₃ (OVU33 A602HH 10VB)			
Wheel Diameter (mm)	208			
Wheel Width (mm)	20			
Wheel Speed, V _s (m/s)	20, max 35			
Work Speed, V _w (m/min)	7, 15 max			
Grinding Condition	Wet Condition (Coolant)			
Workpiece Material	Ti-6Al-4V			
Cut Type	Up -Grinding			
Depth of Dressing (10 μm)	Fine, Single Point Diamond 10			
Dressing Feed	Traverse			
Applied Depth of Cut (DOC, μm)	10	20	30	40
Vibration Frequency (Hz)	100			
Vibration Amplitude (μm)	130			

Table 5.4: Experimental Parameters- Effect of Depth of Cut

a)	Parameters	Level	
		1	2
A	Wheel Speed	20m/s	35m/s
B	DOC	10 μm	20 μm
A x C	Interaction	-	-
C	Work Speed	7m/min	15m/min
B x C	Interaction	-	-
D	Dressing (Fine)	10 μm	10 μm
E	Materials	Ti6Al ₁	Ti6Al ₂

Table 5.5a): Design of Experiment Using Taguchi array.

b)	V _s [m/s]		DOC [μm]		V _w [m/min]	
Trial	A		B		C	
	Level	Value	Level	Value	Level	Value
1	1	[20]	1	[10]	1	[7]
2	1	[20]	2	[20]	2	[15]
3	2	[35]	1	[10]	2	[15]
4	2	[35]	2	[20]	1	[7]

Table 5.5b): Design of Experiment Using Taguchi array.

5.18 Experimental results

	V_s [m/s]	DOC [μm]	V_w [m/min]	F_n (N)	F_t (N)	R_a [μm]	a_e [μm]
NO of Trial							
1	1 [20]	1 [10]	1 [7]	39	12	0.11	3
2	1 [20]	2 [20]	2 [15]	56	43	0.11	9
3	2 [35]	1 [10]	2 [15]	30	22	0.113	5
4	2 [35]	2 [20]	1 [7]	50	43	0.115	9

Table 5.6: Taguchi array. For L4 (2³). No Vibration.

	V_s [m/s]	DOC [μm]	V_w [m/min]	F_n (N)	F_t (N)	R_a (μm)	a_e (μm)
NO of Trial							
1	1 [20]	1 [10]	1 [7]	9	7	0.11	3
2	1 [20]	2 [20]	2 [15]	37	26	0.11	9
3	2 [35]	1 [10]	2 [15]	8	6	0.13	2
4	2 [35]	2 [20]	1 [7]	14	10	0.1	10

Table 5.7: Taguchi array for L4 (2³), with Vibration.

Tables 5.6 and 5.7 are typical model of Taguchi Design of Experiment, which used to determine the effect of the parameters tested upon each other. An standard L₁₆ 2⁸ orthogonal array model was modified to L₄ 2³ and used because of the lake of materials, however, the digit number four (4) represents the numbers of trials, the digit number two (2) represents the level of factors and the digit number Three (3) represents the numbers of the parameters been tested (A, B, C). This provides the most economical testing plan for evaluating the direct effects of four /or eight parameters. According to Taguchi Grove & Davis (1992), the plan may be checked for reliability by running confirmation trials based on the results collected. If the results from the confirmation trials agree with the expected results, then the experimental plan may be considered to be reliable.

5.18.1 Effect of Wheel Speed on Surface Roughness

When grinding at wheel speed in the range of 20 m/s to 35 m/s at table speed of 7m/min, with both the application of vibration and without vibration with the enhance of Taguchi array the results could be used to demonstrate the influence of the grinding wheel speed upon the surface roughness.

Figure (5.20) shows that the surface roughness is significantly influenced by high wheel speed and that reflects the stronger effect of the wheel speed on the surface roughness especially when grinding with vibration assisted.

Vs: 20 & 35m/s, V_w: 7 m/min (Taguchi Array)

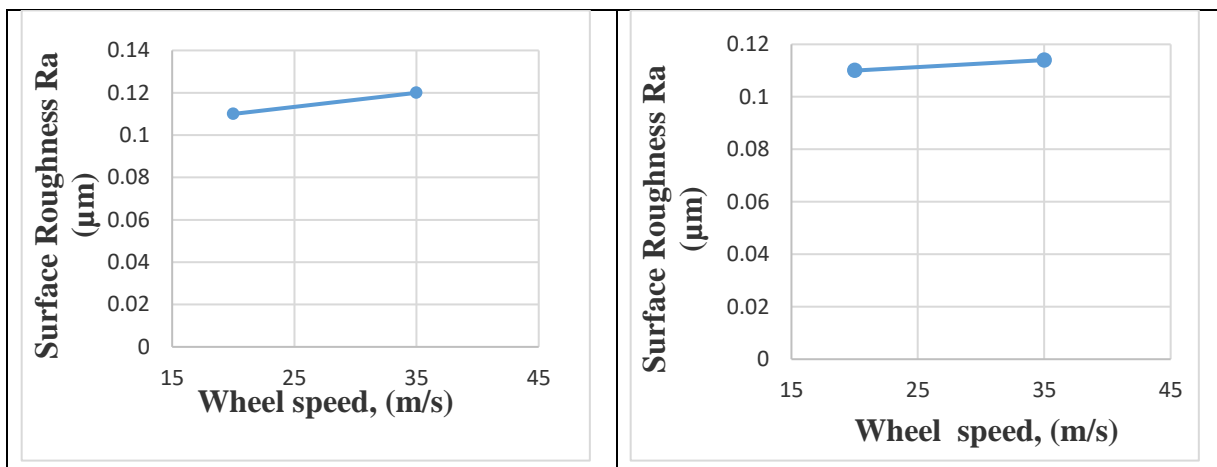


Figure 5.20: Surface roughness; No Vibration Surface roughness; vibration

5.18.2 Effect of Table Speed on Actual Depth of Cut

When grinding at speed in the range of 7 to 15 m/min table speed, at 20 m/s grinding wheel speed, with the application of vibration and without vibration, it has been seen that the table speed had significant effect on actual depth of cut, especially in vibration mode application where the speed line appears to be a steep line which reflects the scale of the influence.

Vs: 20 m/s, V_w: 7 &15 m/min (Taguchi Array)

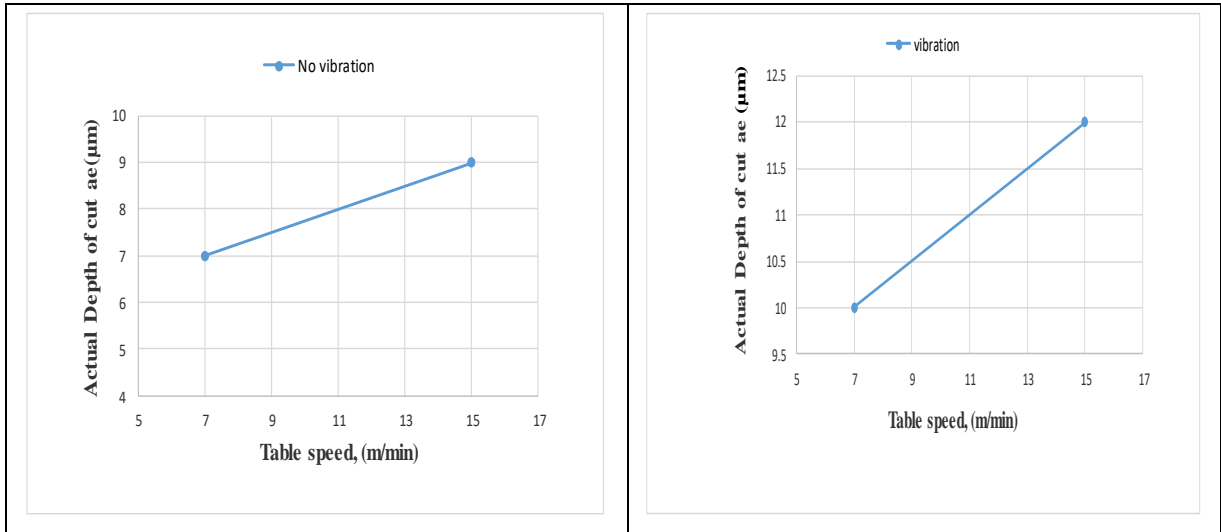


Figure 5.21: Actual depth / No Vibration Actual depth of cut/ Vibration

5.18.3 Effect of Wheel Speed on Cutting Forces

Vs; 20 & 35 m/s, Vw; 7 m/min, DOC; 10 µm (Taguchi Array)

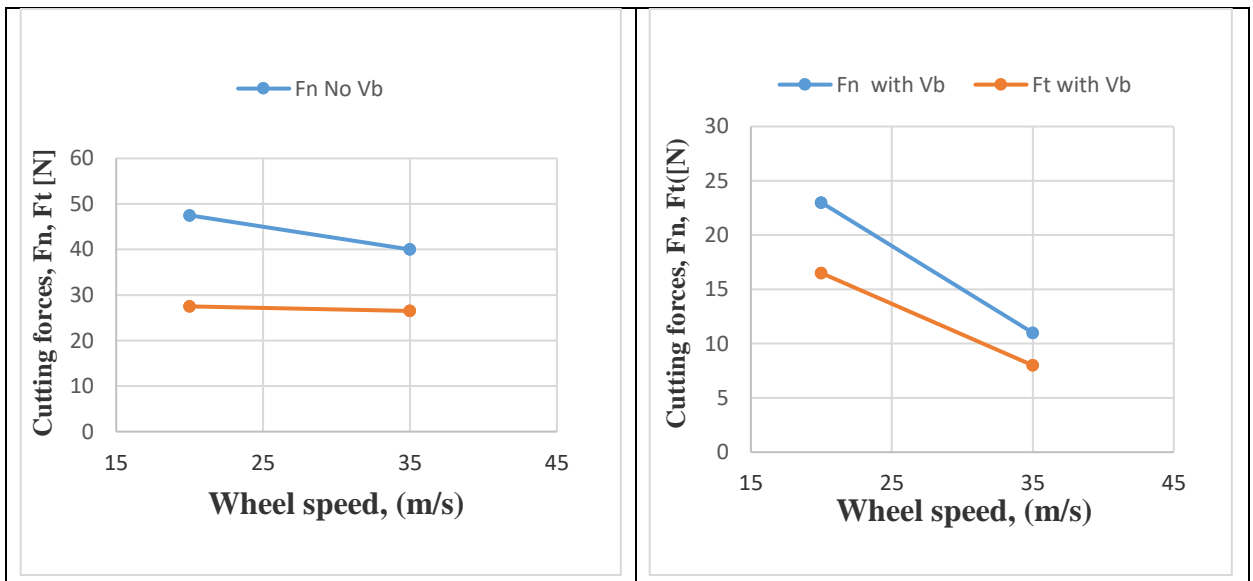


Figure 5.22: Cutting Forces / No vibration Cutting Forces / with vibration

Grinding of (Ti6Al) at wheel speed in the range of 20 to 35m/s, table speed of 7m/min and 10µm depth of cut using Taguchi array, with both the application of vibration and without it, that resulted in the forces values given in Figures 5.22. However, Figures 5.22 shows that the influence of wheel speed on grinding cutting forces is significant, especially with the application of vibration assisted grinding for such a smaller depth of cut (10µm). However, increasing wheel speed resulted in

decreasing the grinding forces, this is due to the shorter period of contact between the work-piece and the grinding wheel.

5.18.4 Effect of Table Speed on Cutting Forces

V_w ; 7 & 15 m/min, V_s ; 20 m/s, DOC; 10 μ m (Taguchi array)

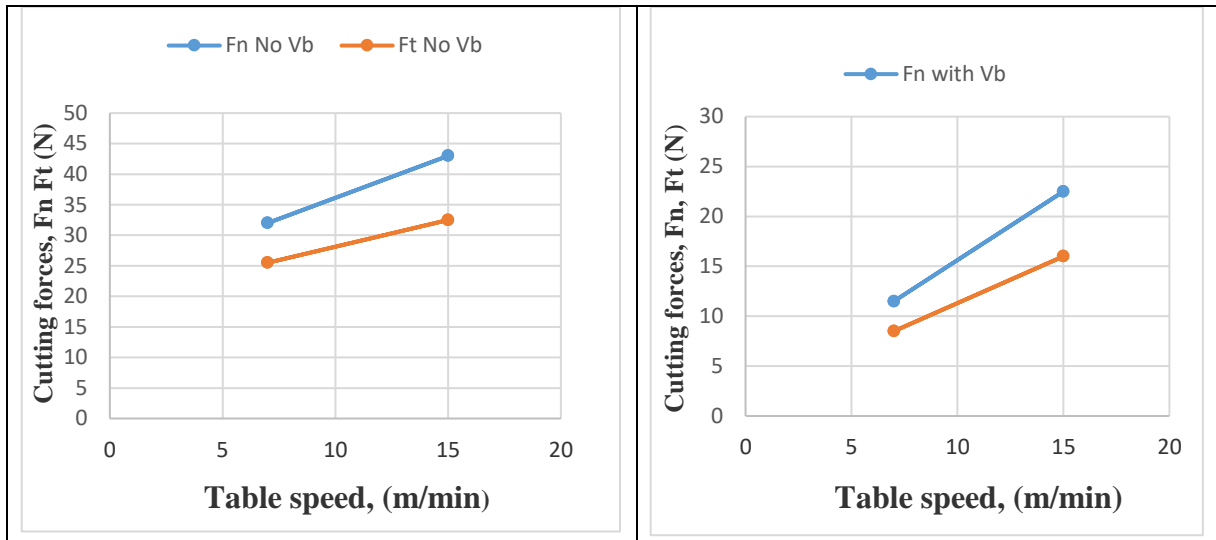


Figure 5.23: Cutting Forces / No vibration Cutting Forces / with vibration

When grinding at table speed in the range of 7 to 15 m/min table speed, 20m/s grinding wheel speed and 10 μ m depth of cut with both the application of vibration and conventional grinding using Taguchi array, the results could be seen clearly in Figure 5.23 that table speed had a significant influence on cutting forces; this is because of the slope of the lines towards the vertical axis.

The results shown in Figure 5.20 up to Figure 5.23 reflected some facts which should be analysed using the Taguchi analysis. It is important to note that the Taguchi approach identifies qualitatively the strongest effects of the input parameters upon other output parameters.

Figure 5.22 shows that the influence of wheel speed on grinding forces for trial 1 is less significant at depth of cut of 10 μ m because increasing the wheel speed decreased the grinding forces, this is due to the shorter period of contact between the work-piece and the grinding wheel.

Figure 5.21 shows that table speed has stronger effect on the actual depth of cut when grinding with vibration.

However, the effects of wheel speed and table speed on actual depth of cut and cutting forces F_n , F_t in this experiment are significant while the influence on the

surface roughness is less significant, if we take into consideration the lower depth of cut at trial one ($10\mu\text{m}$).

However, it has been noticed from Figure 5.20, that grinding wheel topography influences surface roughness directly, hence the effects of the process parameters upon the output parameters such as forces for instance when applying vibration assisted machining are more effective than without vibration assisted.

5.19 Effect of Depth of Cut on Grinding Forces

Figures 5.24 and 5.25 show the results of normal (F_n) and tangential (F_t) forces of grinding in vibration and without vibration.

The results shown in the graphs demonstrate the reduction of grinding forces in the case of applying vibration and non-vibration mode. This can be seen obviously in the graphs where all forces, normal and tangential under vibration assisted grinding decreased significantly by more than 50%. However, a similar conclusion was drawn in Figures 5.25 and 5.26 below where Graphs showed that normal forces were reduced when applying vibration.

However, Figure 5.27 reflects a full grinding cycle of the process, where it can be seen obviously that at the beginning of the cycle, for a few seconds of time there was no force recorded because there was no direct contact between the grinding wheel and the work-piece. Hence, a force started to rise when the grinding wheel touched the first point of the work-piece and it remained in this pattern until the grinding wheel left the last contact point in the workpiece. The time span between the two points (start - finish), was used to specify the actual grinding time and then the table speed depending on the work-piece length.

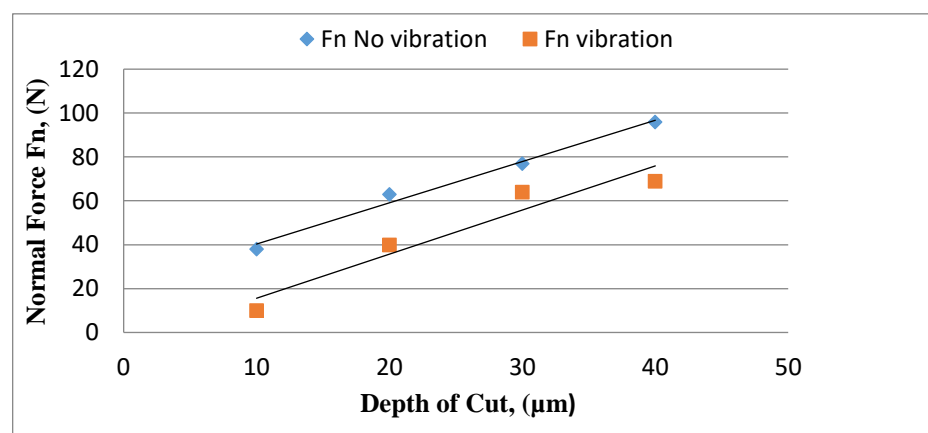


Figure 5.24: Normal force F_n versus depth of cut, Vibration/ No vibration

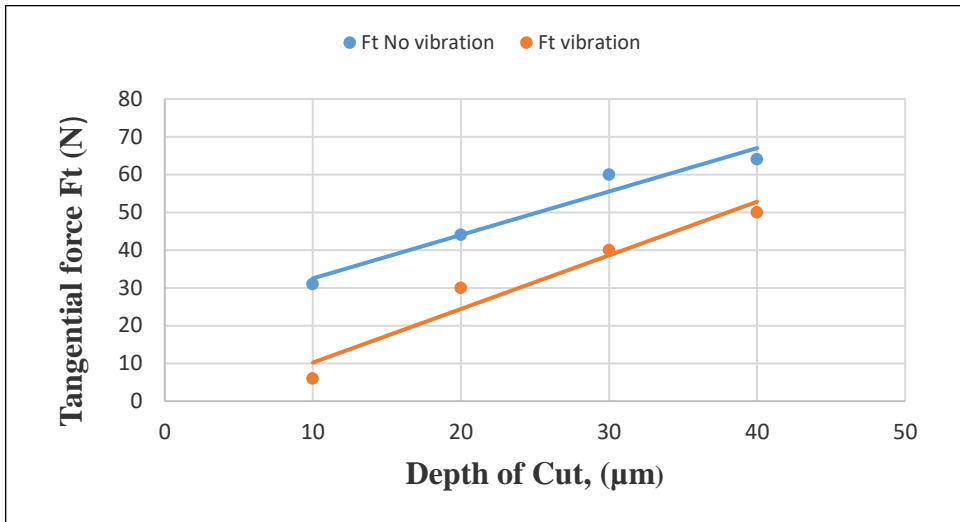


Figure 5.16: Tangential force F_t versus depth of cut/ Vibration/ No vibration

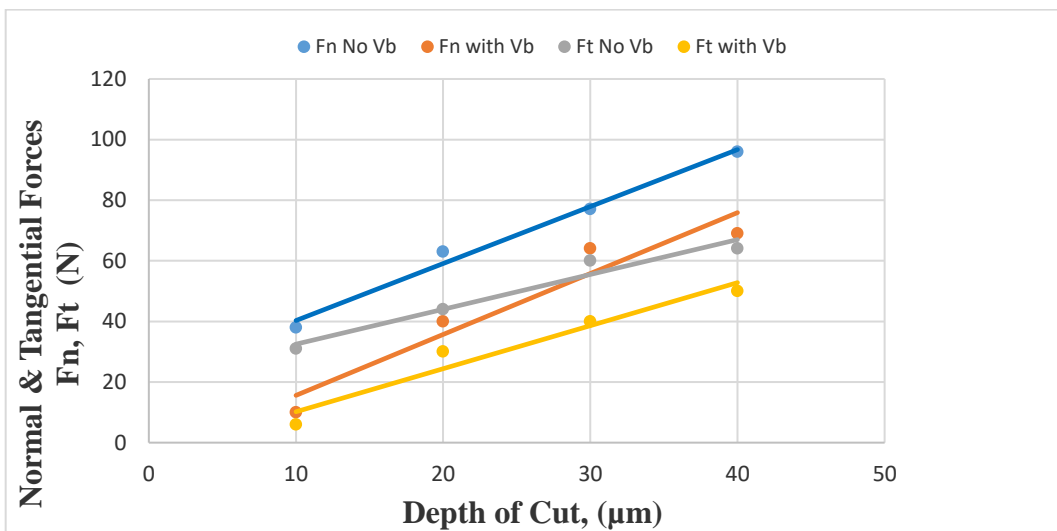


Figure 5.26: Normal & Tangential forces F_n, F_t versus depth of cut/ No vibration/ vibration

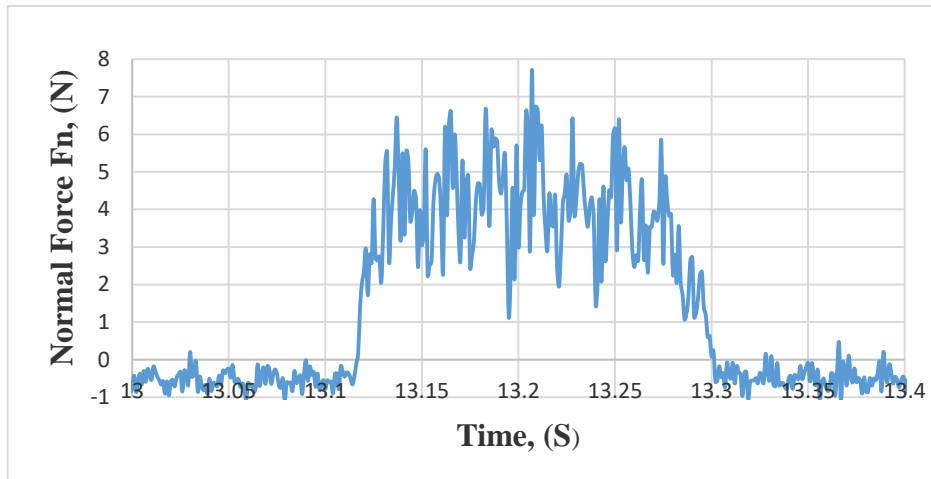


Figure 5.27: Normal force F_n versus Time/ No vibration

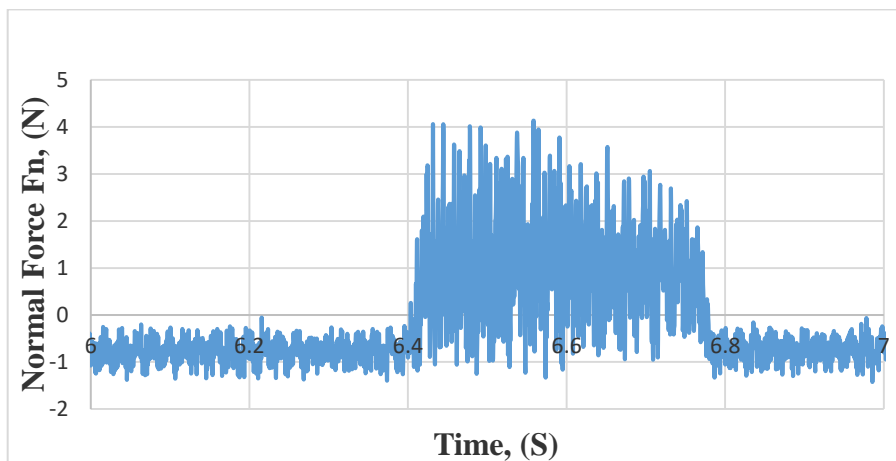


Figure 5.28: Normal force F_n versus Time/ with vibration

5.20 Effect of Depth of Cut on Surface Roughness

The surface roughness of the work-piece was measured after each trial, from 10 μ m up to 40 μ m depth of cut, in three different positions in the work-piece and the average was taken in each measurement.

Then the obtained data was transferred into Excel to create the graphs shown in Figures 5.29, 5.30 and 5.31. However, from these graphs it can be noted that by applying vibration assisted a better quality of the work-piece surface finish was achieved where the measured surface roughness was lower by about 5% than without

vibration. The graphs showed that at low depth of cut with high grinding wheel speed, a better surface roughness was also achieved.

As it has been shown in Figures 5.29, 5.30 and 5.31, it is interesting to see the variation in surface patterns while grinding with and without vibration. It can be noted that by applying vibration, a flat slot gouging pattern obviously appeared on the work-piece surface. This may be the reason that surface roughness Ra was lower in the case of using vibration assisted grinding than without vibration.

However, a surface roughness profile generated by the Brucker contour GTK for depth of cut between 10 to 40 μm gives the indication of a stable grinding wheel profile on the work-piece without chatter, so a good quality surface finish was reached as a conclusion (see Appendices B-3). However, for a better understanding of surface profile a GFM machine was used at a confirmation stage of the investigation.

Furthermore, a similar result was noticed by observing Figure 5.33 where GFM surface measuring machine was used. GFM was able to scan an area of 40*8mm of the work-piece repeatedly. The results reflected a clear and smooth pattern of the surface roughness for both 2D and 3D images in case of grinding under vibration assisted for 20 μm depth of cut. While a poor surface roughness pattern with visual cracks on both 2D and 3D images was obtained under the same conditions when grinding without vibration assisted (see Appendices B-3e).

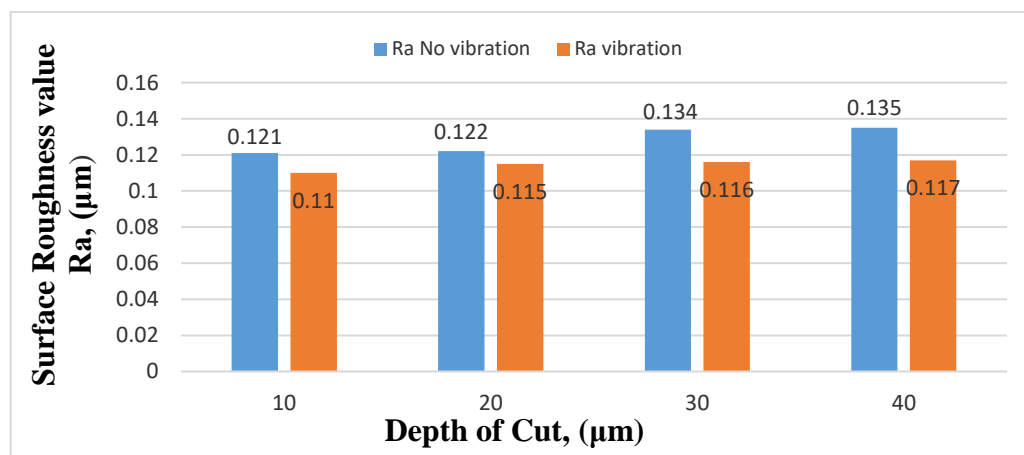


Figure 5.29: The relationship between surface roughness Ra and depth of cut when grinding at feed rate of 15m/min and wheel speed of 20m/s, using coolant.

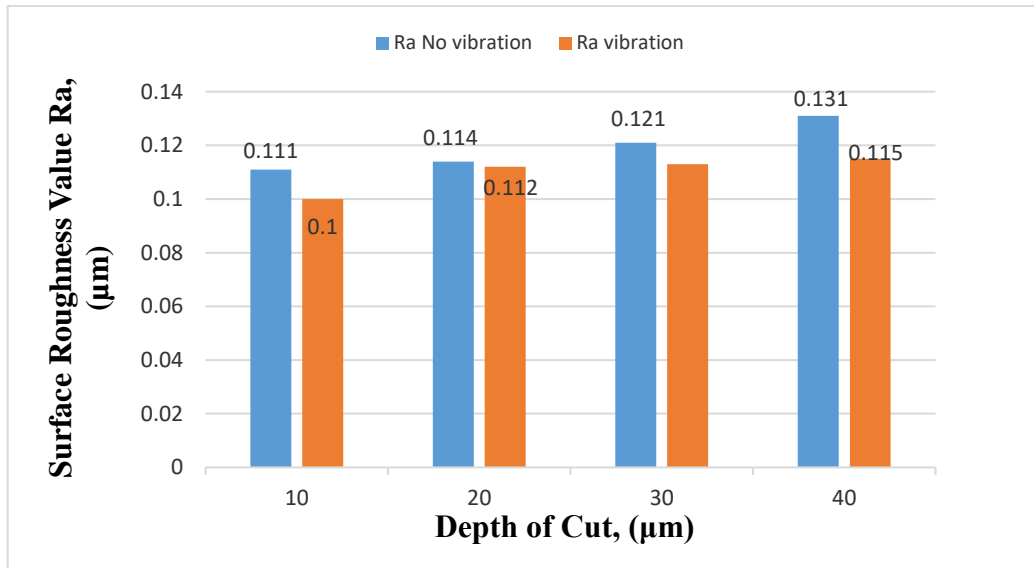


Figure 5.30: The relationship between surface roughness Ra and depth of cut when grinding at 15m/min feed rate and wheel speed of 35m/s, using coolant.

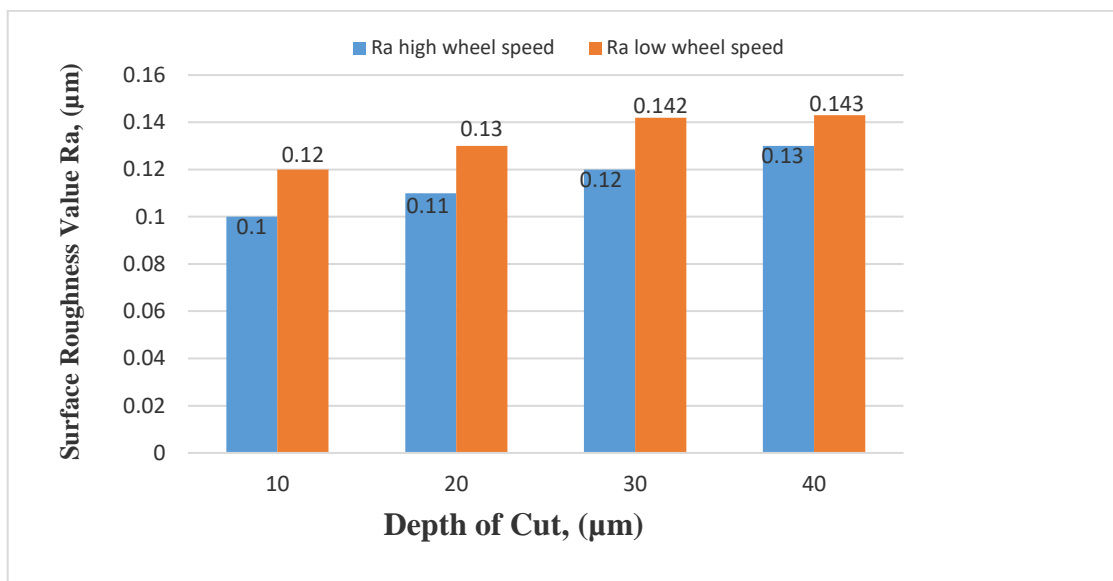


Figure 5.31: The relationship between surface roughness Ra and depth of cut when grinding at feed rate of 15m/min and wheel speed of 20 m/s and 35 m/s /No vibration.

Figure 5.31 shows that at low depth of cut with high grinding wheel speed and high feed rate, a slightly better surface roughness was achieved.

The Figure also shows the surface roughness deteriorated when grinding at high depth of cut and low grinding wheel speed.

5.21 Actual Depth of Cut (a_e)

As has been mentioned before, the materials used for these tests were the Titanium (Ti6Al4V) alloy and nickel alloy (Inconel 718).

To measure the actual depth of cut a_e , the following procedure was performed- the work-piece was ground flat across its width with several spark-out passes. However, a 2 μm measuring clock device was used to measure the depth of cut level before grinding and after grinding with the enhancement of Mitutoyo slip gauges strips ranging from 1.001 mm to 100.000 mm. In this process a slip gauge of specific dimension was ground on parallel datum beside the work-piece where the '0' was obtained, the wheel was then moved across the work-piece width. The difference between the datum 'strip' slip gauge, and the ground 'strip' of the work-piece was measured using the finger clock gauge (see Appendices B-3)

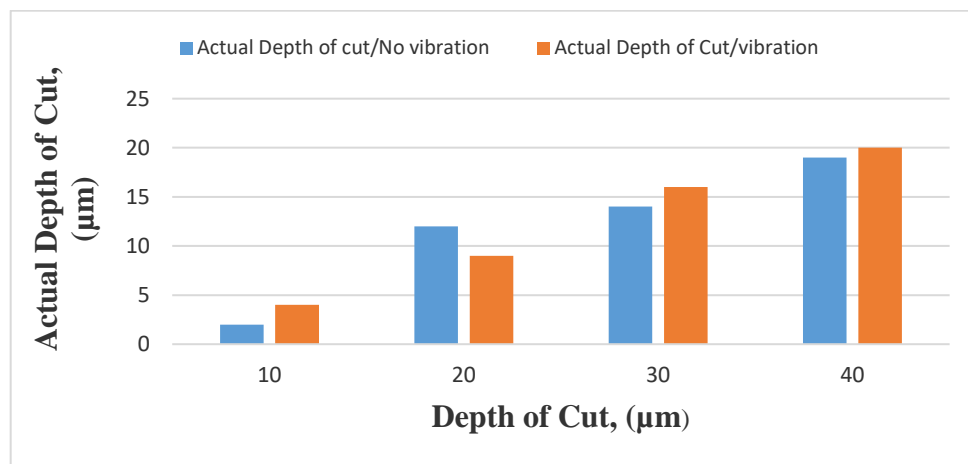
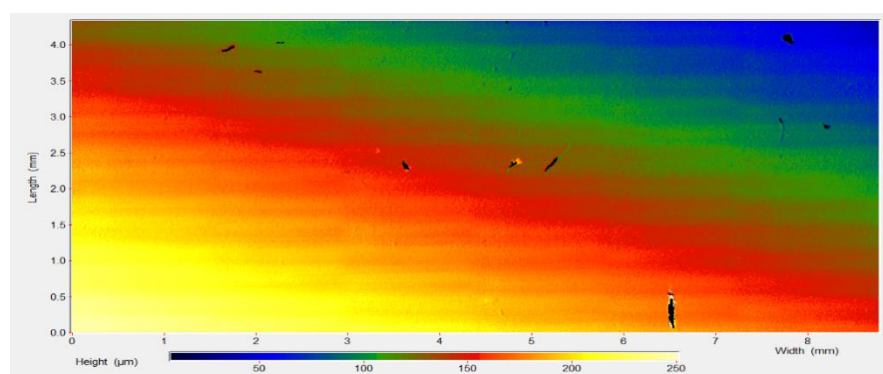
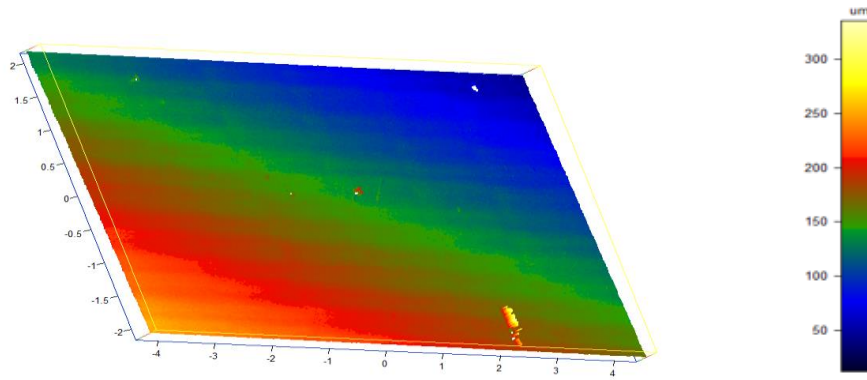


Figure 5.32: The relationship between actual depth of cut and depth of cut when grinding at 15m/min feed rate and wheel speed of 20 m/s, using coolant



2D image.



3D image.

Figure 5.33: GFM Machine Surface roughness pattern

5.22 Summary

Using Design of Experiments Taguchi orthogonal array method, the combinations of the process parameters (inputs parameters) with their levels and measured responses are shown in Figures 5.29 up to 5.33, where the effects of the process parameters upon surface roughness and actual depth of cut are significant when grinding with vibration. Figures 5.27 and 5.28 Showed that grinding forces were improved by about 50% when applying vibration assisted grinding. Figures 5.24, 5.25 and 5.26 showed the variation in Normal and Tangential Forces with Depth of cut when grinding with vibration and without vibration. From the Figures it was observed that by increasing the depth of cut the Normal forces increased due to the increase in average chip thickness.

However, it can be concluded that increasing cutting depth will increase the surface roughness and that can be seen in figures 5.29, 5.30 and 5.31. However, with increasing feed rate and wheel speed, conversely, surface roughness lower and thus the surface quality better.

However, in conclusion a surface roughness that was obtained by applying vibration is better than the quality achieved by conventional ones.

CHAPTER-6

RESULTS

GRINDING OF Ti-6Al-4V

6. GRINDING OF Ti-6Al-4V

6.1 Introduction

A full scale of experimental work with and without vibration assisted grinding was undertaken by employing an “Aluminium Oxide” grinding wheel. This section of the research also represents the final experimental work of implementing vibration-assisted on grinding of titanium Ti-6Al-4V alloy. However, many researchers found that the surface of titanium alloys can easily be damaged and cracked during machining, because of the heat that is generated on the grinding contact zone. Likewise, during machining of titanium Ti6Al4V a similar damage was found.

In this chapter experimental work was carried out testing 4 work-pieces of titanium Ti6Al4V, where a coolant system was also introduced to improve the quality of the work-piece surface finish and to improve the material removal rate. Investigations have been also made on grinding force calculation, grinding force ratio, power consumption, material removal rate, surface roughness and the specific grinding energy as well.

Grinding Parameter	VALUE
Grinding Wheel Type	Al ₂ O ₃ (OVU33 A602HH 10VB)
Wheel Speed (V _s)	17 m/s
Wheel Diameter	208 mm
Work Speed (V _w)	250 mm/s
Grinding Condition	Wet (coolant)
Wheel Feed	Traverse
Workpiece Material	Ti-6Al-4V
Vibration Frequency	100-250 Hz
Vibration Amplitude	130 μm
<i>Applied Depth of Cut</i>	<i>15-45 μm</i>

Table 6.1: Experimental Parameters Setup

6.2 Experimental Methodology

Titanium work-piece bars with the following dimensions: 60 mm length x 8 mm width x 20 mm height are used in the Experiment, where, a surface grinding machine was used to grinding them with application of vibration assisted and with enhance of coolant fluid as well. Where method and procedure are given below, especially the machinability of the materials was tested in terms of four factors given below. However, a crack underneath the workpiece was tested using SEM, and also a method of aching the workpiece surface after grinding with Acids to identify the depths & width of the internal crack. Whilst, cutting forces, power, material removal and wheel wear were also been measured.

- ❖ Concept Design;
 - Machinability concept of hard materials are assessed in terms of four factors:
 - Tool life
 - Cutting Forces
 - Power requirements
 - Surface finish
- ❖ Parameters Design:
 - The selection of control factors (parameters) and their optimal levels
 - The optimal parameters levels and defining boundaries
- ❖ The goal is to find suitable condition to achieve:
 - Improving the surface finish and integrity. Work-pieces of the materials were examined under the SEM (Scanning Electron Microscope).
 - Improve the grinding efficiency
 - Reduce the energy consumption
 - Reduce the grinding wheel wear

6.2.1 Materials

- ❖ Two groups of materials were investigated (Brittle and ductile)
 - Titanium Ti-6Al-4V (hard and brittle material)
 - Nickel Alloy ‘Inconel 718’ (Ductile material).
 - Chip formation & Segmentation. (study under SEM)

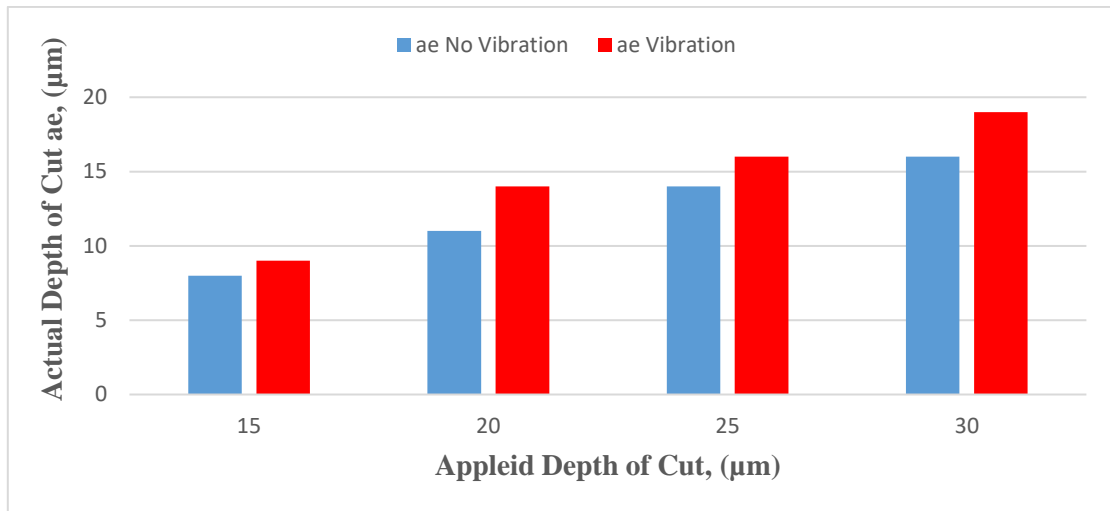


Figure 6.1: Actual Depth of Cut Versus Applied Depth of Cut

Figure 6.1 illustrates the relationship between applied depth of cut (DOC) and actual depth of cut (a_e). The results show that the application of vibration onto grinding secured a better cutting efficiency, regardless of the recorded low cutting forces in superimposed vibration, the actual depth of cut is still higher than conventional grinding. If one were to consider the static deflection on spindle unit, these results show that, by reducing the normal cutting force the vibration allow the subsystem spindle-wheel-grits-work-piece to perform better.

6.3 Actual Depth of Cut and Material Removal Rate

Figure 6.2 illustrates the material removal rate that is in a direct proportional relationship with the actual depth of cut. However, the main purpose here is to define the material removal rate and the specific grinding energy. Figures 6.1 & 6.2 show that the actual depth of cut and the material removal rate have been increased with the increase in applied depth of cut. However, it has also been observed that with the application of vibration assisted increasing in the material removal rate was secured.

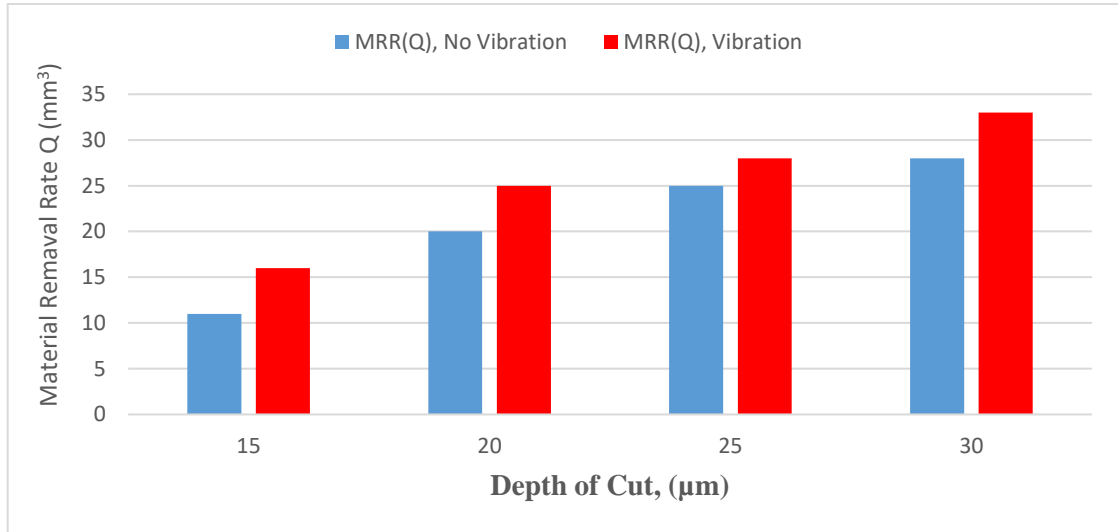


Figure 6.2: Material Removal Rate Versus Depth of Cut

6.4. Grinding Force for Ti-6Al-4V

It has also been proved that the vibration assisted grinding at high feed rate i.e. 250mm/s and low grinding wheel speed for this particular traditional machine (ABWOOD 5025) provided the best material removal rate along with a decrease in cutting forces. On the other hand, one of the disadvantages of grinding at low feed rate at high wheel speed is the risk of thermal damage for the work piece surface due to excessive rubbing and friction leading to burn out.

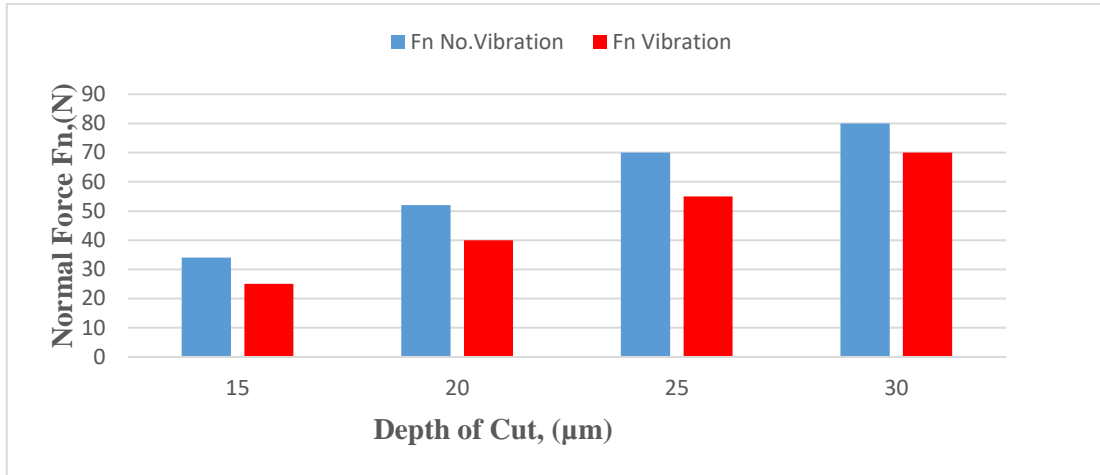


Figure 6.3: Normal force Vs depth of Cut

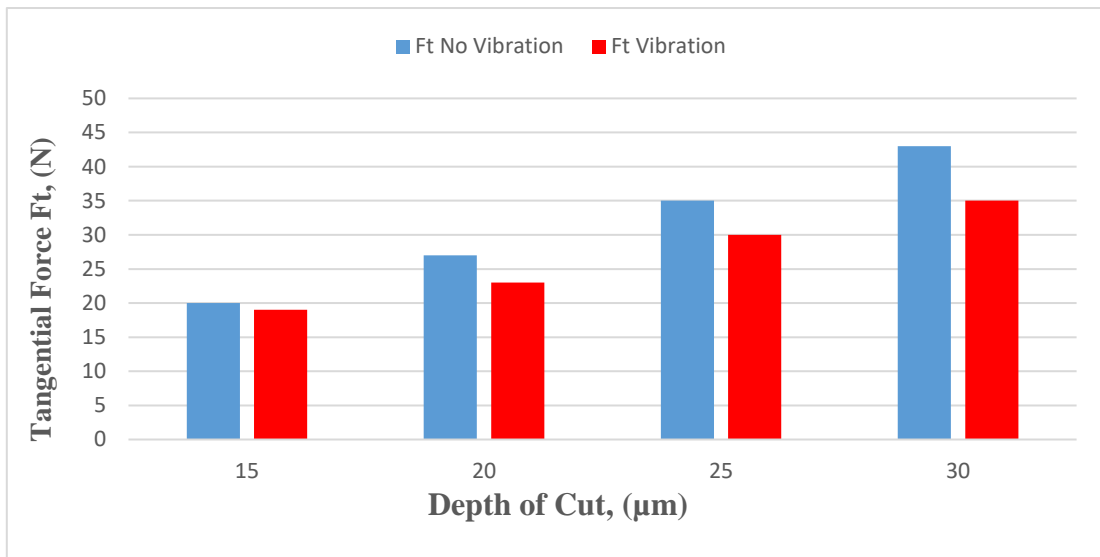


Figure 6.4: Tangential Force Vs Depth of Cut

Figures 6.3, 6.4 and 6.5 represent the relationship between grinding cutting forces in the vertical direction (F_n) and in the tangential direction (F_t). However, the third force (F_a) acting in the axial direction was neglected because it has a very small value in comparison to the other two forces. These forces were measured during the grinding process in both cases with and without vibration. As a results of the trials it has been noticed that cutting forces were increased with the increase of applied depth of cut. In addition to that, these forces, values differ significantly with the implementation of vibration assisted, from the forces that obtained in the conventional grinding.

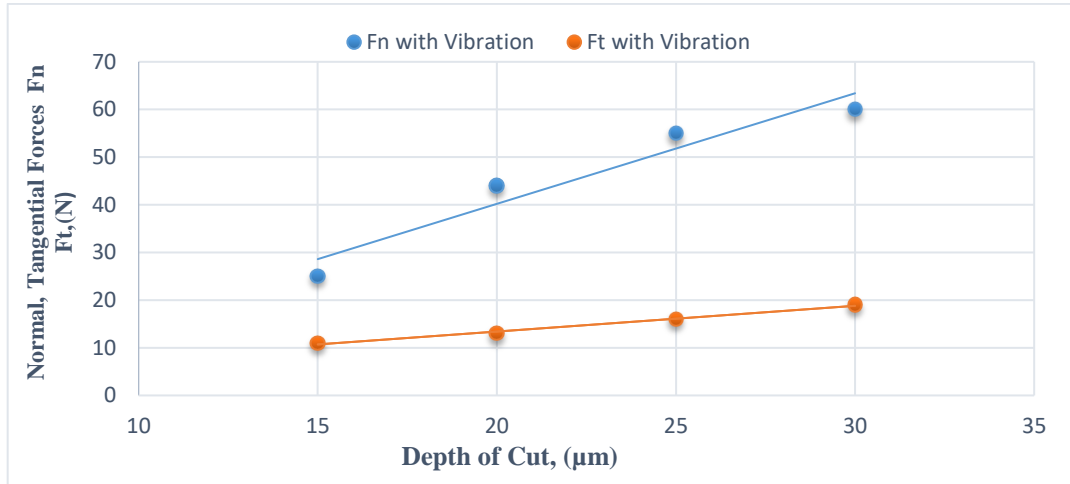


Figure 6.5: Normal and Tangential forces for Ti-6Al-4V as a function of depth of cut when grinding with vibration at 20m/s wheel speed & 250mm/s feed rate.

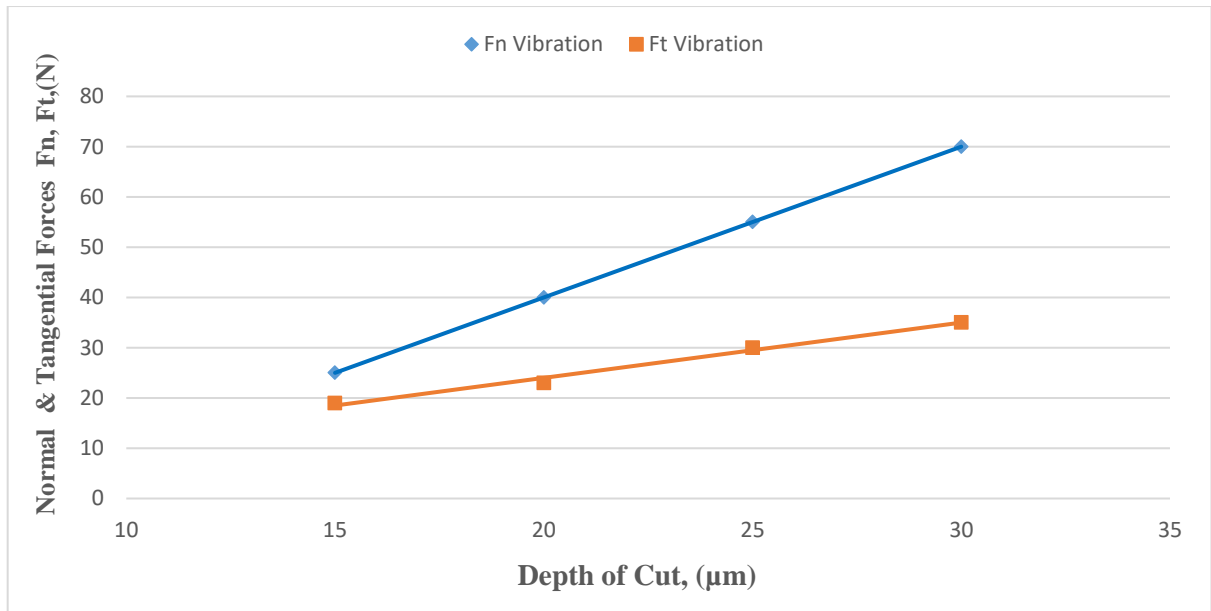


Figure 6.6: Normal & Tangential Forces Versus Depth of Cut at 17m/s Vs

Figures 6.3 up to 6.6 illustrate the process performance in terms of cutting forces, Normal force (F_n) and tangential force (F_t). However, both measured forces represent a relationship that has been affected by two parameters of the process, these two parameters are the actual depth of cut and the frequency. Referring to the previous trials in chapter 5, the frequency was fixed parameter (100 Hz) in the process, because such an assumption allows the desired maximum oscillation amplitude of 130 μm to be achieved. Consequently, it was observed that grinding cutting forces increase with

the increase in depth of cut. The cutting forces in vibration assisted grinding trials show a slight decrease in its values, this reflects improvement in the process. The normal forces decreased by around 50% and the tangential force decreased by about 45%. However, it has been observed that at low depth of cut the improvement is marginal.

6.5 Surface Roughness

Surface texture and profile can be defined as follows: at some scale surfaces of manufactured components have structure or defects that may affect their function or durability. Often these arise through changes that happen during manufacturing process such as tool wear leading to a rougher surface. In order to control these processes effectively and to ensure that components meet their designed specification it is necessary to have methods for examining and characterising the surface quality. Surface roughness determines a range of component characteristic such as the ability of lubrication and reflectance durability. Hence, surface roughness quality is influenced by various parameters such as;

- Machine parameters such as static and dynamic behaviour and spindle system.
- The grinding process parameters such as wheel speed, table speed, applied depth of cut and dressing depth.
- Grinding wheel characteristics such as grain material, grain size, grade structure and grain dimensions.
- Work-piece material such as mechanical properties and chemical composition.

Generally, the longitudinal surface roughness has a lower value than traversal value, and therefore, used in the industry. Roughness parameter Ra is defined to be the most used international parameter of roughness. It is the mean of the roughness profile from the mean line. For a better accuracy, the surface roughness has been measured using the TYLOR HYBSON surface texture machine.

Figure 6.7 depicts the measured surface roughness of the work-pieces during grinding with vibration assisted and without vibration. The results reflect that the surface roughness worthiness with increase of depth of cut and became better with increase of wheel speed. Here, a reduction in surface roughness of about 9% was achieved with the application of vibration assisted. This improvement in surface roughness shows that the desired surface finish quality of the products could be achieved by the implementation of vibration assisted grinding. Moreover, in this investigation the effect of process conditions on surface quality was compared. Based on the investigation results, it has been noticed that the surface roughness deteriorates with

increasing the depth of cut and becomes better with increasing the feed rate and wheel speed. From previous study it has also been proved that coolant application allows to achieve better surface roughness to be achieved, reduction in grinding cutting forces and also to impose direct impact on the environment (Brinksmeier, 1998).

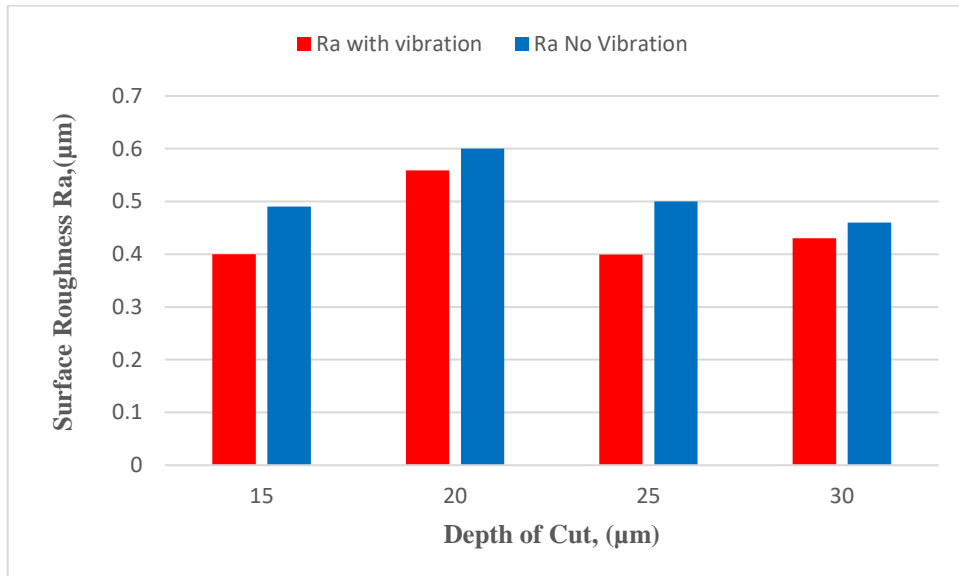


Figure 6.7: Surface roughness Ra for (Ti-6Al-4V) when grinding at 17m/s wheel speed.

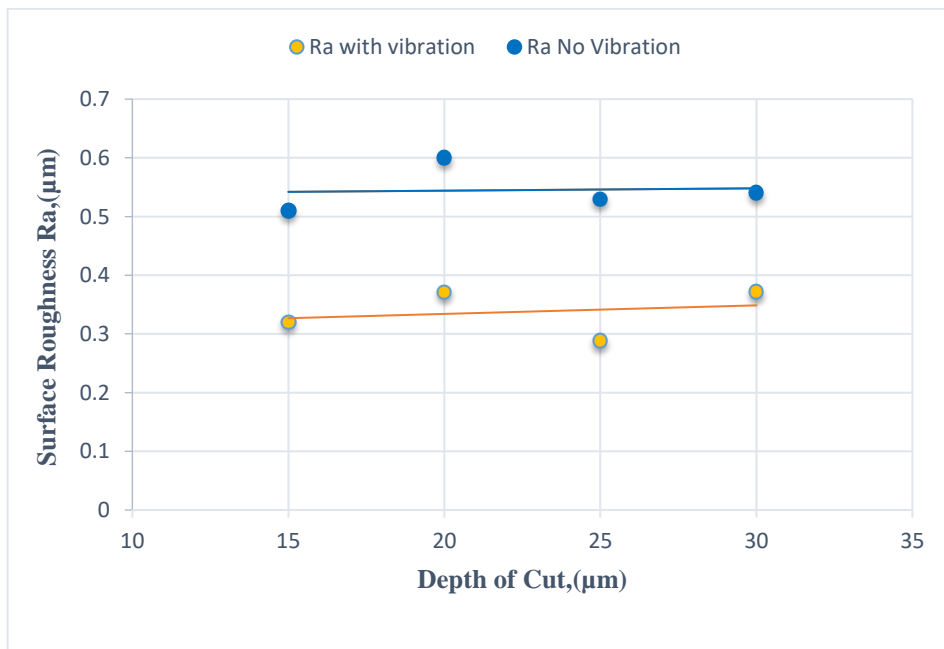


Figure 6.8: Surface roughness Ra for (Ti-6Al-4V) when grinding at 20m/s wheel speed.

Surface roughness is an important factor in predicting the performance measure of any machining process. In grinding process, surface roughness is one of the important factors in assessing the quality of ground component. Operating parameters such as grinding wheel speed, feed rate, depth of cut, work material properties, grinding wheel composition and coolant application are variables that effect the surface roughness quality in the grinding process.

From Figures 6.7 and 6.8 it has been noticed that by applying vibration assisted a better quality of the work-piece surface finish was achieved. Where the measured surface roughness was lower by about 15% to 25% with reference to surface roughness achieved without the application of vibration. The graphs also show that at low depth of cut with high grinding wheel speed, a better surface roughness has been also achieved. Appendix -d shows few images of surface roughness profile obtained from the (TAYLOR HOBSON) machine.

Another key issue is that grinding at wheel speed of 35m/s, with the application of vibration assisted grinding at low depth of cut such as 15 a 20 μm , can cause chatter on the work-piece surface, due to the high wheel speed. However, burnout on the work-piece surface was noticed at higher depths of cut of 25 μm and above, this burnout could be clearly seen by naked eyes in a shape of a shadow area above the work-piece surface. This occurred due to the high temperature on the contact zone between the work-piece and the cutting tool.

Nevertheless, when grinding at low wheel speed (17m/s) and high feed rate (250mm/s), no burnout was seen and no smear as well. It has also been noticed that under similar grinding conditions, at low feed rate of 125mm/s for the ABWOOD surface grinding machine, the whole work-piece surface was burned out completely while the grinding quality was very poor in general. In conclusion, increasing the grinding wheel speed tends to increase the risk of thermal damage.

Hence, it has been well known that more than half of the energy in the grinding process is converted to heat, if this phenomenon is not controlled that will generate a chatter, plus the possibility of work-piece surface burnout.

6.6 Grinding Energy

The specific grinding energy (e_c) is the main key performance indicator in grinding technology. However, the specific grinding energy is also defines by the grinding power required to remove one unit volume of material per one unit of grinding time. The Lower e_c the better the better the performance. e_c can be reduced by either

decreasing power consumption or increasing the volume of metal removed. However, e_c has been considered to be the most fundamental factor for any machining process efficiency, which can be given as follows:

$$e_c = P/Q \quad (\text{J} / \text{mm}^3)$$

Where: e_c is the specific energy, P = Power and Q = Removal Rate.

Actual Depth of cut (μm)	Removal Rate (mm^3/s)	Power (w)	Specific grinding Energy (J/mm^3)
8	22.08	350	15.9
11	30.36	875	29.8
14	38.64	1050	23.17
16	44.16	1330	30.11

Table 6.2: The relationship between actual depth of cut, material removal rate and specific grinding energy

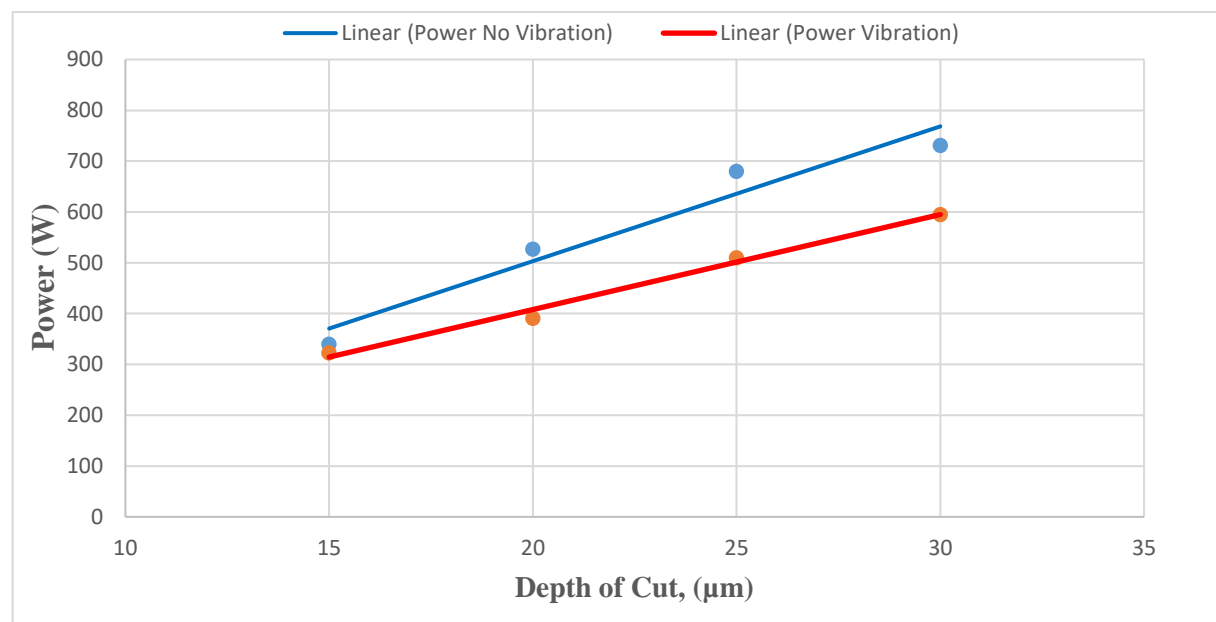


Figure 6.9: Power Consumption VS Applied Depth of Cut

6.7 Power Consumption

Figure 6.9 above shows that power consumption is a function of applied depth of cut. This figure depicts that the application of vibration assisted reduces the power consumption. This reduction reaches up to 35%. The total improvement in power consumption proved that vibration assisted has advantages over conventional grinding.

6.8 Specific Grinding Energy

Figure 6.10 below illustrates the specific grinding energy as a function of material removal rate and reflects that the specific grinding energy is quite low as the result of the superimposition of vibration to grinding in comparison to conventional grinding.

Figure 6.11 and Figure 6.12 portray the specific cutting forces as a function of wheel speed where it seen that the specific cutting force decreases with the increase in wheel speed. It is also seen that the superimposed vibration outperformed conventional grinding by 35%.

It has been seen that the application of vibration on grinding leads to an average reduction in power consumption of 35% or more.

However, any increase in cutting edge density λ will increase the specific grinding energy where energy consumption will be high.

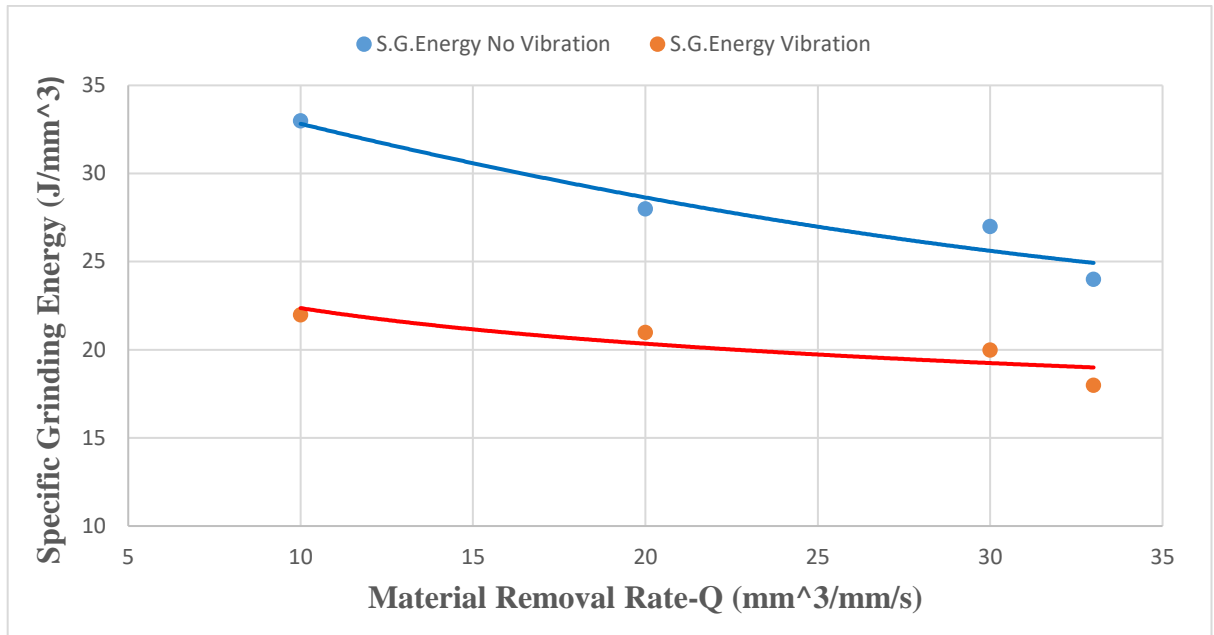


Figure 6.10: Specific Grinding Energy (J/mm³) VS Material removal Rate

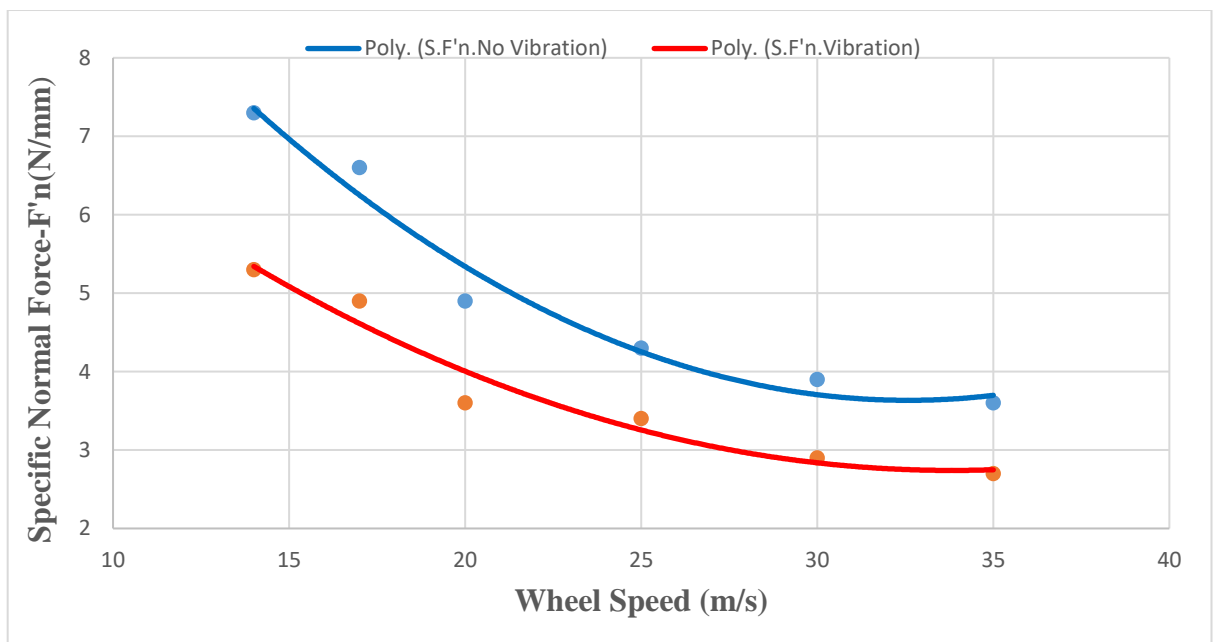


Figure 6.11: The effect of wheel speed on specific normal forces.

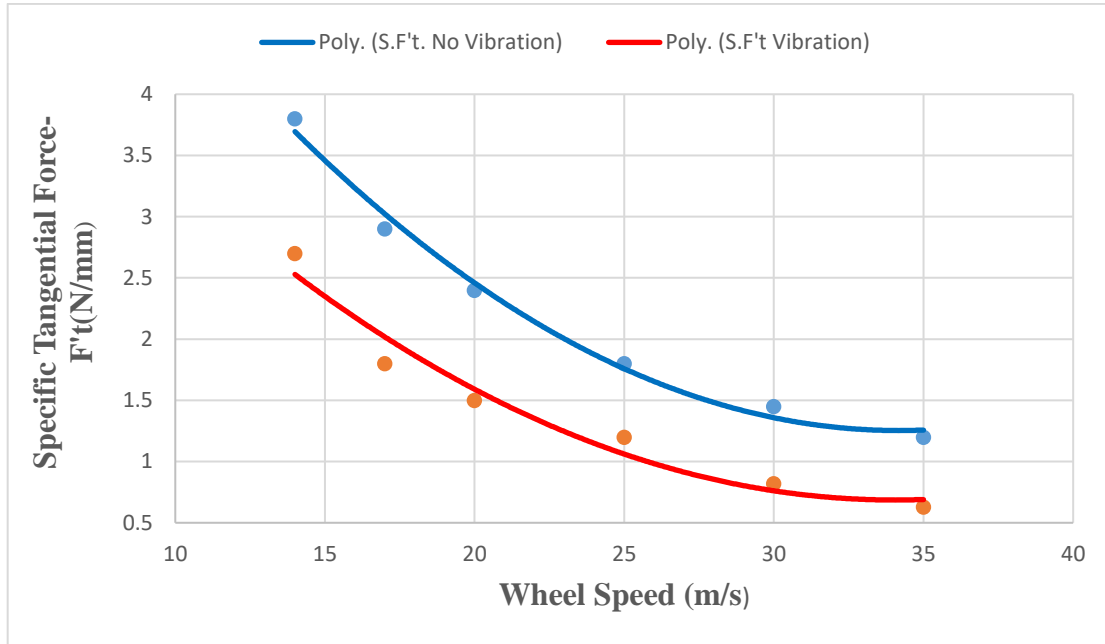


Figure 6.12: The effect of Wheel Speed on Specific tangential Forces

6.9 Boundaries identification

From the experimental findings better performance boundaries for high quality grinding were assumed as follows:

- Grinding wheel speed is 17m/s
- Feed rate is 250mm/s
- Applied depth of cut 15-30 μm
- Dressing between 4-14 μm
- Displacement 130 μm
- Frequency 100Hz
- Minimum Depth of Cut between 15-30 μm are the optimum conditions to be applicable to minimize surface roughness, burnout and chatter. Because, smaller depths of cut in the range of 10 μm and below are not desired for hard materials, due to the limitation for the machine tool use but could be employed on a stiffer machine, equally vibration seems not to reduced cutting forces for depth of cut below 15 μm because of the effect of the conventional grinding machine spindle specification. Hence, the grinding wheel doesn't remove the required amount of material from the work-piece at lower depth of cut,

because of the spindle unit back-lash is in the range of cut $10\mu\text{m}$. Nevertheless, applying vibration assisted at $15\mu\text{m}$ depth of cut and above reduced the normal forces remarkably. However, the reduction in normal forces per width unit ground is important for wheel wear, the load on the wheel and the work-piece, all these factors' accuracy are highly required in the industry.

6.9.1 Workpiece surface quality

The experimental results reveal that the following factors are the main factors which influence surface quality:

- The dressing depth
- The feed rate
- The coolant
- The grade of the grinding wheel
- The grinding wheel structure and the wheel speed

It has been seen in Figures 6.7 and 6.8 above that the superimposed vibration has a clear advantage over conventional grinding. However, the dressing has key effect on the roughness of the surface.

Figure 6.7 shows that at dressing depth of $14\mu\text{m}$ where, figure 6.8 illustrates an average of $0.55\mu\text{m}$ and $0.35\mu\text{m}$. On average the vibration assisted grinding secured an improvement of 25~30 percent in surface finish quality over conventional grinding.

6.10 Summary

In this chapter titanium alloy (Ti-6AL-4V) machinability was investigated experimentally, as the boundary conditions for grinding this alloy on a surface grinding machine were found (suitable grinding parameters such as wheel speed, feed rate and applied depth of cut at fixed frequency and fixed amplitude) to secure better quality of surface roughness and cutting forces reduction. Then the trials were conducted to achieve specific cutting force decreases, material removal rate improvement and decrease in specific grinding energy. In conclusion it has been seen that the superimposed vibration outperformed conventional grinding by 35%.

It has also been seen that the application of vibration assisted on grinding leads to an average reduction in cutting forces and power consumption of 35- 45% or more.

It is to notice that in these experiments, the coolant was applied at a very low flow rate and at atmospheric pressure.

The results showed that at low depth of cut with relatively high grinding wheel speed, a better surface roughness, low specific grinding energy and high material removal rate were achieved. However, in this study, grinding at high wheel speed namely 35m/s, with the application of vibration assisted grinding at low depth of cut such as 15 a 20 μm , induced chatter on the workpiece surface. Conversely, some burnout on the workpiece surface was noticed at higher depths of cut of 25 μm and above. In addition, as expected, low feed rate of such as 125mm/s resulted into complete burnout of the workpiece.

This problem of machining titanium was resolved by lowering the grinding wheel speed (17m/s) and increasing the feed rate (250mm/s) and no burnout nor chatter were observed. Consequently, one could state that, increasing the grinding wheel speed without adequate feed rate, lead to a risk of thermal damage.

CHAPTER 7

RESULTS

GRINDING OF NICKEL ALLOY (INCONEL 718)

7. GRINDING OF NICKEL Alloy (INCONEL 718)

7.1 Introduction

In this chapter the performance of vibration assisted grinding was investigated using Nickel alloy along with grinding trials in conventional grinding.

7.2 Experiment Objectives:

- To find out a relationship between the process output parameters and the process input parameters
- To compare grinding without vibration & with vibration.
- To investigate the material removal rates, cutting forces and surface roughness,
- To measure the actual depth of cut & to calculate the specific grinding energy
- To Investigate the wheel wear

The experimental process parameters are given in Table 7.1 and Tables 7.2 and 7.3 illustrate the results

Grinding Parameters	Values
Grinding Wheel Type	(Al ₂ O ₃ : VU33 A602HH 10VB
(V _s) Wheel Speed (m/s)	17m/s (1300 rpm)
(V _w) Work Speed (mm/s)	250
Grinding Condition	Wet Condition
Workpiece Material type	Nickel Inconel 718
Cut Type	Up -grinding,
Depth of Dressing	14 μm/ Single Point Diamond
Applied Depth of Cut- DOC-(μm)	15, 20, 25, 30
Vibration Frequency (Hz)	100
Vibration Amplitude (μm)	130

Table 7.1: Grinding Parameters (Set-up Parameters)

Trial	Process		Parameters	Parameters	
	V_s		V_w (m/min)	<i>Applied DOC</i> (μm)	<i>Actual DOC</i> a_e , Actual (μm)
	(m/s)	<i>rpm</i>			
1	17	1300	15	15	5
2	17	1300	15	20	7
3	17	1300	15	25	10
4	17	1300	15	30	11

Table 7.2: Experimental Results/ With the Application of Vibration Assisted

Trial	Process		Parameters	Parameters	
	V_s		V_w (m/min)	<i>Applied DOC</i> (μm)	<i>Actual DOC</i> a_e , Actual (μm)
	(m/s)	<i>rpm</i>			
1	17	1300	15	15	4
2	17	1300	15	20	6
3	17	1300	15	25	9
4	17	1300	15	30	10

Table 7.3: Experimental Results/ Without the Application of Vibration Assisted

7.3 The Effect of Applied Depth of Cut on Forces

The aim is to measure and investigate the grinding process output parameters for nickel Inconel 718. The results of the measurement enable us to carry out a comparative investigation between grinding output parameters of nickel. Hence, the grinding forces, the material removal rate and the surface roughness have been measured and illustrated in the graphs below.

Figure 7.1 reflects the normal force as a function of applied depth of cut. The normal force values increased with the increase of depth of cut. However, the influence of vibration assisted grinding on the normal force values was significant, as it can be seen from graph 7.1, that the normal force reduced by 45% with the application of vibration similar grinding conditions for conventional grinding.

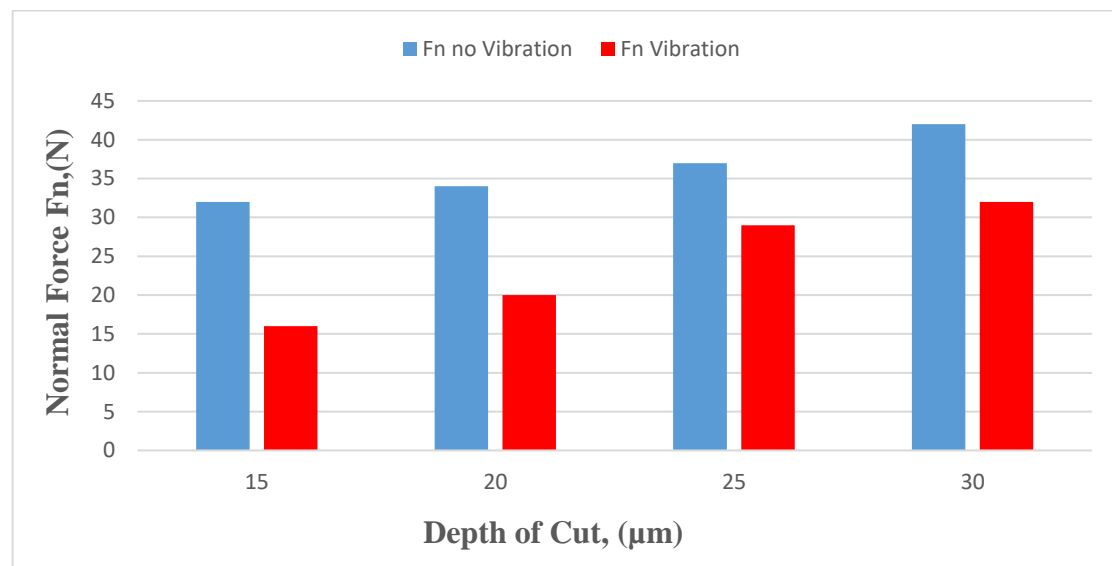


Figure 7.1: Normal force (Inconel 718) as a function of depth of cut when grinding with / without vibration at 17m/s wheel speed, 250mm/s table speed.

Figure 7.2 below illustrates the tangential force as the result of the effect of the applied depth of cut when grinding without and with vibration assisted grinding. Similar to normal force, the tangential force decreased significantly by about 45%, in comparison to grinding without vibration values.

In addition to that, figure 7.3 reflects similar comparison results, in which it appeared obviously that the values of the tangential force are lower than the values of the

normal force in both grinding cases, without vibration and with vibration assisted grinding.

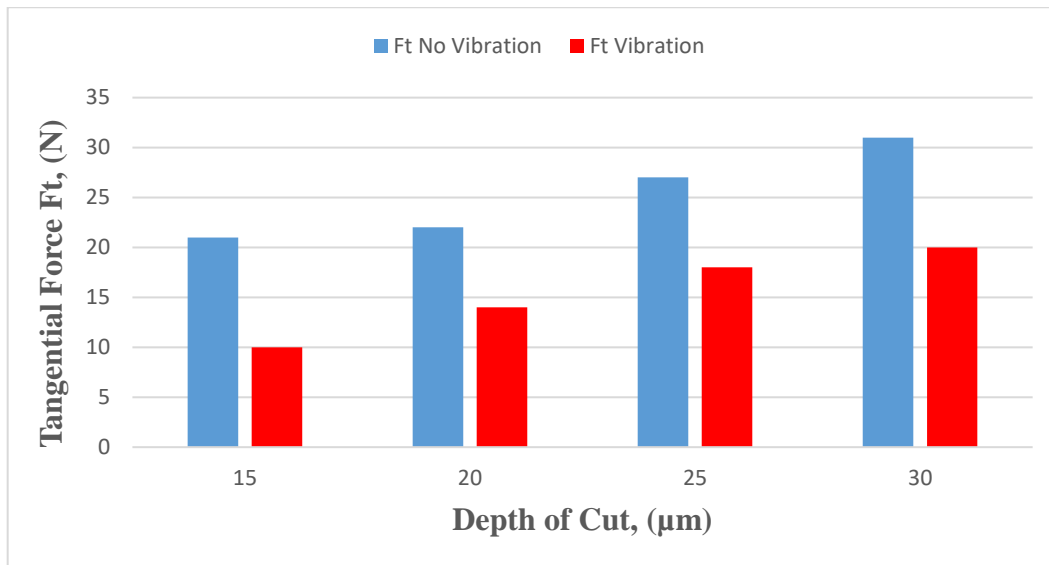


Figure 7.2: Tangential force (Inconel 718) as a function of depth of cut when grinding with/without vibration at 17m/s wheel speed, 250mm/s table speed.

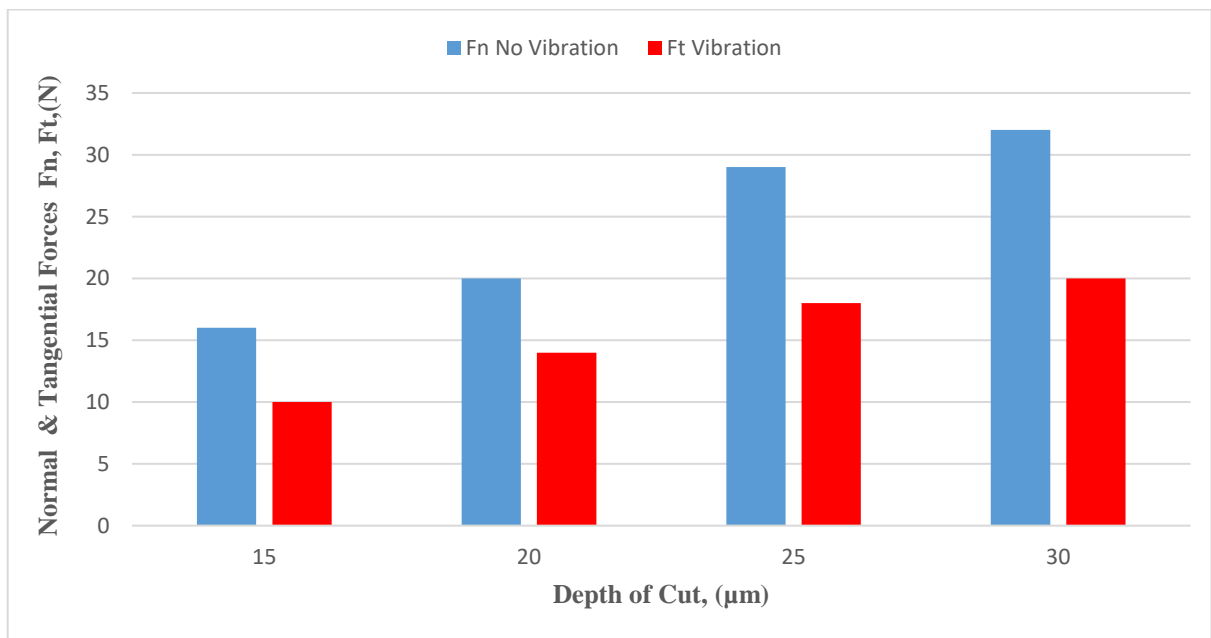


Figure 7.3: Normal & Tangential forces (Inconel 718) as a function of depth of cut when grinding with/without vibration at 17m/s wheel speed, 250mm/s table speed.

7.4 Material Removal Rate (MRR) Results

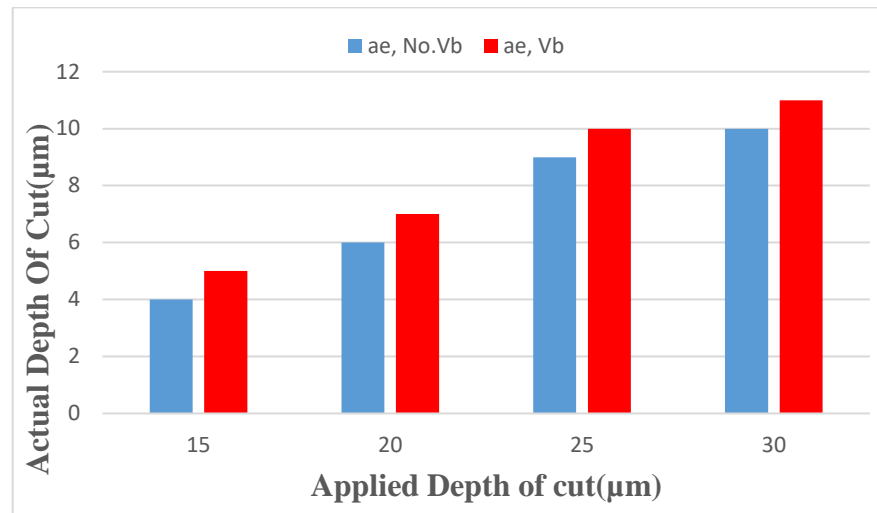


Figure 7.4: The Effect of Applied Depth of Cut on Actual Depth of Cut

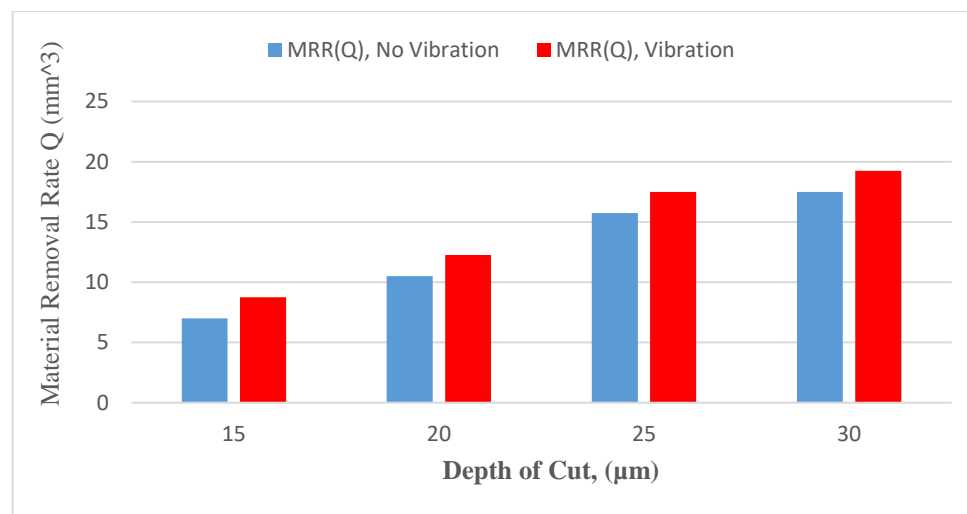


Figure 7.5: The Effect of Applied Depth of Cut on Material Removal Rate

Figures 7.4 and 7.5 give the results of the measured actual depth of cut versus the applied depth of cut. This measured actual depth of cut is used to calculate the material removal rate (MRR) in both cases of the grinding process, with and without vibration assisted grinding. The results also reflect the increases of material removal rate with the application of vibration to grinding. However, as has been mentioned before, the material removal rate is a very important factor in the industry because it describes the performance of the grinding wheel and the quality of the cutting process.

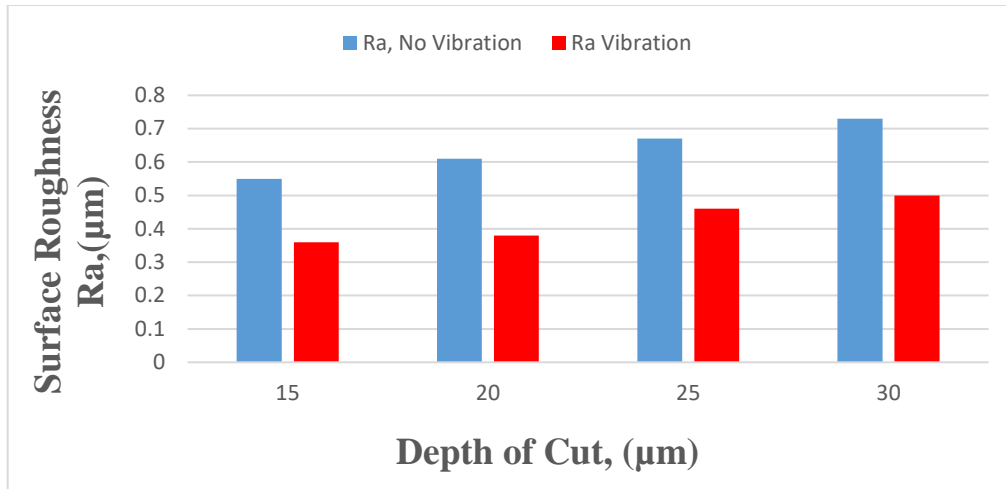


Figure 7.6: The Effect of Applied Depth of Cut on Surface roughness

7.5 Surface Roughness

Figure 7.6 above shows the variation in surface roughness from good quality at low depth (15 μm) of cut to poor quality at high depth of cut (30 μm). Hence, the depth of dressing and coolant fluid are also important factors that could influence surface roughness quality. However, since the machinability of nickel alloy described to be poor due to the risk of workpiece surface damage during grinding process because of the this material low thermal conductivity, high chemical reactivity and strong adhesion with the cutting tool, vibration assisted machining using soft aluminium oxide grinding wheel with the enhance of coolant fluid was introduced to tackle these problems. Figure 7.6 shows that an improvement in surface roughness was achieved with application of vibration assisted grinding, where the red bars in the Figure give that indication, in comparison to the blue bars which represent the surface roughness in case of grinding without the application of vibration assisted.

Figure 7.6 illustrates the results of the measured surface roughness where it appears that the surface roughness for vibration assisted grinding (red bars) is much better in its quality than the one in conventional grinding. The overall improvement of the surface roughness was in the range of 15-20%.

7.5 Process Power and Specific Grinding Energy

Figures 7.7 and 7.8 illustrate the grinding power and the specific grinding energy (e_c) versus the applied depth of cut and the material removal rate respectively. They also show that with the increases in depth of cut the power requirements increased. Equally, an improvement of about 50% in power consumption with the implementation of vibration assisted grinding was achieved. Consequently, the specific grinding energy reflects this-improvement, as it decreases with the application of vibration assisted grinding with an average of $19 \text{ J/mm}^3/\text{mm/s}$.

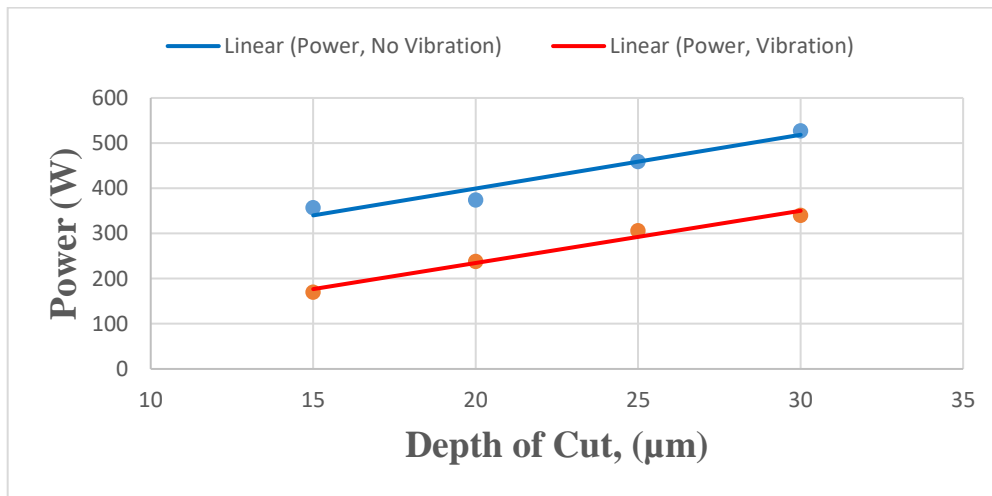


Figure 7.7: Grinding Power Consumption Vs Applied Depth of Cut

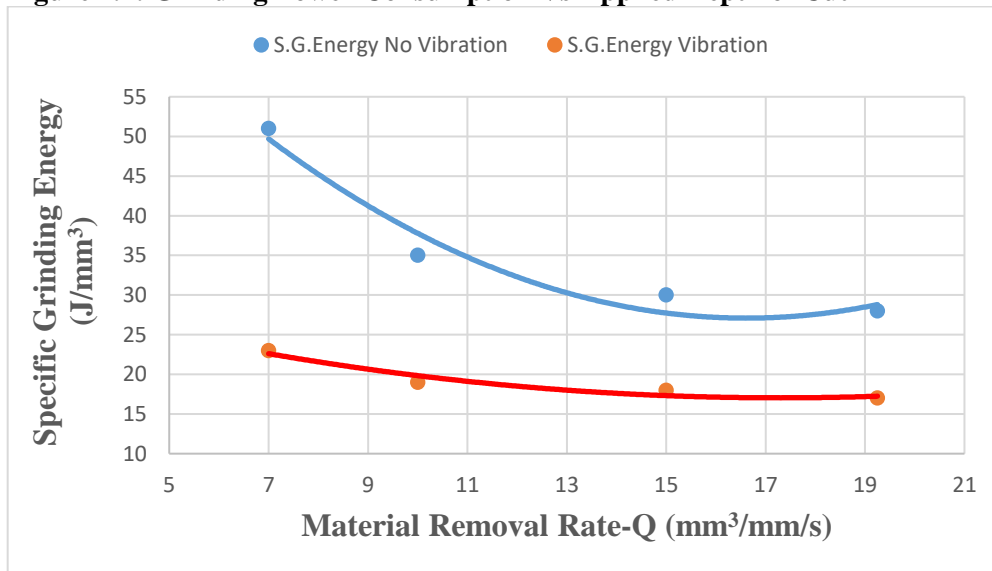


Figure 7.8: Specific Grinding Energy VS Material Removal Rate

7.6 Conclusion

Grinding of nickel alloy didn't differ too much from grinding of Ti6Al4V as both of them are difficult to-machine aerospace materials. Hence, the conclusion has been drawn that the system consumed less energy with the application of vibration to grinding. The results showed that for grinding nickel Inconel 718 the cutting forces were reduced by (35%) with the applied vibration. As contrast the conventional grinding system consumed much more energy to remove the same amount of material volume per unit. Furthermore, the surface roughness measured by stylus (TAYLOR HOBSON) shows that applied vibration for grinding of nickel improves surface roughness quality by 20%, while it increased the material removal rate by 15%. This result is in accordance with a previous study carried out at LJMU laboratory by Andre and Tsakoumis (2014).

CHAPTER 8

RESULTS

**PROCESS PERFORMANCE IN GRINDING ADVANCE
AEROSPACE MATERIALS**

8. PROCESS PERFORMANCE IN GRINDING ADVANCE AEROSPACE MATERIALS

8.1. Introduction

In this chapter the features of the aluminium oxide wheel are described and a comparison in performance between two different aerospace materials is also given. However, the idea behind this comparative study is to explicitly show the performance of vibration assisted and its beneficial in grinding advanced aerospace materials in terms of forces reduction, tool life extension surface finish and material removal rate improvement. However, these findings exposed for a better understanding of low frequency vibration and its possible uptake by the industry for further practical application in real industrial processes. Here though aluminium oxide grinding wheel is not the best choice to grind these though gummy and brittle material, the performance this wheel helps to show the capability of the superimposed vibration with its promising performance even in worst machining conditions.

8.2 The choice of Aluminium Oxide Wheel

Softs wheels including the aluminium oxide wheel allow for stable operation of the grinding process where cutting forces and surface roughness remain stable. This is attributed to the constant release and renewal of the wheel's abrasive grains. However, since the increase in cutting force occurred as a results of the wheel's abrasive grains wear which lead to their release because of the low hardness and retention capacity of the grinding wheel bond, the opposite is also correct.

Furthermore, this constant release of abrasive grains leads to a decrease in the wheel diameter which results in G- ratio drop. On the other hand, if the wheel of choice is a hard bond abrasive grains wheel then the excessive increase in tangential cutting force caused by the wear of the abrasive grains lead to high energy consumption which causes an increase in the grinding zone temperature and then thermal damage and surface roughness deterioration.

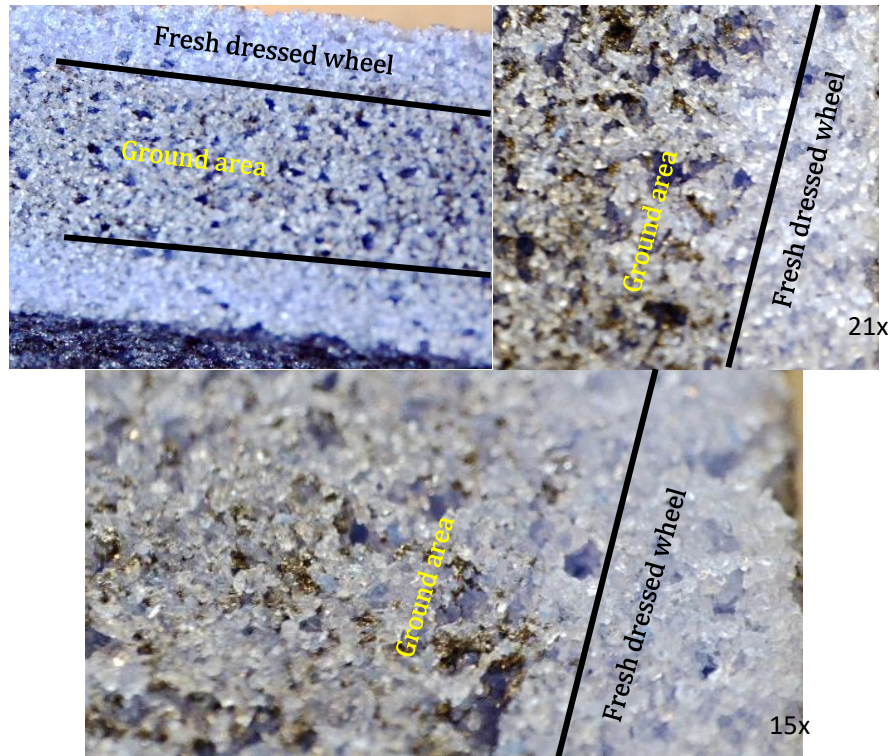


Figure 8.1: Image of the wheel surface after series of test grinding showing no clogging

8.3 Process performance in Titanium and Nickel alloys

The process parameters used in this experiment are 17m/s wheel speed, 250mm/s feed rate and applied depth of cut varied between 10 to 35 μm . The following graphs in Figures 8.2, 8.3, and 8.4 reflected the experimental results of normal cutting forces (F_n) in grinding without and with vibration for two different aerospace materials namely Ti-6Al-4V and nickel Inconel 718. Here identical conditions of grinding operation were used, and the graphs illustrate the performance of both materials as a function of applied depth of cut.

However, Ti-6Al-4V appears to have the highest demand of cutting forces, in comparison to nickel Inconel 718 in both cases of grinding, without vibration and with the application of vibration. Furthermore, the projection of forces requirement for nickel Inconel 718 shows the lowest normal force in comparison to Ti-6Al-4V this is because of the low amount of material removal rate in grinding of nickel. This low material removal is attributed to the toughness of the materials from one hand and from the other hand it is also attributed to the type of grinding wheel that has been employed (soft aluminium Oxide Grinding Wheel Al_2O_3 (OVU33 A602HH 10VB)), rather than hard CBN or Diamond wheel

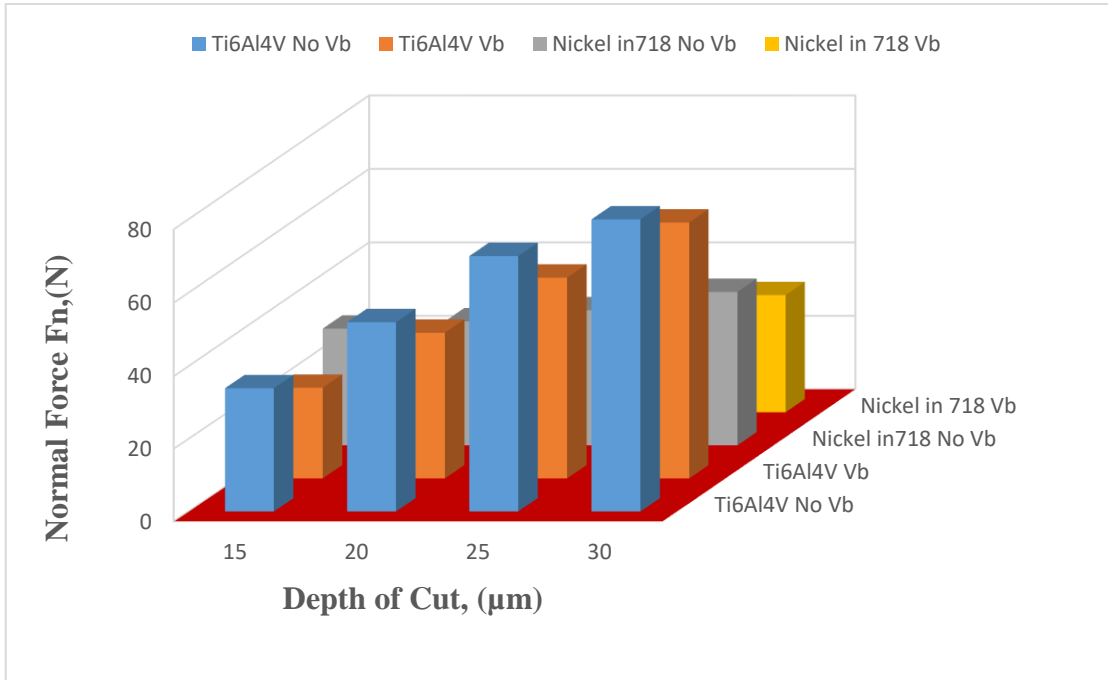


Figure 8.2: Normal Force Versus Applied Depth of Cut for Titanium and Nickel alloys

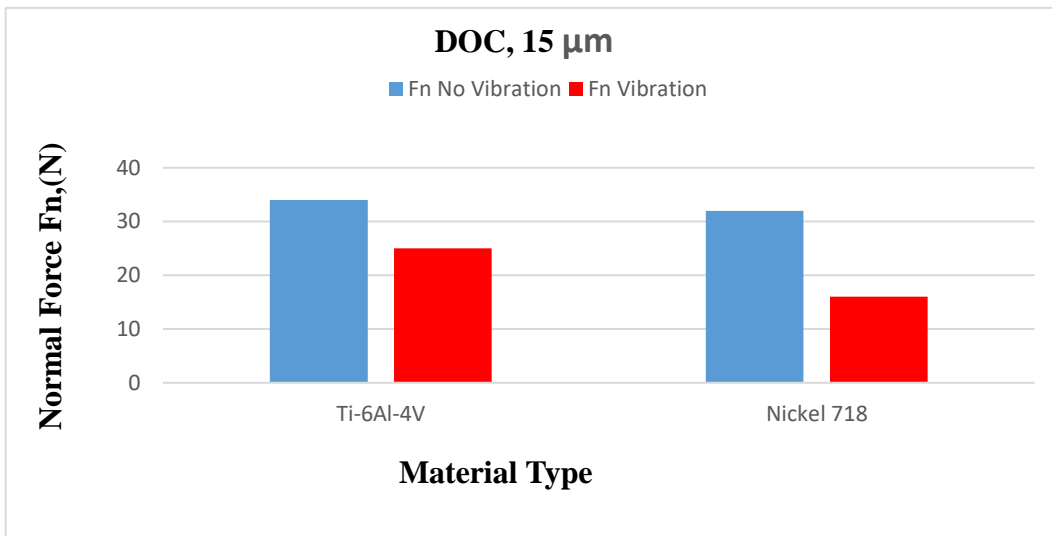


Figure 8.3: Normal Force for titanium and Nickel alloys (15 m)

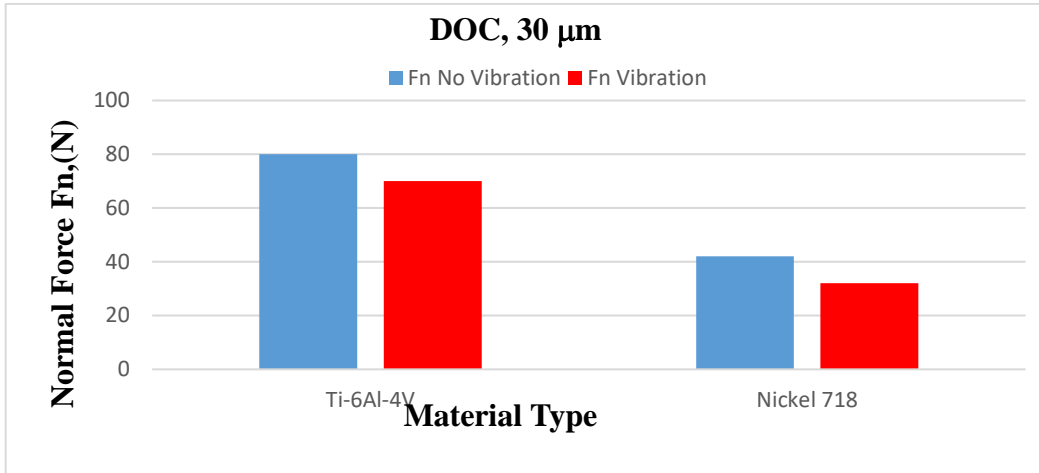


Figure 8.4: Normal Force for Titanium and Nickel alloys (30 · m)

Figures 8.5, 8.6 and 8.7 illustrate the relationship between the tangential force and the applied depth of cut when grinding the two advanced aerospace materials with and without the application of vibration assisted under similar grinding conditions. The tangential forces showed opposite indication in values compared to the normal forces, as it appears lower for nickel and higher for Ti-6Al-4V. Hence, this result indicated the advantageous of nickel upon the Ti6Al4V and other aerospace material in terms of forces requirement, energy consumption and tool life issue.

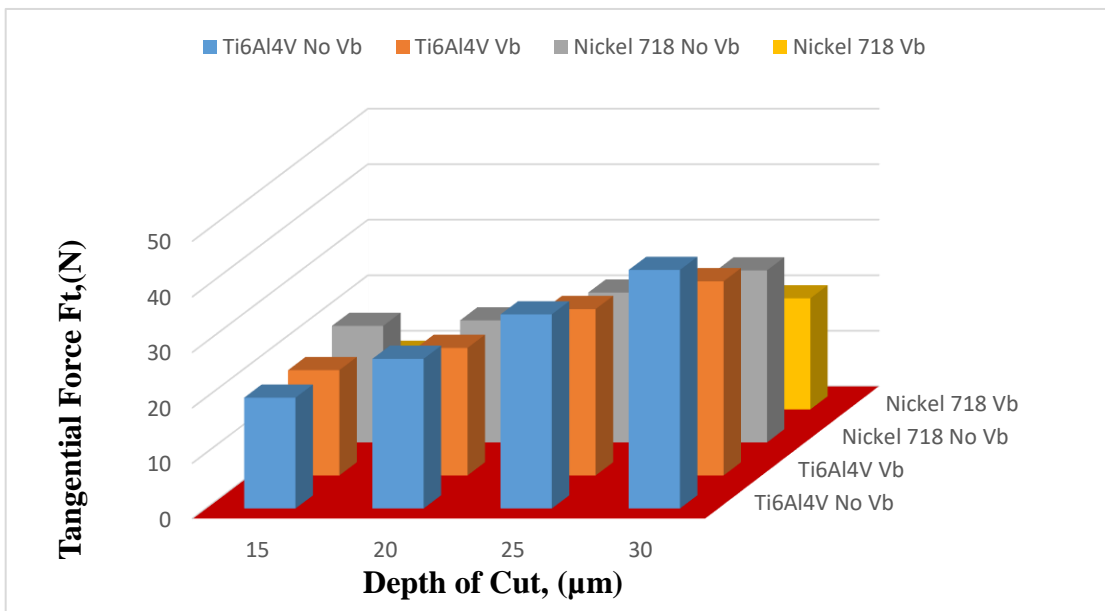


Figure 8.5: Tangential Force Versus Applied Depth of Cut for Titanium and Nickel alloys

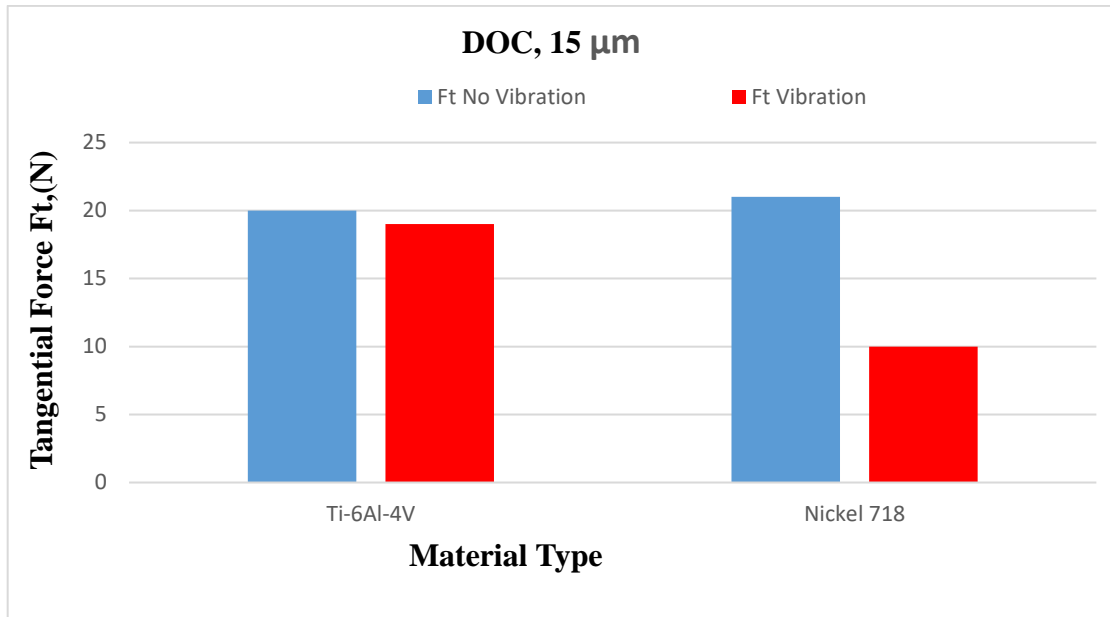


Figure 8.6: Tangential Force Titanium and Nickel alloys (15 · m)

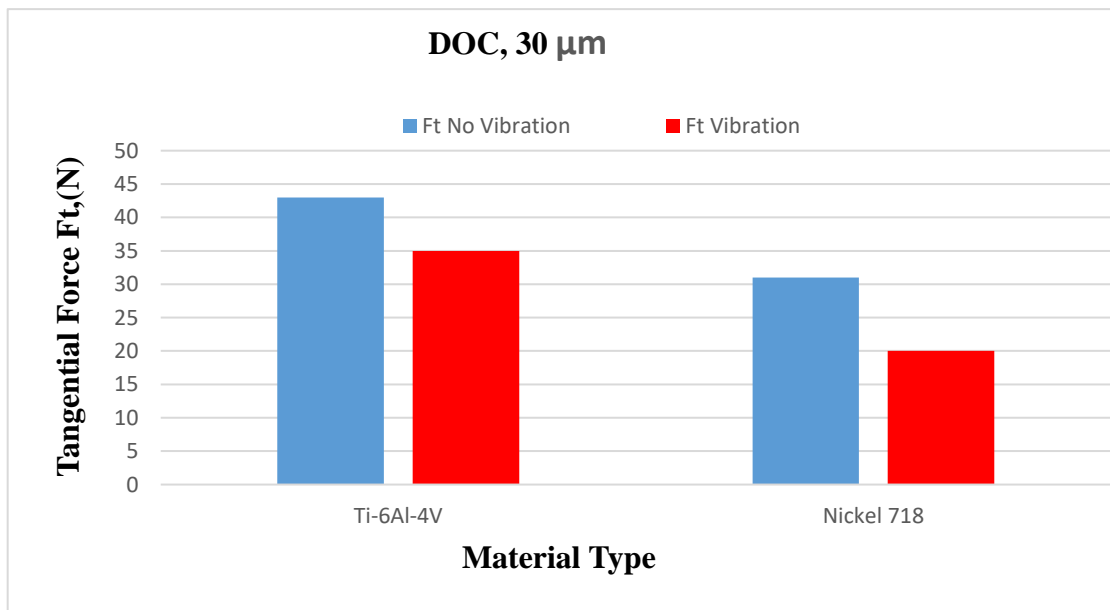


Figure 8.7: Tangential Force for Titanium and Nickel Alloys

8.4. Power and Specific Grinding Energy

Figures 8.8 and 8.9 show the power consumption when grinding titanium and Nickel alloys under similar grinding conditions (e.g. 15μm & 30 μm depth of cut), at 17m/s wheel speed and 250mm/s feed rate.

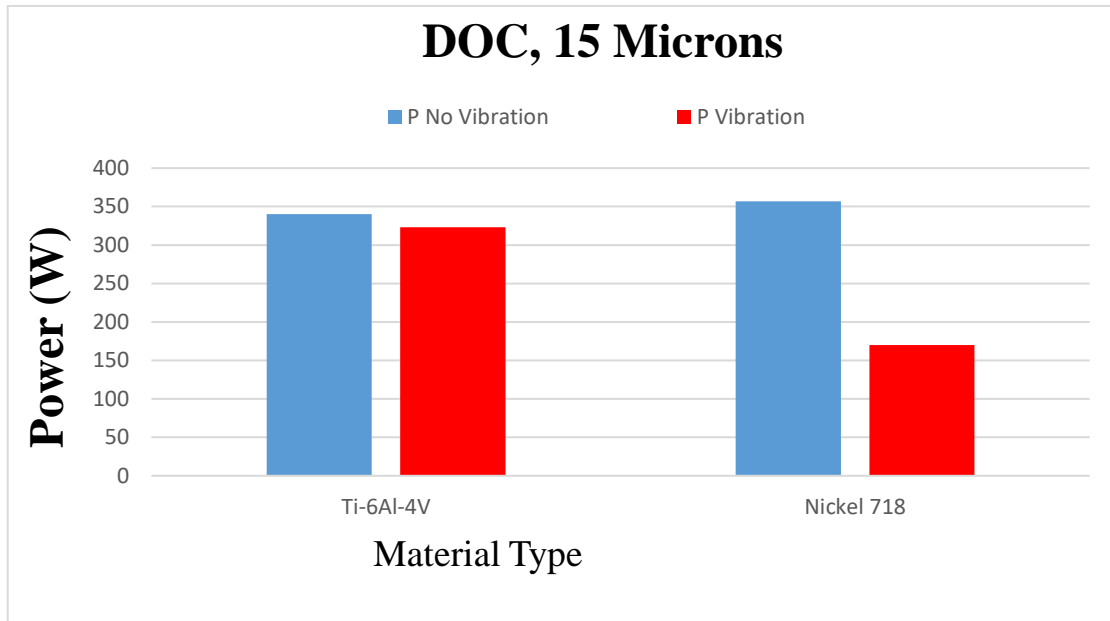


Figure 8.8: Power Consumption Versus Applied Depth of Cut for Two Materials (15 μm)

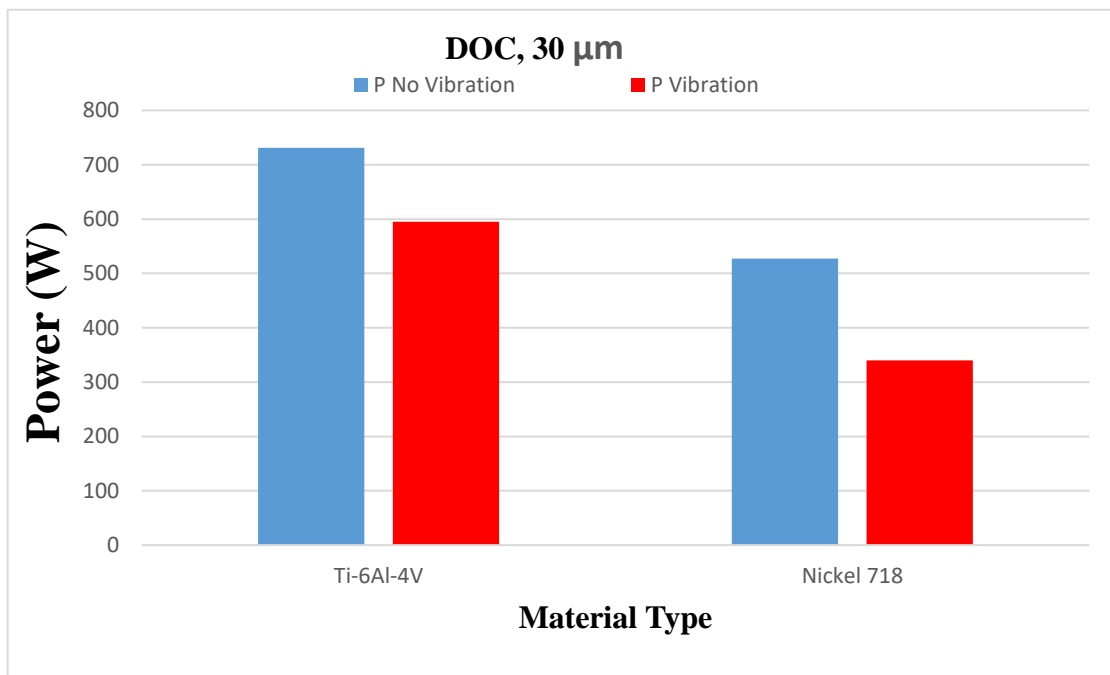


Figure 8.9: Power Consumption Versus Applied Depth of Cut for Two Materials (30 μm)

The Figures also show that the application of vibration assisted reduced the power consumption. This finding is well highlighted especially in case of grinding nickel alloy where vibration secured 35% less power consumption than the power that could be consumed in conventional grinding.

Figures 8.10 upto to 8.12 represent the relationship between the specific grinding energy and the material removal rate for two advanced aerospace materials. The nickel alloy Inconel 718 has higher specific grinding energy than the titanium Ti6Al4V. However, from cost perspective fact, the lower specific grinding energy the better.

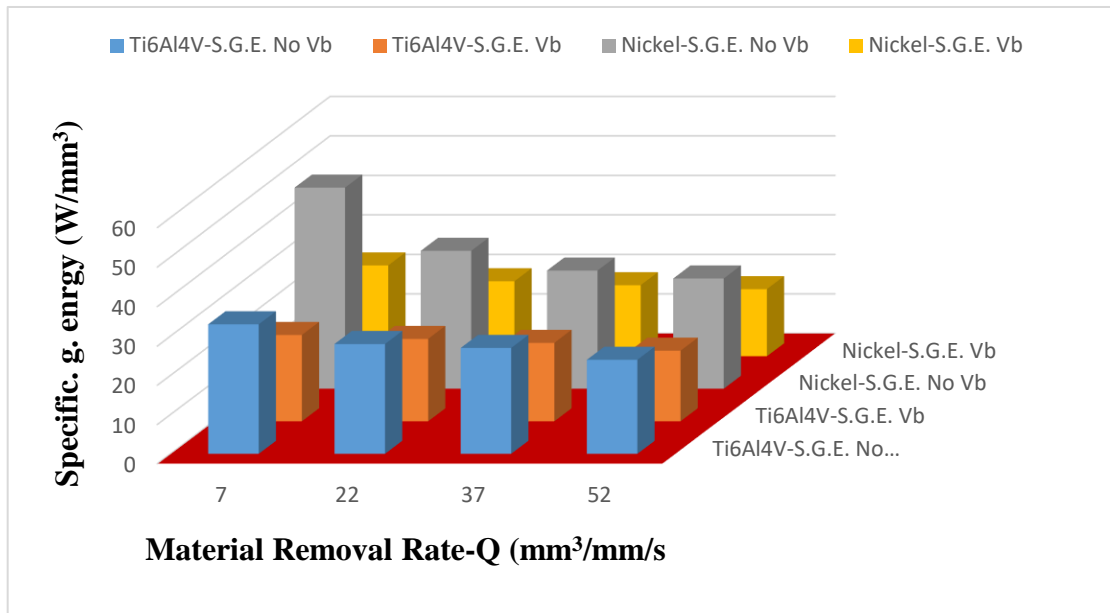


Figure 8.10: Specific Grinding Energy for Titanium and Nickel

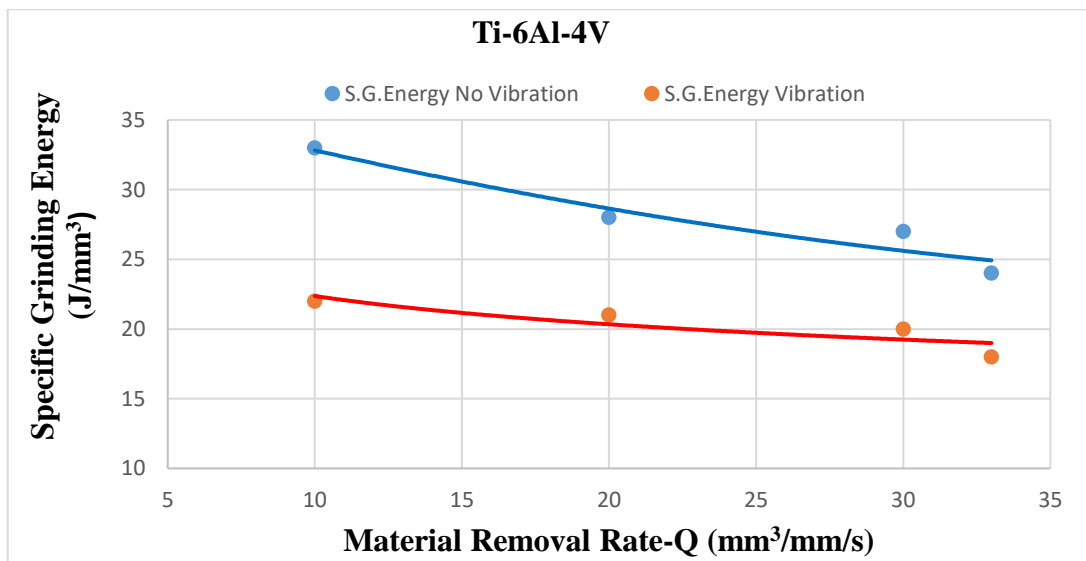


Figure 8.11: Specific Grinding Energy Versus Material Removal Rate

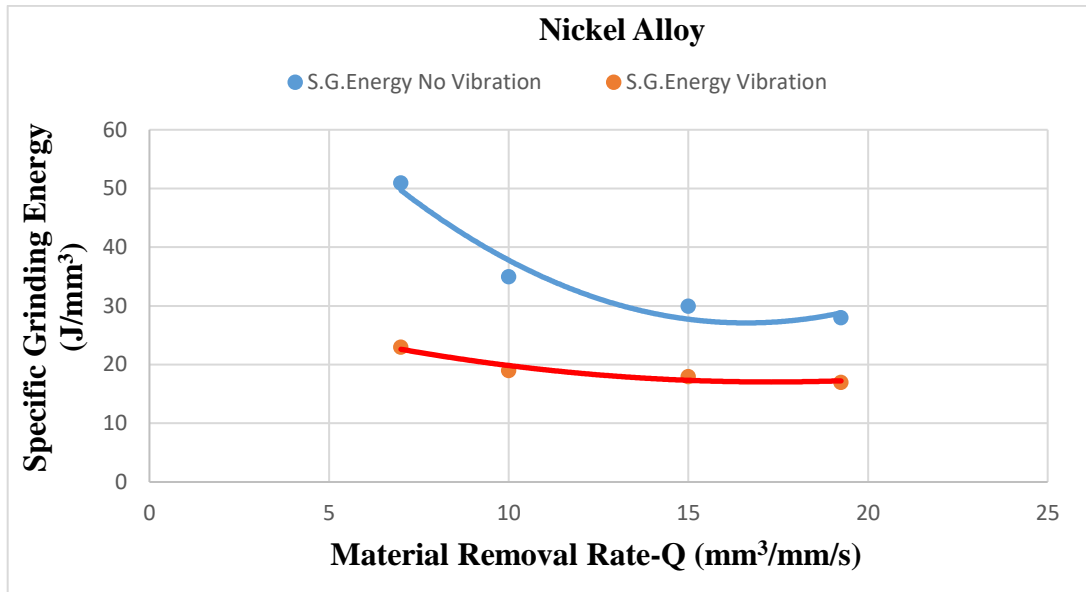


Figure 8.12: Specific Grinding Energy Versus Material. Removal Rate.

8.5 Material Removal Rate

Figures 8.13, 8.14 and 8.15 illustrate the variation in material removal rate for the two aforementioned advanced aerospace materials. The graphs in these Figures showed that for 15 μ m, and 30 μ m depth of cut, the measured material removal rate with application of vibration is more much higher (10%) than in the conventional grinding. However, Figure 8.15 depicts the overall performance of both materials in grinding with and without vibration. Here it is seen that Inconel 718 performed better than Ti6Al4V with the superimposed vibration. Hence, it can be seen that nickel alloy has an increased material removal rate than titanium.

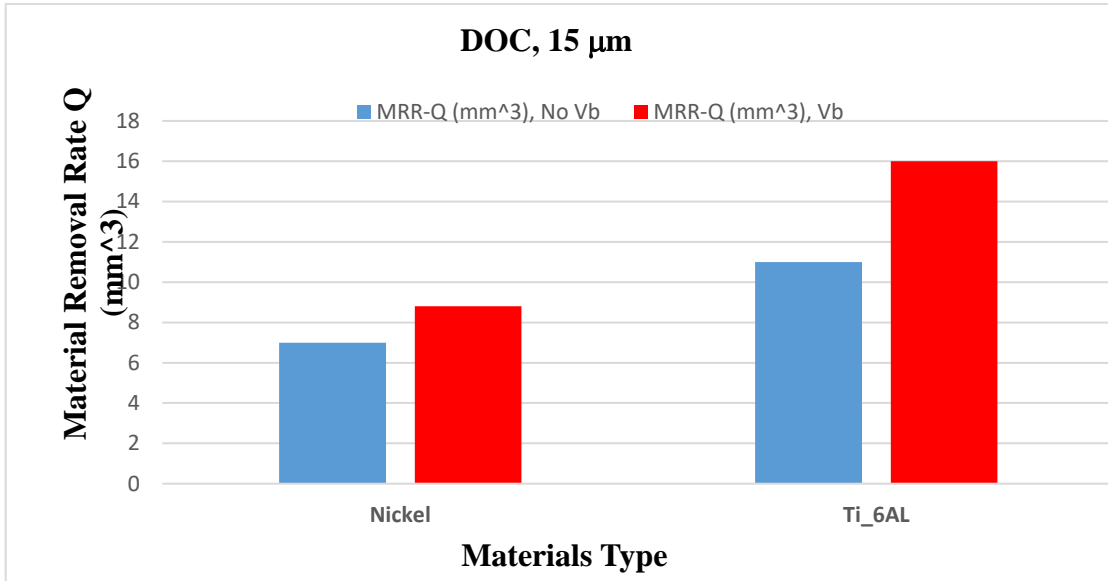


Figure 8.13: Material Removal Rate Titanium and Nickel alloys (15 μm)

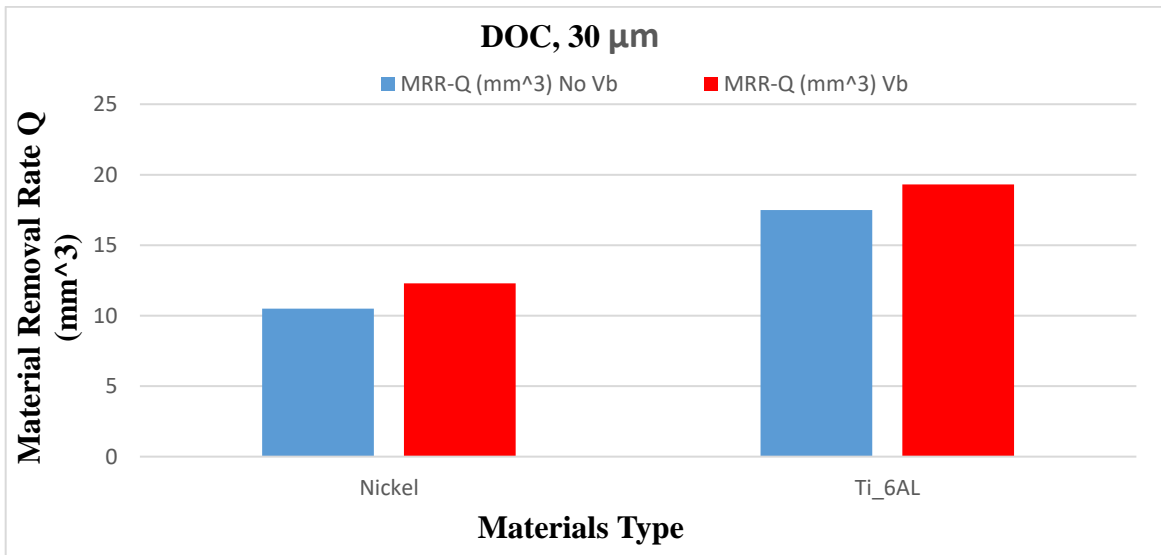


Figure 8.14: Material Removal Rate Titanium and Nickel Alloys (30 μm)

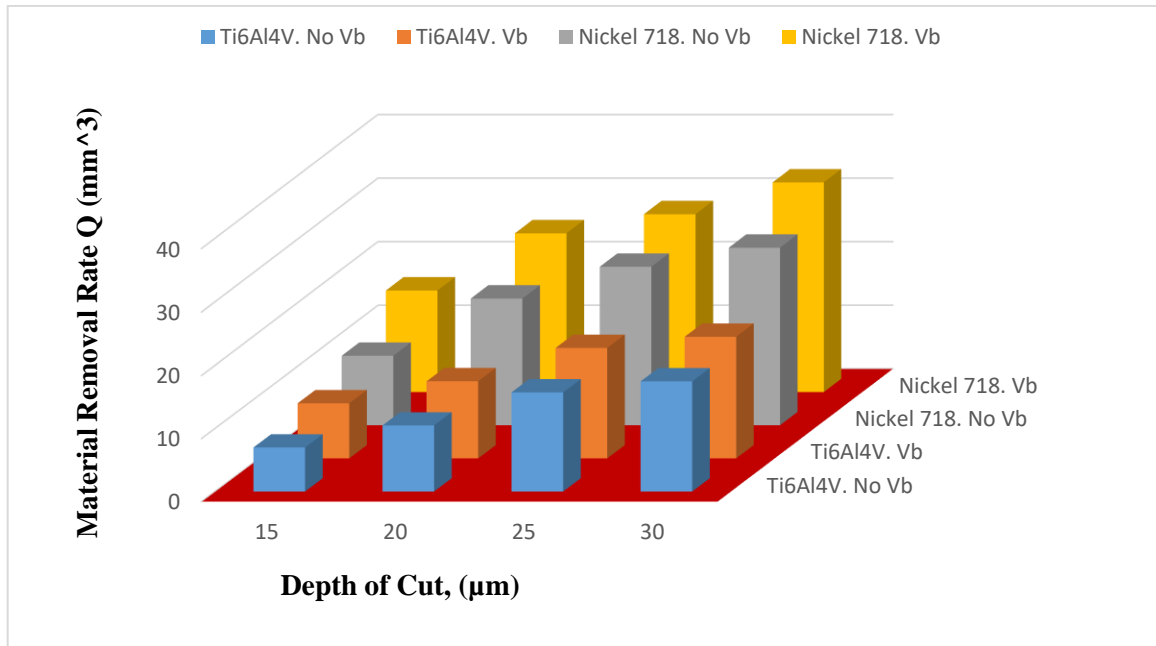


Figure 8.15: Material Removal Rate for Nickel Alloy & Ti-6Al-4V, Without / With Vibration.

8.6. Surface roughness (Ra)

Figures 8.16 and table 8.2 illustrate the variation in surface finish quality in terms of roughness Ra. Although the quality of the surface roughness depends highly on the applied depth of cut and the depth of dressing, in this case the stiffness of the material and its mechanical properties play an important role, as these materials are described as being among the most difficult to machine, and this has been recognised by K. Kocman (2011). These two aerospace materials surface' roughness is easily to be damaged during any machining process due to their poor machinability: low thermal conductivity and high chemical reactivity cause heat generation during machining, and strong adhesion as well, between the work piece and the cutting tool. All these reasons led to poor surface quality.

However, the results show that improvement in surface roughness was achieved with the application of vibration, and this was achieved by operating at moderate grinding wheel speed, 17 m/s, feed rate of 250 mm/s and with 14μm depth of dressing. Nevertheless, under these grinding conditions with the application of vibration and

with enhancement of coolant, the surface roughness 'Ra' for nickel alloy Inconel 718 appeared to be better quality than the surface roughness of Ti6Al4V (25%).

DOC	Nickel Alloy		Ti-6Al-4V	
	Ra No Vb	Ra Vb	Ra No Vb	Ra Vb
15	0.55	0.36	0.49	0.40
20	0.61	0.38	0.6	0.55
25	0.67	0.46	0.5	0.41
30	0.73	0.5	0.45	0.42

Table 8.1: Surface roughness measurement for $V_s = 17\text{m/s}$, $V_w = 250\text{mm/s}$

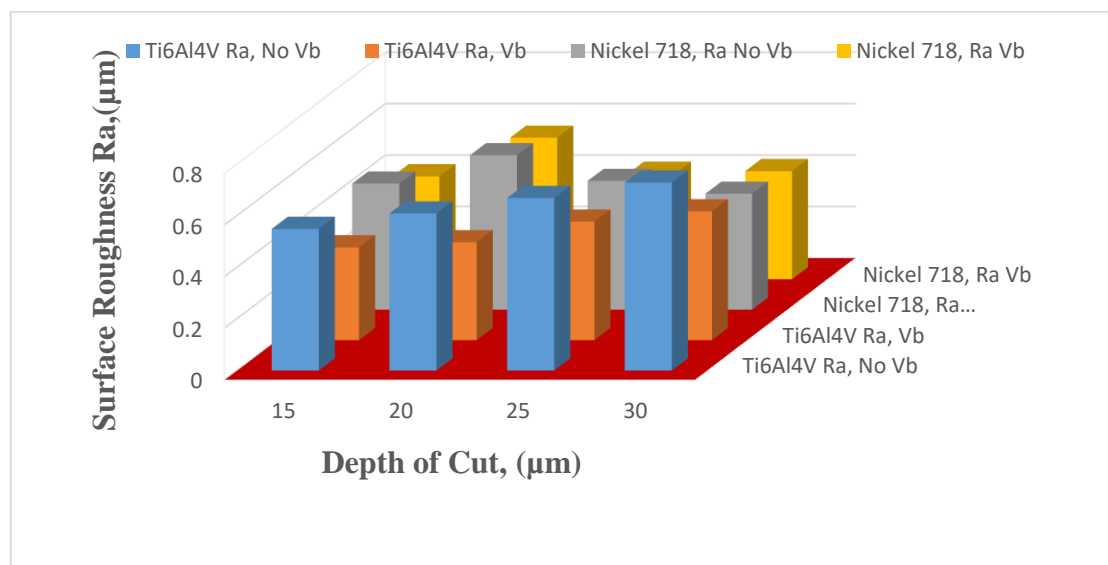


Figure 8.16: Surface Roughness for wheel speed 17 m/s and work speed 250 mm/s

8.7 Wheel Wear

Wheel wear by definition is the amount of material that is moved out of the wheel during grinding process and the grinding wheel wears out. Mostly in fine grinding, a

wheel becomes dull rather than sharp, at some point of the grinding process the wheel need to be dressed. However, in general the grinding wheel performance deteriorates in three different ways such as:

- i. Gradual wear of the grains which lead the wheel to become dull.
- ii. Loading of workpiece material into the wheel surface
- iii. Losing the wheel sharpness.

Therefore, wheel wear is classified into three different mechanism types as followed:

- 1- Attritions wear, which involve slow dulling of the abrasive grains
- 2- Grain fracture wear which refers to removal of abrasive fragments from the grain due to internal stress
- 3- Bond wear refers to the acting force on the grain caused stresses that exceed the fracture stress of the bond.

Moreover, wheel wear can be measured via a correlation of the amount of material ground, known as grinding ratio (G-ratio). That is equal to the volume of wheel material removed to the volume of workpiece material removed.

8.8 Wear Observation and Testing

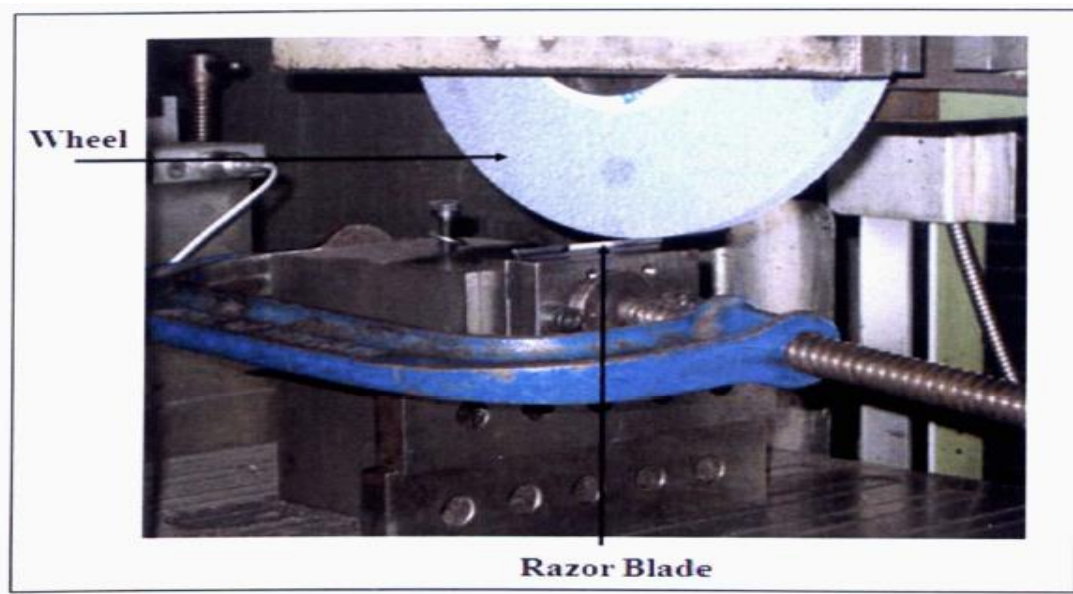
An initial observation of wheel state has showed no clear sign of wheel clogging or wear. This is illustrated in Figure 8.1, where one can see that wheel is still clean and open with not clogging. The dark area marked “Ground area” is the part of the wheel that was used during grinding and the part marked “Fresh dressed wheel” shows the initial wheel state after dressing. Comparing these two areas it is seen that the wheel is not damage and not warn out. However, wheel wear tests are planned for the last stage of experiments, where continuous grinding with given depth of cuts and given time will used to characterise wheel wear performance and to derive the G-ratio.

Figure 8.1: Image of the wheel surface after series of test grinding showing no clogging, the experiment here, was conducted with an aluminium oxide grinding wheel (OVU33 A602HH 10VB) using Nickel 718 and Ti-6Al-4V

The wheel was dressed before each trial and a given amount of material from each workpiece was removed in several grinding passes, starting from 20 μ m and up to 1000 μ m for the titanium alloys and up to 600 μ m for the nickel alloys. These trials were repeated with the application of vibration and without the application of vibration at 17 m/s wheel speed and feed rate of 250 mm/s.

Subsequently, a razor blade was used to replicate the wheel wear profile as illustrated in Figure 8.17 the replicated inverse profile on the blade was measured using Taylor Hobson surface texture measurement machine with a stylus. This machine shown in Figure 8.18 was equipped with computerised special software able to scan the blade edge and to produce the wheel surface texture. The results and profiles of the measurements are shown in appendices D.

Test using Razor Blade Method:



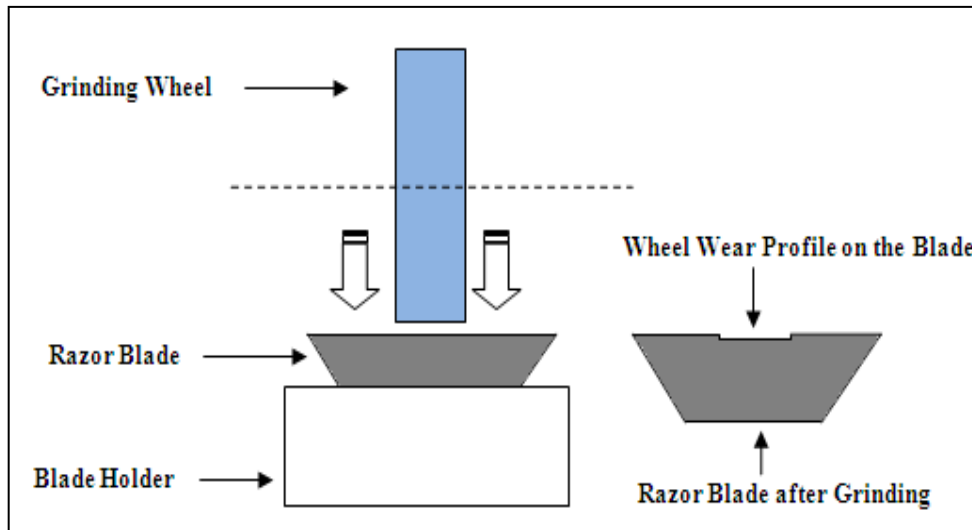


Figure 8.17: Wheel Wear Test Using Razor Blade Method

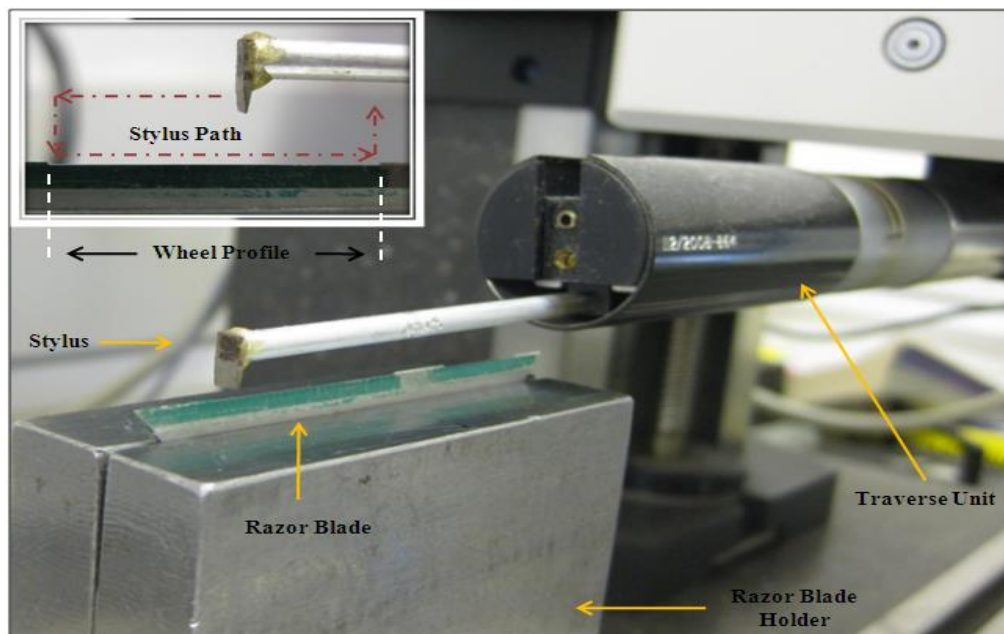


Figure 8.18: Wheel Wear Test Measurement Configuration

Figure 8.19 illustrates the results of both cases grinding with vibration and without vibration. It appears that the wheel wear for the Ti6Al in conventional is much higher than that for nickel which gives an indication that this grinding wheel seemingly inadequate, can be used for Ti6Al4V if the cost of the wheel is taken in to consideration.

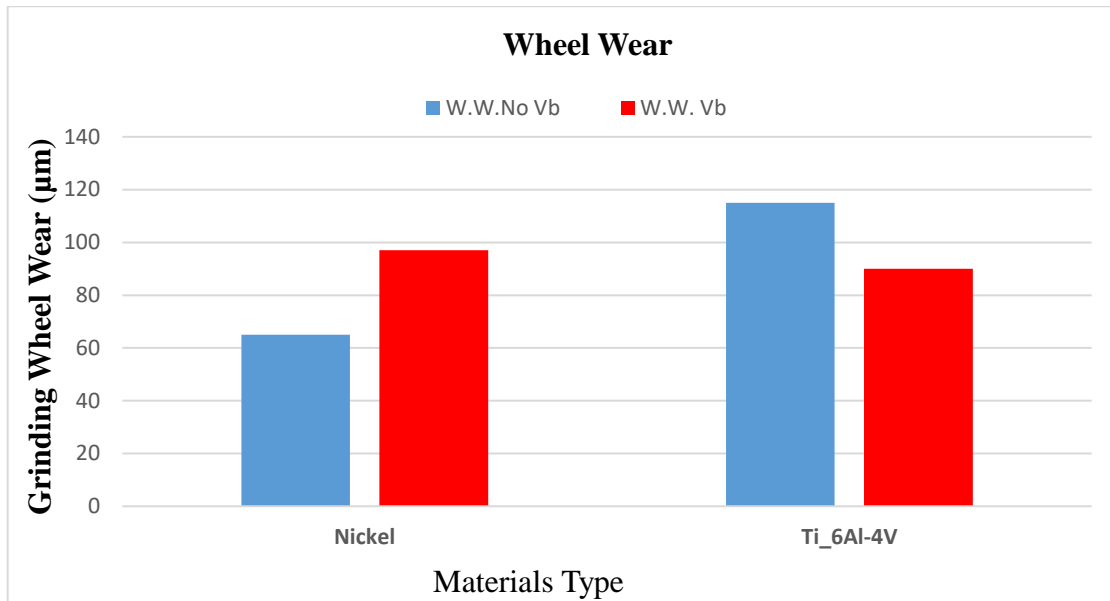


Figure 8.19: Wheel wear

8.9 Material Removed

The results presented in figure 8.20 demonstrate the amount of material ground of the work-pieces in wear test, that evolved from 20 µm up to 1000 µm then the material removed was calculated. It is observed here that in both materials, the application of vibration secured a higher material removed than that without vibration. This evidences improved cutting efficiency of vibratory process and its ability to reduce not only cutting forces but also the tool wear.

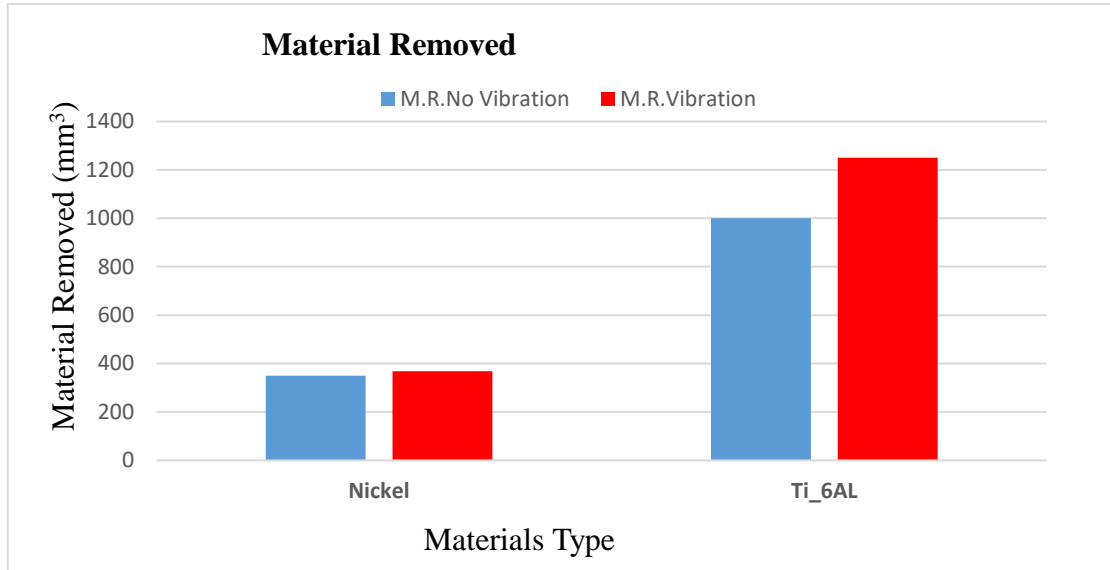


Figure 8.20: Material removed

8.10 G-Ratio

The G-ratio is defined by the amount of material being ground per unit wheel width to the volume of wheel worn per unit wheel width. **G-ratio** = V_w/V_s

Where V_w = Volume of metal removed (in.J/ mm³) and V_s = Volume of wheel wear (in.mm³).

Rowe. Second Edition stated that a high G- ratio may be in excess of 5,000, is possible for hard grinding wheels whereas for difficult to machine material, the G-ratio might be as low as 1. Moreover, the experiments outcome are in agreement with Rowe's statement (B. Rowe. Edition 2) and secures reasonable G-ratio as shown in figure 8.21 it is to admit that the soft aluminium oxide wheel is not hard enough for grinding hard aerospace materials. However, an improvement in the G- ratio was achieved by the vibratory grinding of titanium alloy, but a net decrease is observe in nickel alloys.

In general the G-ratio variation in Figure 8.21 reflects that the wheel wear strongly depends on wheel speed and work speed at high removal rate (Batako et al., 2012). However, a G-ratio of less than 3.5 achieved is slightly acceptable, especially at 17m/s wheel speed and 1mm depth of cut because that the aluminium oxide wheel grains wearied excessively at high level.

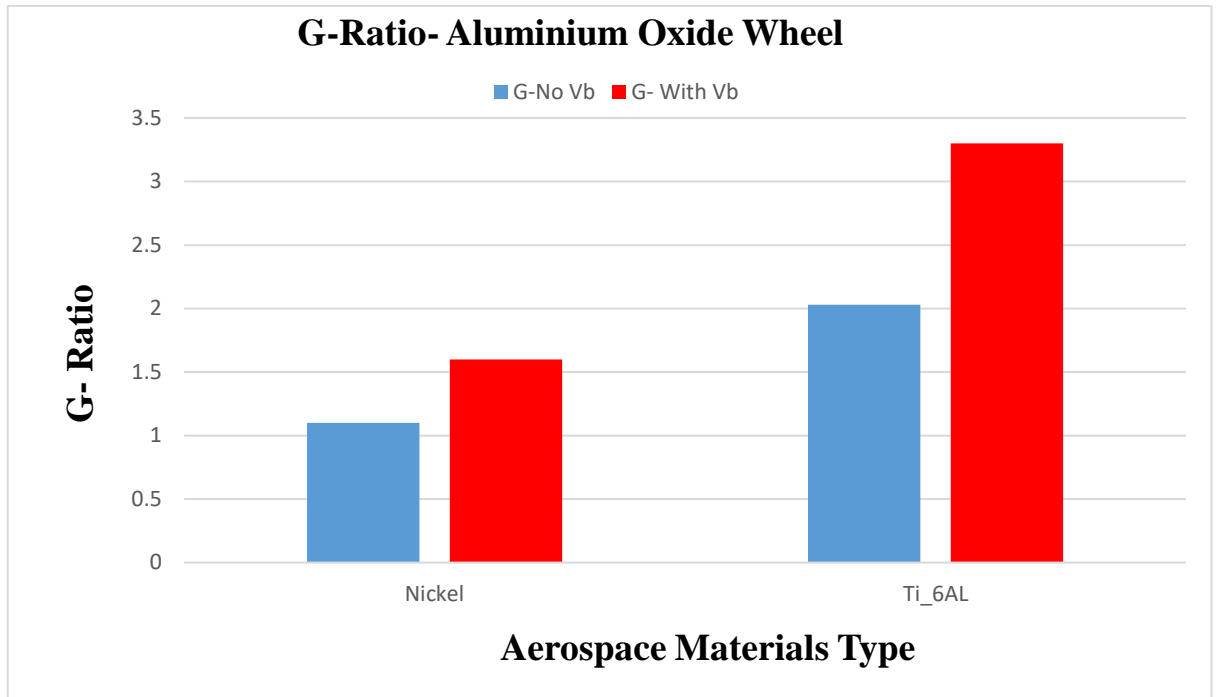


Figure 8.21: Grinding G-ratio

8.10.1 MATLAB Software Modelling For Single Grain Grit to achieve Chip length Calculations

Single Grain Grit Diameter 120 μm , grinding time 0.001 second, Frequency 100Hz, Depth of cut 3 μm , Feed rate 250mm/s, Wheel speed 17m/s, Amplitude 130 μm .

The Model below had been run in MATLAB to prove that vibration assisted grinding is better off than grinding without vibration assisted. It has been noticed that from the modelling for a single grain grit aluminium oxide wheel cutting tool, that the chip length is taller in vibration assisted grinding by 1.5% and also smaller in terms of thickness, which proved the claim of force reduction, wheel wear reduction as well and improvement in the material removal rate.

```
>> run('C:\Users\GNREIBRA\Desktop\lclg.m')
```

```
lg = 0.4899 (Geometrical contact length= chip length at no vibration mode)
```

```
T = 0.0020
```

```
lc = 0.4955 (Real contact length= chip length at vibration mode)
```

$dl_percent = 1.5\%$ (Increase in chip length in percentage)

8.11 Concluding Remarks

The conducting surface roughness for Inconel 718 was much better with the superimposed vibration than that of Ti6Al4V while the material removal rate was the inverse the forces and the process energies were lower in nickel alloy than Ti6Al4V grinding with and without the superimposed vibration

The results also showed the benefit of vibration assisted grinding in terms of wheel wear, material removal rate and grinding force ratio. Hence, it has been noticed the applied vibration assisted increased material removal and extended wheel life by 35% In titanium alloys, (See modelling above in MATLAB Software).

CHAPTER-9

**DISCUSSION, CONCLUSION &
RECOMMENDATIONS**

9. DISCUSSION, CONCLUSION & RECOMMENDATIONS

9.1 Discussion

The aim of this project was to investigate into the benefits of vibration assisted grinding of difficult-to-cut aerospace materials, the machining of which pose a great challenge. This challenge was met by employing a piezo-actuator that vibrated the work-piece during surface grinding process. Periodic oscillations were applied in the perpendicular direction of the grinding direction. The purpose was to reduce the cutting forces, to improve the surface quality of the work-piece, along with the material removal rate and to extend the tool life.

A literature review was undertaken to get good understanding of any work been done so far in this field in the past and currently, after a comprehensive search it was found that very limited publications in this subject were in access. However, most of the work been done in the past was in the field of ultrasonic vibration by imposing high frequencies oscillations which could reached up to 100kHz [REF. The reason behind this idea because it has been proven that the bigger the amplitude the better the surface quality might be achieved of the ground product [].

The vibration mechanism allowed the whole system to vibrate the work-piece in a direction perpendicular to the grinding direction at 100 Hz vibration frequency with a displacement to 130um.

Several equipment were tested as well including the traditional surface grinding machine ABOOD with its maximum grinding wheel speed of 6000rpm, while the material under investigation was identified, machined, prepared, and characterised Via “Electrons Scan Microscope”. A data acquisition with PC was set to capture grinding data for analysis.

By employing design of Experiment Taguchi orthogonal array the combinations of the process parameters were designed in which the depth of cut, the feed rate and the grinding wheel speed were chosen to grind Inconel 718 and Ti6Al4V with an aluminium oxide wheel. The grinding forces, the surface roughness, the specific grinding energy and the material removal rate were investigated.

The results showed that the grinding forces reduced remarkably when vibration assisted was applied especially at higher depth of cut, as trials for both normal and

tangential forces reflected force reduction of 45% while the surface roughness was decreased for all depth of cut when vibration assisted was applied.

However, these results reflected that Taguchi design of experiment arrays was a suitable method to examine the effects of grinding process parameters upon each other. Hence, it was found that when vibration assisted imposed, the depth of cut values influence directly the cutting forces, as when grinding at high depth of cut the forces were reduced by 30%. On the other hand, the influence of table speed and wheel speed were also specified and it was found that at higher table speed and higher wheel speed a higher reduction in forces and power was achieved (30%). Similar results for surface roughness were obtained when high wheel speed was used with applied vibration, and a better quality of the ground work-piece surface was achieved as well.

Furthermore, when vibration assisted grinding applied the values of actual depth of cut obtained were slightly low because of the work-piece been displaced very much. Thus a 20% material removal rate was secured.

After the preliminary experiments a set of experiments were carried out with similar grinding conditions and similar grinding parameters arrangement for titanium Ti6Al4V alloy and nickel Inconel 718, for all these sets of experiments a closed-loop control system setup was also used to control the vibration- assisted grinding process. The closed-loop control system kept the given vibration amplitude constant during the experiments.

A similar procedure as in the preliminary experiments was repeated for the grinding of titanium Ti6Al4V alloy where the vibration –assisted was also applied here. The results gave a reduction in cutting forces of 30% was observed for both tangential and normal forces especially at high depth of cut. Whilst the power consumption and the specific grinding energy were also reduced remarkably. On the other hand, the material removal rate was increased and the surface roughness quality was also improved.

Moreover, for this particular aerospace material the grinding parameters boundaries were found and specified for the ABWOOD traditional surface grinding machine (17m/s wheel speed, 250mm/s table speed, 15- 30 μm depth of cut and 14 μm depth of dressing), these boundaries obey the conditions of preventing the work-piece from being burnout or smeared.

These set of experiments were conducted and repeated again with another hard to machine aerospace material namely nickel Inconel 718 alloy, where vibration was also introduced with coolant.

However, although the material is too hard to be cut with soft grinding wheel, a reasonable amount of material was moved especially at higher depth of cuts. The results showed that the grinding cutting forces were reduced by 35% when vibration-assisted was applied. Consequently the power consumption and the specific grinding energy were reduced while better quality of surface roughness was achieved. The obtained surface roughness was measured using the stylus surface texture machine, and the appendices reflected the surface roughness profile pattern.

A comparative procedure between two hard aerospace materials been made to validate the investigations results. The results showed that nickel Inconel 718 got slightly advantages over Ti6Al4V in terms of surface roughness quality, forces and power consumption. Nickel alloy required low forces and then low power in comparison to Ti6Al4V, especially when vibration-assisted was applied. Meanwhile, Ti6Al4V got also one advantage over nickel particularly in material removal rate, as the material removed for this alloy is much higher than that of nickel because of the soft aluminium oxide wheel grains size and toughness.

Finally, since wheel wear is a factor of wheel life, the aluminium oxide grinding wheel type (Al_2O_3 (OVU33 A602HH 10VB) was employed to observe a specific amount of material removed repeatedly. Hence, several grinding trials were carried out for both materials, starting from 20 μm and up to 1 mm depth of cut. The results showed that the wheel wear decreased when vibration assisted was applied. In addition to that, the removed materials in both cases higher when vibration assisted was applied. The G-ratio calculations proved that vibration assisted has positive influence on the grinding process, this could be seen from the increase of 40% G-ratio value in case of Ti6Al4V grinding.

9.1.1 Single grit Cutting dynamics-chip length

Due to the periodic oscillating of the work-piece in vibration assisted grinding, smaller chips will be formed during each cycle. However, the higher the vibration frequency the shorter the period time of the cycles. By means that many cycles took place at short interval of time. Thus, that means a short chip can be formed (chip

segmentation). Furthermore, this opposite to conventional grinding where continuous and large chip can be produced.

For given grinding parameters such as:

- 1) Grinding wheel diameter $\phi = 208\text{mm}$
- 2) Grinding wheel speed $V_s = 17\text{m/s}$
- 3) Grinding wheel speed $V_w = 250\text{mm/s}$
- 4) Wheel type: UV33A602HH10VB1/
- 5) Depth of cut $a_p = 20\mu\text{m}$
- 6) Workpiece length 46.4 mm
- 7) Workpiece width 11mm
- 8) Workpiece Rockwell hardness (31.3)
- 9) Vibration frequency = 100Hz ,
- 10) vibration amplitude = $130\mu\text{m}$
- 11) Grit size $60\mu\text{m}$
- 12) Contact length $l_c = l_g = \sqrt{d_s a_p}$
(l_g is the geometrical contact length)

$$= \sqrt{208 * 0.02} = 2.039\text{ mm}$$

Period of oscillation $t = 1/\text{Frequency} = 1/100 = 0.01\text{s}$

Then the chip length could be calculated by solving equation (4) in chapter as follow:

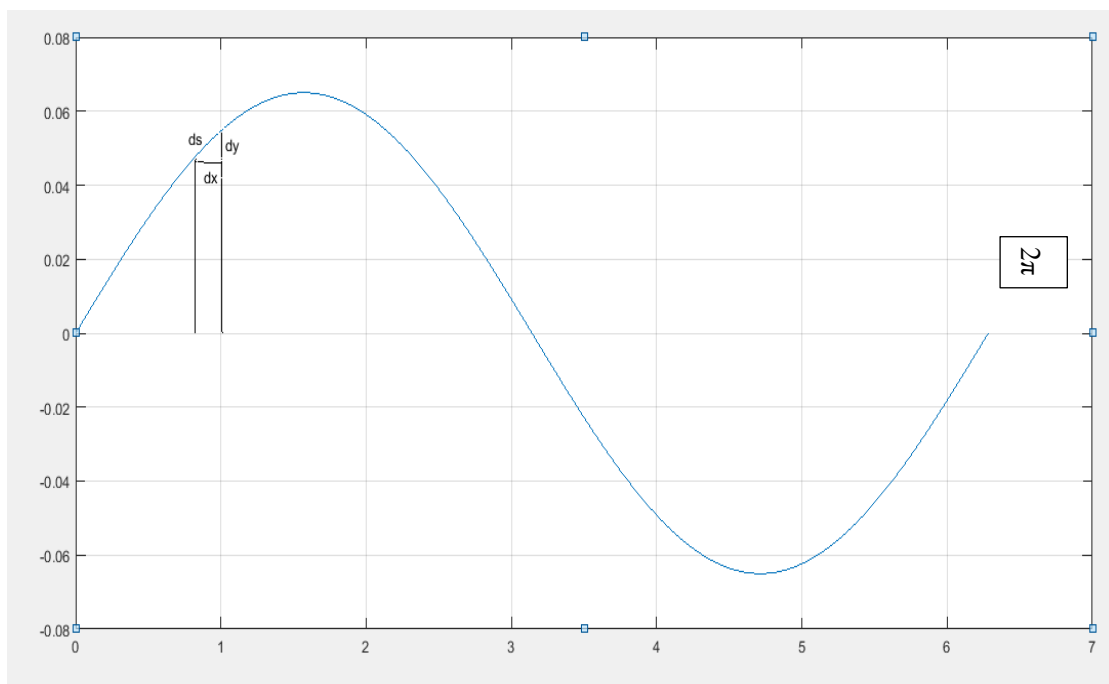
$$l_c = l_g = \sqrt{\left(\frac{d_s}{2}\right)^2 - \left(\frac{d_s}{2} - a_p\right)^2}$$

$$\left(\left(104\right)^2 - \left(104 - 0.2\right)^2\right)^{1/2} = 6.48\text{mm (Contact length) =}$$

$$\sqrt{(208/2)^2 - (208/2 - 0.2)^2} = 6.48\text{ mm without vibration on workpiece}$$

	Length (μm)	Perimeter (μm)
Min	10.11	
Max	10.11	
Range	0.00	
Average	10.11	
Total	10.11	
Deviation	0.00	
Count	1	

Name	Item	Result
L1	Length	10.11 μm
TR1	Perimeter	117.72 μm



9.2 Conclusions

This research project investigates extensively into vibration- assisted technique for surface grinding process. A novel vibratory system has been developed to vibrate the work-piece in a perpendicular direction to the feed rate to achieve specific displacement. A reliable experimental system setup was developed to accommodate the jig, the work-piece holder and the work-piece. The vibration frequency was imposed to the jig via piezo-electric actuators at low power consumption

Experiment setup configuration was constructed on a closed-loop control system to keep the vibration parameters constant during grinding process at all time.

This study is aimed to find out what are the benefits of superimposed vibration in the perpendicular direction (Axial direction to the machine spindle) for surface grinding. However, this new approach has not been implemented before. Thus a new mechanism of imposing oscillation to the work-piece was developed (perpendicular direction).

It was shown that vibration assisted reduces grinding cutting forces and power consumption and improves surface finish quality as well. The reason why vibration assisted reduced cutting forces because due to the small chips formed by the cutting grits that cut in two direction due to sinusoidal motion. This means that the grits operated on three sides namely front and the two axial sides, this led to the recorded increased material removed during the tests.

With the increase in depth of cut, table speed and wheel speed beside the applied vibration this lead to efficient grinding process performance. However, Surface finishes, are related directly with feed rate, therefore with lower feed rates, better quality surface finish was achieved for both aerospace hard materials under investigations (Ti6Al4V & nickel Inconel 718). Hence, it has been proven that the better quality of surface roughness can be achieved when grinding at low feed rate in both cases conventional and with applied vibration assisted. The reason why vibration assisted improve surface roughness because the lapping effect of the cutting tool traverse movement over the catted area which allows remove materials debris left from previous cycle.

It has been proven that vibration assisted grinding prevent wheel loading and extend tool life due to the reduced duration of cutting tool contact with the work-piece.

Finally, it has been proven also that the superimposed vibration assisted led to wheel wear reduction and increased material removal rate.

-
- Throughout the literature, diamond and CBN wheels are used for grinding hard and brittle material, however extensive wear and surface damage have been reported [93]. Therefore, the author assumes *to have contributed to the knowledge* with the use of a non-suitable Aluminium oxide wheel to successfully grind hard to machine aerospace material.

It is stipulated that for vibration assisted machining the tool disengagement secured by $V_w < 2\pi af$ is key to lower forces and successful machining. However, in this investigation the oscillation was applied in the wheel axial direction. Therefore, this condition of tool disengagement was observed. Nevertheless, the results were surprisingly positive and outperformed conventional mode of grinding and this is new finding because up to the knowledge of the author this has not been reported in the literature.

- The application of low frequency vibration in wheel axial direction extended tool life by 30%, which is a promising output. This is because, the oscillation led the grit to cut in two direction, that increased the material removal rate, though keeping a reduced load on the wheel as no clogging was observed.
- The findings of this show that the condition of tool disengagement for gaining benefits of vibration is not always the fundamental prerequisite vibratory performance. It showed that positive effects of superimposed vibration can be obtained without tool disengagement. This reveals a new phenomenon that always has been inherent to ultrasonic cutting where amplitude is small and does not allow full disengagement of tool.

Keynotes:

Scientifically it was demonstrated mathematically how vibration assisted reduces cutting forces when applied to grinding.

The reason why that might occurred because when the superimposed oscillation or resonance grinding applied to the workpiece, at a certain point in the process a zero time situation will occur where the cutting tool has no full cutting force, because of the resonance affect which act in intermittent or lapping side effect. At this moment the force dropped to its lowest values, as the workpiece displacement generated in this case allows the cutting tool to cut into two direction, as that help to reduce the cutting forces and extends the cutting tool life. The reason why the forces reduces because of the thinner thickness and longer chip that been produced as the result of grinding in

vibratory mode. Also due to the minimum contact between the tool edge and the workpiece that helps also to reduce any load on the cutting tool.

Scientifically that can be explained if a geometrical model of a single grit of a grinding wheel is considered, where the grit diameter is d_s and the geometrical contact length is l_g , the depth of cut is a_p . Thus the cutting force can be given by F_t which is a function of the average chip cross section area A_m , and V_c is the volumetric material removal for the grid which is considered to be constant whilst the cross section area A_m is not constant as the chip length and thickness are variable and not constant. Then the only parameter that is subjected for reduction with longer chip length in vibration cutting mode is the tangential force F_t . Thus vibration reduces the cutting force F_t , the equations from 1 to 14 in chapter 4 illustrate this finding. Then and only then, if the chip length L_c become longer (vibration mode), F_t the tangential force will become smaller that means low force. In the other hand, if the chip length L_c become smaller conventional grinding, the tangential force F_t become bigger. Therefore vibration assisted application reduces force because of the thinner and longer catted chip in vibratory grinding

However, from this study three important findings were reached. These findings considered to be state of the arts in this field.

Firstly I have managed successfully through this investigation to grind hard to machine aerospace materials employing aluminium oxide wheel with the enhancement of vibration assisted machining. The investigation results revealed that also grinding with vibration is better off than grinding conventionally.

Secondly the obtained results support and validate the idea of employing super abrasive grinding wheels such as CBN and diamond wheel has negative effects on the workpiece surface quality in terms of cracks, thermal damage and high operation cost.

The application of superimposed vibration assisted machining which depends fundamentally on the resonance grinding oscillation theory, to machine hard aerospace materials shows great results especially nickel and Ti6Al 4V Where there were improve in material removal rate, the surface roughness and reduction in cutting forces and power consumption, at the same time it enhanced to extend the wheel life.

Thirdly for the first time in this field the application of low vibration frequency was introduced on the perpendicular direction of the feed rate into the workpiece to secure suitable displacement that match a low excitation that required to reduce the power consumption.

The results proved that vibration assisted machining when applied in this direction reduces the load on the cutting tool, consequently the cutting forces were reduced and wheel wear as well, this led wheel life extension by about 30%.

Experimentally via calibration a desired amplitude of 130 μ m was found to match low vibration frequency of 100Hz

In addition to that, and for the first time also the formed chip length was calculated and measured in both cases conventionally and with the implementation of vibration assisted machining where the two length were compared together.

The chip length in case of vibration grinding was longer by about 1.5% than that of conventional grinding, the SEM results also proved that 117 μ m length. Chip thickness measured 10 μ m.

Moreover, the choice for low frequency and high displacement came after all the previous studies have been reviewed, where the use of high frequency proved to be too risky to damage the surface roughness of the work-piece, increase the tool wear and harming the machine, the equipment and the operator as well. In the other hand, the choice for high amplitude because in the previous study the application of low amplitude proved that was not efficient enough to allow for sufficient coolant fluid to be trapped between the cutting tool and the work piece in the contact zone. Hence, a large amplitude of 130 μ m was obtained by calibration to obey the task of allowing enough coolant fluid to reach the grinding contact zone to help extract the heat generated by the grinding process.

9.3 Recommendation for future work

It is strongly recommended for future work to use high speed grinding machine with supper abrasive wheel.

It would be more beneficial to use ABAQUS/ CAE be used to create models and simulation a single micro-grinding vibration assisted.

REFERENCES

REFERENCES

1. A. D. L. Batako. V. Tsiakoumis (2014), An experimental investigation into resonance dry grinding of hardened steel and nickel alloys with element of MQL. *International Journal of advance manufacturing technology* (2015) 77: 27-41. London
2. A. R. C. Sharman, D. K. Aspinwall, R. C. dewes, P. Bowen. (2001) 'Workpiece surface integrity considerations when finish turning gamma titanium aluminide, University of Birmingham, Birmingham B15 2TT, UK. *Journal of Materials Processing Technology, Wear* 249 (2001) 473-481.
3. Alfares, M. & Elsharkawy, A. (2000) 'effect of Grinding Forces on the vibration of grinding Machine Spindle System'. *International Journal of machine Tools & Manufacture*, 40, pp.2003-2030.
4. Alut, W. (1989), Types of grinding Wheels. In: King, R. I. & Hahn, R. S. ed. *Handbook of Modern Grinding Technology*, chapman and hall, New York, pp.72-87.
5. Astashev, V. K., Babitsky, V. I., Kolovsky, m. Z. (2000), *Dynamics and Control of Machines*. Springer-Verlag, Berlin
6. Albizuria, J., Fernandesb, M. H., Garitaonandiab, I., sablzac, x., Uribe-Etxeberriac, R., Hernandez, J. M. (2006) 'An active system of reduction of vibrations in a centreless grinding machine using piezoelectric actuators' *International Journal of Machine tools & Manufacture, Vol. 47, Issue10, pp, 1607-1614*.
7. Altintas, Y., "Manufacturing Automation: Metal Cutting Mechanics, Machine Tool Vibrations and CNC Design". Cambridge University Press, Cambridge, UK, 2000.
8. Astash, K., and Babitsky, I. "Ultrasonic cutting as a nonlinear (vibro-impact) process". Vol. 36, pp.89-96.(1998)
9. Axinte, A., Gindy, N., Fox, K., and Unanue, I. "Process monitoring to assist the workpiece surface quality in machining". *International Journal of Machine Tools & Manufacture*, Vol. 44, pp. 1091-1108. (2004)

-
10. Baldwin, W. H. (1931). The story of Nickel. III. Ore matte, and metal. *Journal of Chemical Education*, 8(12): pp. 23-25.
 11. Bradley, C., and Wong, S. (2001) "Surface texture indicators of tool wear- a machine vision approach". *International Journal of Advanced Manufacturing Technology*, Vol.17, pp. 435-443.
 12. Babitsky, V., and Kalanishilov, N. "Ultrasonically turning in aviation material". *Journal of Materials Processing Technology*, Vol. 132, pp.157-167. (2003)
 13. Babitsky, V.I. (1995) 'Autoresonant Mechatronic System' *Mechatronics*, Vol.5, No.5, pp.483-496
 14. Babitsky, V.I. (1998) '*Theory of Vibro-Impact Systems and Applications*' (Russian revised translation, Nauka, Moscow, publish year 1999.
 15. Babitsky, V.I. (1998) '*Theory of Vibro-Impact Systems and Applications*' Springer-Verlag, Berlin Heidelberg
 16. Babitsky, V. I. Veprik, A. M. (1998), 'Universal Bumpered Vibration isolator for Severe Environment' *Journal of Sound and Vibration*, (1892) 269-292.
 17. Barczak, L.M., Batako, L.M., Morgan, M.N. (2010) 'A study of plane surface grinding under Minimum Quantity Lubrication (MQL) condition' *International Journal of machine Tools & Manufacture*. Volume 50(11)
 18. Baines-Jones, V.A. (2010) '*Nozzle Design for Improved Useful Fluid Flow In Grinding*' LJMU Doctoral Dissertation, Record No. 000877481.
 19. Barczak L. (2010). Application of Minimum Quantity Lubrication (MQL) in Plane Surface Grinding, PhD Thesis
 20. Batako, A. D. L. & Koppal, S. (2007), Process monitoring in high efficiency deep grinding-HEDG' *Journal of physics: Conference series* 76012061.
 21. Batako, A. D., Rowe, W. B., Morgan, M. N. (2005) 'Temperature measurement in High efficiency deep grinding' *International Journal of Machine Tools & Manufacture*, 45, pp. 1231-1245

-
22. Brinksmeier, E., Heinzl, C., Wittmann, M. (1999) 'Friction, Cooling and Lubrication in Grinding' *CIRP Annals- Manufacturing Technology*, Vol. 82, Issue 2, pp.581-598.
 23. Bonifacio, M. And Diniz, E (1994). Correlating tool wear, tool life, surface roughness and tool vibration in finish turning with coated carbide tools. *Wear*, Vol. 173, pp. 173-144.
 24. Brehl D.E, Dow T.A, Garrard K, Sohn A (2006). Microstructure fabrication using elliptical vibration-assisted machining. *Proc ASPE 39*, pp. 511–5114.
 25. Brehl DE, Dow TA (2007), editors. Vibration assisted machining technology. *Proc ASPE 40*:pp.175-176.
 26. Brehl, D (2008). Review of vibration assisted machining. *Precision Engineering*, Vol. 32, pp. 153-173.
 27. Brinksmeier, E., Minke, E., and Nowage, L Residual stresses in precision components". The 5th International Conference on industrial Tooling, Vol. 10-11, pp. 1-21.(2003)
 28. Brucker, D. "remarks on the wearing process in grinding". *Industrie anzieger*, Vol. 8, pp. 23-28.(1960)
 29. Cerniway M. (2005), Elliptical Diamond Milling: Kinematics, Force and Tool. Msc Dissertation, Graduate Faculty, North Carolina State University.
 30. Chern and L., and Change, C, (2006), Using Tow-Dimensional Cutting for Micro- Milling *International Journal of Tools & Manufacture*, Vol. 46, pp.659-666.
 31. Chen, X. & Rowe, B. W. (1996) 'Analysis and Simulation of the Grinding Process. Part II: Mechanics of Grinding' *International Journal of Machine Tools and Manufacture*, v36, issue8, pp.883-896.
 32. Chen , X. & Rowe, B. W. (1996) 'Analysis and Simulation of the Grinding
 33. *International Journal of Machine Tools & Manufacturing*. 36 (8): 871-906

-
34. Chen, X., & Rowe, W. B., Mills, B., Allanson, D. r. (1998) 'Analysis and Simulation of the Grinding Process, part IV: Effect of wheel wear', *International Journal of machine Tools Manufacture* 38 (1-2) pp.41-49.
 35. Chen H., Tang I., Zhou W. (2013). An experimental study of the effects of ultrasonic vibration on grinding surface roughness of C45 carbon steel.
 36. Cheng, C.H., Tony, L. Schmitz, G. Scott, D. (2007) 'Rotating Tool Point Frequency Response Prediction Using RCSA' *Machining Science and Technology*
 37. David A. Stephenson, John S. Agapiou, (2006) *Metal Cutting Theory and Practice*, 3rd Edition.
 38. De Vries, D. (1910), *Milling machines and milling practice: a practical manual for the use of manufacturers, engineering, students and practical men*, London, E. & F.N. Spon, limited; Spon & Chamberlain, New York.
 39. D. M. Grove & T. P. Davis, *Engineering, quality and Experimental Design*, Longman Science and Technical, 1992).
 40. D. Rugg, (2003). The Current Status of Titanium Alloy Use in aero-Engines, Proceedings of the 10th World conference on Titanium (Ti-2003). Hamburg, Germany, Vol.IV, pp.2727-2735, ISBN:3-257-30306-5.
 41. Donachie M. J. Jr. (1998). *Titanium, A Technical Guide*. Metal Park, OH: ASME International, ISBN 0-87170-309-2.
 42. Dagnall, H., (1997), '*Exploring Surface Texture*' Taylor and Hobson publication, list No. 600-14/98.
 43. Deutsche N. "Determination of surface Roughness Values Ra, Rz, Rmax, with Electric Stylus instruments-Basic Data". Berlin Beuth Verlag, GmbH, (1974).
 44. Ewad H. (2013), *Development of a closed loop control system for two Dimensional Vibration assisted machining*, MPhil, LJMU, 2013.
 45. Ewad H, Chen X, Yu D and Batako ADL (2016), *Development of a control system for Vibration Assisted Grinding*, LJMU GARS conference. June 2016

-
46. Emsley J, (2011), Nature's building blocks, Oxford University press.
 47. Ebbrell, S. (2003) 'Process requirements for Precision Grinding' (Doctoral Dissertation) Retrieved From John Moores University Library database, Record Number: 000717781
 48. Eiji, u. (1982) 'Theory of Cutting and Grinding', Mechanical engineering publications, Beijing.
 49. Filiz, S., Cheng, C. H., poweli, K.B., Schmitz, T.L., Ozdoganlar, O. B. (2009) 'An Improved Tool-Holder Model for RCSA Tool-point Frequency Response Prediction' *Precision Engineering* 33 pp. 26-36
 50. Filipowski R., Marciniak M. (2000) Techniki obróbki mechanicznej i erozyjnej.
 51. Garcia-Gardea, e., Kapoor, S.G., Wu, S.M. (1980) 'Analysis of Grinding dynamics by dynamic Data system Methodology' *International journal of Machine Tool Design and Research*, v.21 No.2 pp.99-108
 52. Groover, P. "Fundamental of Modern Manufacturing: materials Processes and Systems". Third edition, John Wiley & Sons, Inc.2007.
 53. Gallemaers J P, Yegenoglu K, Vatovez C, (1986); Optimizing Grinding Efficiency with Large Diameter CBN Wheels; Int. Grind. Conf. Philadelphia, USA SME86-644, pp 38-39.
 54. Hanasaki, S., Fujivara, j., wada, T., Hasegawa, y. (1994) 'Vibratory creep feed grinding' *Trans. Japan Soc. Mech. Eng.*, 60 (573), 1829-1834.
 55. Howes, T. (1990) 'assessment of the Cooling and Lubrication properties of grinding Fluids' *Ann. CIRP* 39, 1, pp.313-316.
 56. Huang, G. L. & Sun, C.T. (2006) 'The dynamic Behaviour of a piezoelectric actuator bonded to an anisotropic elastic medium' *International journal of Solids and structures* v.43 pp. 1291-1307
 57. Hui Ding, Rasidi Ibrahim, Kai Cheng, Shi-Jin Chen. (2010) 'Experimental study on machinability improvement of hardened tool steel using two dimensional vibration-assisted micro-end-milling'. Brunel University, Uxbridge, UB8 3PH, UK. *International Journal of Machine Tools & Manufacture*, 50 (2010) 1115-1118.

-
58. Ihsan, K., Mehmet., B. (2008), Experimental Examination of main cutting Force and surface Roughness Depending on Cutting Parameters ' *Journal of Mechanical Engineering* ' 5492008)7-8, 531-538
59. Inman, D. J. (1996) 'Engineering Vibration' Prentice-Hall Inc., United States of America.
60. J.-S. Kwak, "Application of Taguchi and response surface methodologies for geometric error in surface grinding process" *Int. J. Mach. Tools Manuf.*, vol. 45, no. 3, pp.327-334, (2005).
61. Jackson, A. (2008) ' *An Investigation of Useful Fluid Flow in Grinding* ' LJMU Doctoral Dissertation, record No. 000820129
62. Jiang, Y., TANG, X., Zhang, W. X., Song, Q. H., Li, B.B., Du, B. (2007) 'An Experimental investigation for Dynamics Characteristics of Grinding Machine' *Key Engineering Materials* Vol.329 pp.767-772.
63. K. Kocman, "Application of Magnetic correlation analysis on the choice and correction of cutting parameters for automated manufacturing systems" *Manuf. Technol.*, vol. 11, pp.28-32, 2011.
64. Kermani, M.R., Patel, R., Moallem, M. (2005) 'Flexure Control Using Piezostack Actuators: design and Implementation' *IEEE/ASME Transactions on Mechatronics* v.10, No 2.
65. Kohli, S. P.; Guo, C; Malkin, S. Energy Partition for Grinding with Aluminium Oxide and CBN Abrasive Wheels, *ASME Journal of Engineering for Industry*, v.117, p. 160-168, 1995.
66. Kalpakjian S. and Schmid S. R. (2010). *Manufacturing Engineering and Technology*; Six edition in SI units. Prentice Hall, Singapore
67. Kim, Y, Shen, F., and Ahn, H. "Development of surface roughness measurement system using reflected; laser beam". *Journal of Materials Processing Technology*, Vol.130-131, 2002, pp. 662-667.
68. Kim, J., and Lee, E. "Study of ultrasonic vibration cutting of carbon fibre reinforced plastic". *International Journal of Advanced Manufacturing Technology*. Vol. 12, 1996, pp.78-86.

-
69. Marsi, S. F. (1972), 'Forced Vibration of a Class of Non-Linear Two-Degree- of Freedom Osillators', *Int. J. Non-Linear Mechanics*. Vol. 7, 663-674
70. Malkin, Stephen (1989), *Grinding Technology: Theory and Applications of Machining with Abrasives*, Society of Manufacturing Engineers, Dearborn, Michigan.
71. Malkin, S. & Cook, N .H .(1971) 'The Wear of grinding Wheels, part 1: Attritious Wear', *Transaction of ASME Journal of Engineering for Industry* 93, pp1120-1128.
72. Malkin, S. & Guo, C. (2008) 'Grinding Technology- Theory and applications of Machining with Abrasives' Second Edition, Industrial Press Inc, New York.
73. Malkin S., (1984), "Grinding of metals: Theory and application," *Journal of applied Metalworking*, America Society for Metal, Vol. 3, no. 2, pp.95-109.
74. Moriwaki, T., and Shamoto, E (1991). Ultraprecision Diamond Turning of stainless steel by applying ultrasonic vibration. *Annals of the CIRP*, Vol. 40, pp. 559-562.
75. Maroju, N., K., Kanmani Subbu., S., Vamsi Krishna P. Venugopal A., *Vibration Assisted Conventional and Advanced Machining: A Review*. 12th Global Congress on Manufacturing and Management, GCMM (2014).
76. Matsumura, T. (2005) *Glass machining with micro-end mill*. Japan Society of Mechanical Engineers (JSME), Vol. 1, pp. 139-158.
77. Marinescu, I. D., Rowe B., Dimitrov, B., Inasaki, I. (2004) 'Tribology of Abrasive Machining Processes' ISBN: 0-8155-1490-5 William Andrew, Inc. USA
78. Marinescu I D, Rowe W B, Dimitrov B, Inasaki I, (2005); *Tribology of abrasive Machining processes*, William Andrew publication.

-
79. Marinescu, I. D., Hitchiner, M., Uhlmann, E., Rowe, B. W., Inasaki, I. (2007) Handbook of Machining with grinding Wheels' CRC Press, Taylor and Francis Group LLC, New York USA.
80. Moriwaki, T. & Shamoto, E., (1991) ' Ultraprecisiion diamond turning of Stainless steel by Applying Ultrasonic Vibration' Kobe University japan vol.40 No.1
81. M. Ramulu, T. Branson, D. kim, (2001). A study on the drilling of composite and titanium stacks, Compos. Struct.54, pp. 67-77.
82. M.H. Loretto. Intermetallics in turbines and compressors for aero-engines, in: proceedings of the Third international Charles Parsons Turbine Conference on materials Engineering in Turbines and compressors, Newcastle upon Tyne, UK, (1995).
83. Nageswara Rao, Muktinutalpati, (2011). Materials for Gas turbine – An overview.
84. Noel Williamson Mechanical Tech, student, April (2014), Dr. Govindan. Assistant professor, Kannur Kerala India, Vibration- assisted Grinding with a Newly Developed Rotary Mechanism using Induction Motor
85. National Instruments Corporation. (1994) (Lab VIEW Data acquisition VI Reference Manual for Windows). Part Number 320536B-01.
86. Oberg, E., Jones, Franklin D., Horton, Holbrook L., and Ryffel, Henry H. (2000), Machinery's Handbook, Industrial Press Inc., New York, p.1190
87. O. bilek., J. Javorik, D. samek., (2013). Statistical analysis of surface roughness in grinding of titanium. ISBN: 978-1-61804-243-9.
88. Prasanna M. Mahaddalkar, Michelle H. Miller (2013). Force and thermal effects in vibration-assisted grinding.
89. Prasanna M. Mahaddalkar. Michele H. Miller (2014), 'Force and thermal effects in vibration-assisted grinding' International Journal Advance Manufacturing Technology. 71:1117-1122
90. Qi, H.S. (1995) 'A contact length model for grinding wheel-workpiece contact' PhD thesis. LJMU. UK.

-
91. Qi, H.S., Mills, B. & Rowe, W.B. (1994), 'an analysis of real contact length in abrasive machining processes using contact mechanics' *Wear* 176, pp 283-294
92. Qu, w., Wang, K., Miller, M.H., Y., Chandra, A. (2000) 'Using Vibration-Assisted Grinding to reduce Subsurface damage'. *Journal of the International Societies for Precision Engineering and Nanotechnology*, V. 24, pp. 329-337
93. Qi, H.S., Rowe, W.B., Mills, B. (1997) ' (1997) ' Experimental investigation of contact behaviour in grinding' *Tribology International*, vol. 30 No 4pp 283-294
94. Rowe W. B (2014). *Principles of Modern Grinding Technology*, William Andrew, publication, Second Edition.
95. Rui C. (2002) *Assessment of Vitrified CBN Wheels for Precision Grinding*. Volume. 44. Issues 12-13, pp. 1391-1402.
96. Rowe, W.B., Qi, H.S., Morgan, M.N. & Zheng, H.W. (1993) *the real Contact Length in Grinding based on depth of Cut and Contact Deflections*. Proc. Thirtieth International MATADOR Conference. UMIST, Macmillan. Pp.187-193
97. Sao Carlos. (2014). *Analysis of surface roughness and hardness in hardness in titanium alloy machining with polycrystalline diamond tool under different lubricating modes*. Vol. 17. No. 4.
98. Sabine, T., Anne, M. Zoubier. B., (2016) *Tool Wear and Cutting forces under cryogenic machining of titanium alloy (Ti17)*.
99. Shamoto E, Suzuki N, Tsuchiya E, Hori Y, Inagaki H, Yoshino K (2005). *Development of 3-DOF ultrasonic vibration tool for elliptical vibration cutting of sculptured surfaces*. *CIRP Ann*, vol. 54, no. 1, pp. 321-324, 2005.

-
100. Tawakoli, T. (1993) 'High efficiency Deep Grinding' VDI-Verlag GmbH, *Mechanical Engineering Publication, London*
 101. Teicher, U., Ghosh A. (2006). On the grindability of Titanium alloy by brazed type monolayered superabrasive grinding wheels. *International Journal of machine tools and manufacture* 46(6), pp. 620-622.
 102. Tsiakoumis V. I, (2011) an investigation into Vibration assisted Machining - Application to surface grinding Processes, PhD Thesis LJMU.
 103. Van Arkel, A. E.; de Boer, J. H. (1925). Preparation of pure titanium, zirconium, Hafnium, and thorium metal. *Zeitschrift fur anorganisch & allgemeine Chemie*, V.48. 345-50.
 104. Venables, M. (2006) 'It's a [Grinding Technology]' *Manufacturing Engineering* Volume 85, Issue 4, pp. 42-45
 105. Warren R. De Vries. *Analysis of Material Removal Processes* (2012), Publisher: Springer New York, ISBN-13:9781461287599.
 106. Wood B, Robert S (1972). *History of the milling machine*. In *studies in the history of Machine Tools*, Cambridge, Massachusetts, USA, and London, England: MIT press, ISBN 978—0262-73033.
 107. Wells, L and J. *Travis*, "LabVIEW for Everyone," Prentice Hall PTR, Upper ... Fluids," Manuscript in progress, Northern Illinois University, DeKalb, IL, 1998.
 108. Weixing Xu, Liangchi Zhang, and Yongbo Wu, (2016), effect of tool vibration on chip formation and cutting forces in the machining of fiber-reinforced polymer composites, Vol. 90, Issue 1-4, pp. 1145-1154.
 109. Xiao M, Sato K, Karube S, Soutome T (2003). The effect of tool nose radius in ultrasonic vibration cutting of hard metal. *International Journal of Machine Tools & Manufacture*, 43, pp. 1375–1382.
 110. X. Chen, W. B. Rowe, R. Cai, precision grinding with CBN wheels, *Internal Journal of Machine tools and Manufacture*, Vol.42, pp.585-593, (2002)

-
111. Younis, M., Sadek, M.M., El-wardani, T. (1987) 'A New Approach to Development of a Grinding force Model', *Transactions of ASME Journal of Engineering for Industry*, 109, pp.306-313.
 112. Yin, S. & Shinmura, T. (2007) 'Vibration- assisted Magnetic Abrasive Polishing' *Key engineering materials* Vol. 329, pp 207-212.
 113. Yang W. H., Tarn Y. S (1998). Design Optimization of cutting parameters for turning operations based on Taguchi method, *Journal of Materials processing Technolog*, 84, pp. 122-129
 114. Zhang, B., Hu, Z., Luo, Deng, Z. (2006) 'Vibration-Assisted Grinding- m Piezotable Design and Fabrication' *Nanotechnology and Precision Engineering* Vol. 4 No. 4, pp. 282-292.
 115. Zhou M, Eow Y, Ngoi, B, Lim E (2003). Vibration-assisted precision machining of steel with PCD tools. *Mater Manufacture Process*, vol. 18, 2003, pp.825-834.
 116. Zhang, H., Zhang, J., Huo, M. (2006) 'study on ultrasonic Vibration Assisted Grinding in Theory' *Material Science Form*. Vol. 532-533, pp 773-776
 117. Zhang, P. & Miller, H, M. (2003) 'Grinding wheel loading with and without vibration assistance' *Proc. Of the ASPE annual Meeting* pp455-458 Michigan Technological University, Houghton, MI
 118. Zhong, Z. W., Yang, H. B. (2004) 'Development of a Vibration Device for Grinding with Microvibration.' *Materials and Manufacturing Processes* 196, pp: 1121-1132
 119. Zhou, Z.X. & Van Lutterwelt, C.A. (1992) ' The real contact length between grinding wheel and work-piece-A new concept and a new measuring method' *Ann CIRP*, 41, pp. 387-391.

WEB- BASED SOURCES

1. (<http://shawandgoodwin.co.uk/capacities-capabilities/3041542>
2. (www.matweb.com accessed 14,15,16,27 June 2014).
3. (<http://www.thomas-sourmail.net/coatings/materials.html> accessed 5 July 2014).
4. (<http://www.supplieronline.com/propertypages/Inconel718.asp> accessed 2 October 2014).

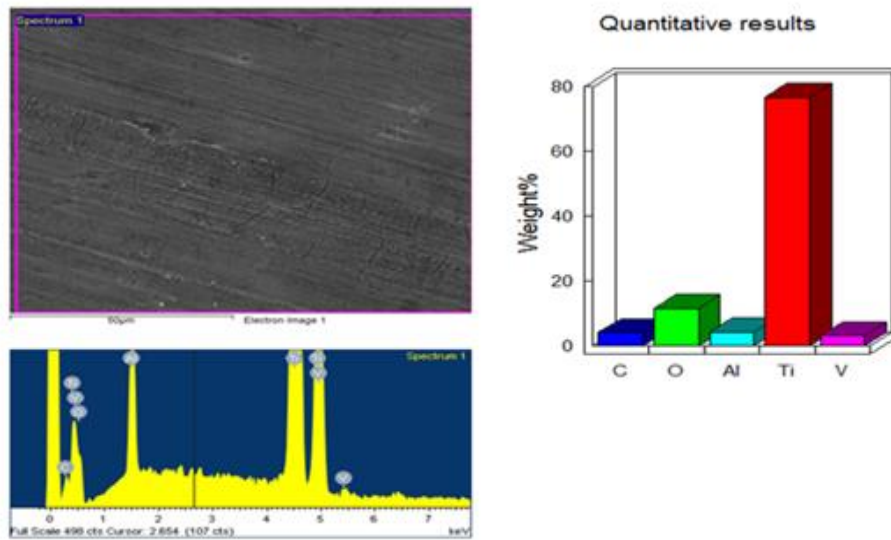
-
5. (<http://www.globalspec.com/reference/63221/203279/5-3-grinding-forces-power-and-specific-energy> accessed 15 October 2014).
 6. (<http://www.mfg.mtu.edu> accessed 10 November 2014).
 7. (www.gordonengland.co.uk/hardness/rockwell.htm).
 8. (www.totalmateria.com).

APPENDICES

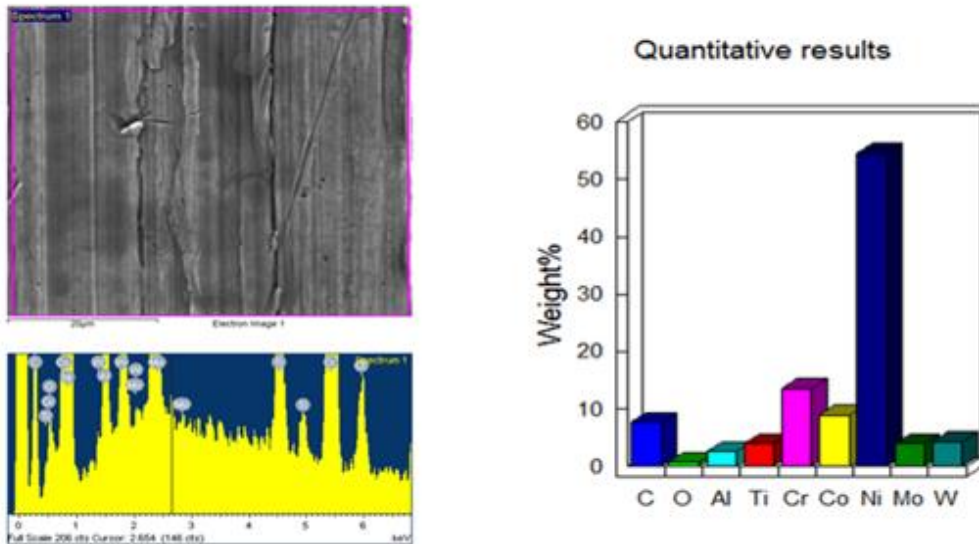
APPENDICES

APPENDIX - A

A-1 Chemical Composition Identification.



A-2 High- grade Titanium aluminide (TiAl).



A-3 Nickel alloy Inconel 718

A-4 Material Chemical & Physical Properties

Elements	Mechanical properties	Chemical properties	Physical properties	Electrical properties	Thermal properties	Component elements properties
Fe Ti 70	Hardness:31	Atomic nr:22	Density:4.7g/cc	Electrical resistivity:0.00017 Ohm-cm	Melting point: 1550-1600C Specific heat:0.525j/g-C	Ti=65-75% Al=21% Nb=4% O=7%
Nickel Alloy 718bar	Hardness:40	Atomicnr:28	Density: 8.32g/cc	Elect-resistivity: 0.000101ohm-cm	Specific heat capacity: 0.544j/g-C	Ni=52% C=7% Cr=19% Mo=4% Ti=1%

A-5 Materials Rockwell hardness Tests Results.

Material	Average hardness	
	X-direction	Y-direction
Inconel 718	40.3	37.3
Ti 1 (High-garde TiAl)	30.7	31.3
Ti2 (TiAl Tubine blade)	28.6	25.3

Table 6.1: Materials Rockwell hardness Tests Results.

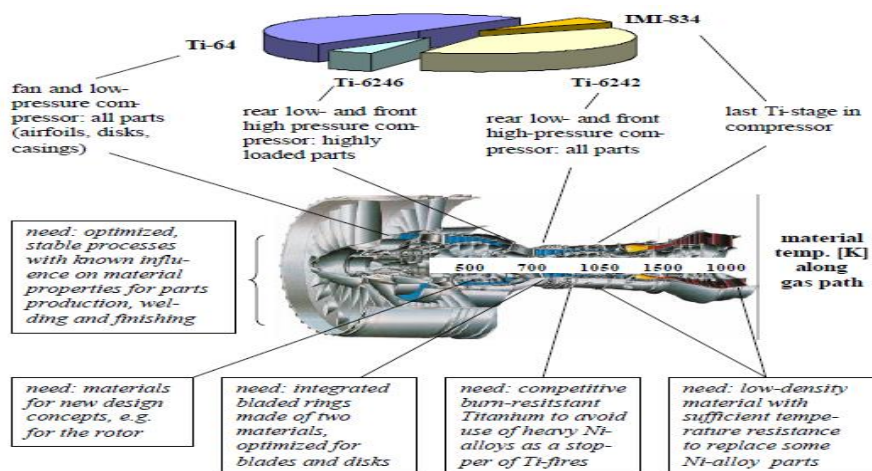
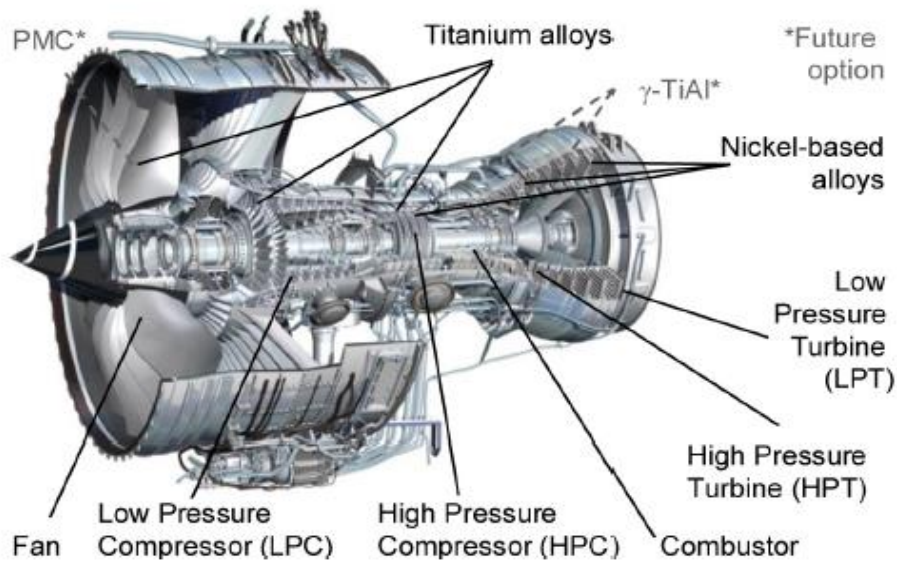
Titanium Ti6Al4V

Test NO	X-direction	Y-direction
1	31	30
2	30	30
3	29.5	29.5
Total	90.5	89.5
Average	30.2	29.8

High -Grade Titanium

Test NO	X-direction	Y-direction
1	30	29
2	31	30
3	31	30
Total	92	89
Average	30.7	29.7

A-6 Material Applications



Aero-engines future requirements (J.Esslinger).

MTU Aero Engine, Munich, Germany 2010.

APPENDIX-B

B-1 Dynamometer Calibration Table

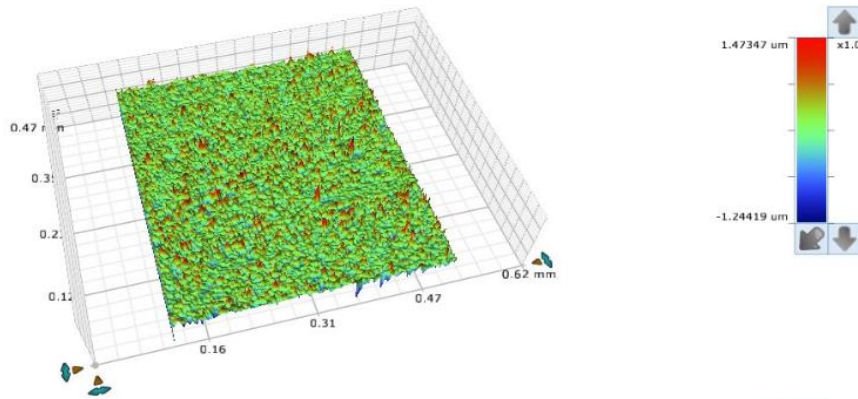
Load.N	F _z V	F _z .mV	Load.N	F _x V	F _x .mV	Load .N	F _y V	F _y .mV
10	5.02	0.023	10	5.013	0.015	10	5.042	0.044
20	5.05	0.053	20	5.041	0.043	20	5.052	0.054
30	5.088	0.091	30	5.06	0.062	30	5.078	0.08
40	5.114	0.117	40	5.08	0.082	40	5.101	0.103
50	5.13	0.133	50	5.113	0.115	50	5.141	0.143
60	5.18	0.183	60	5.13	0.132	60	5.165	0.167
70	5.208	0.211	70	5.17	0.172	70	5.183	0.185
80	5.24	0.243	80	5.19	0.192	80	5.21	0.212
90	5.27	0.273	90	5.22	0.222	90	5.23	0.232
100	5.306	0.309	100	5.245	0.247	100	5.25	0.252
110	5.333	0.336	110	5.269	0.271	110	5.28	0.282
120	5.365	0.368	120	5.29	0.292	120	5.303	0.305
130	5.39	0.393	130	5.31	0.312	130	5.32	0.322
140	5.43	0.433	140	5.33	0.332	140	5.35	0.352
150	5.46	0.463	150	5.35	0.352	150	5.37	0.372
160	5.49	0.493	160	5.37	0.372	160	5.4	0.402
170	5.5	0.503	170	5.39	0.392	170	5.42	0.422
180	5.51	0.513	180	5.42	0.422	180	5.46	0.462
190	5.53	0.533	190	5.445	0.447	190	5.49	0.492
200	5.56	0.563	200	5.48	0.482	200	5.51	0.512

Loads Used to Measure the Forces Acting on The Tangential, Normal and Axial Directions.

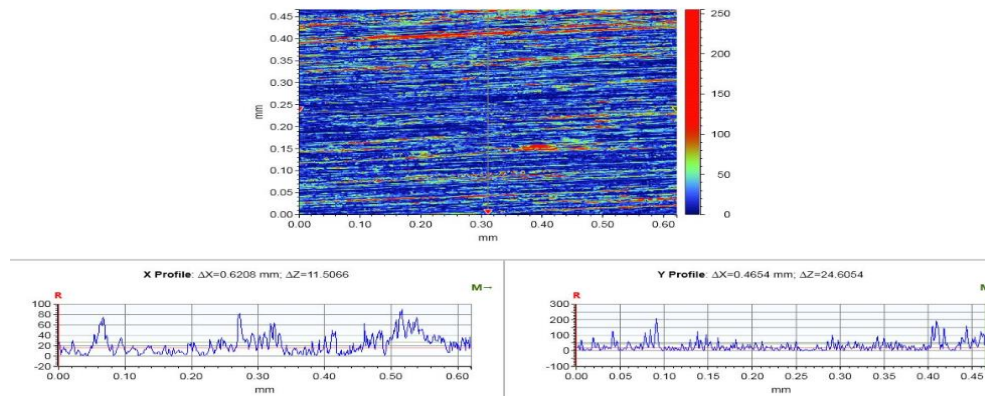
B-2 Taguchi array. For L₈ (2⁷). With interaction

	V _s	a _e	-	V _w	-	Dre	R _a	F _t	F _n	R _a	DOC
	A	B	A x C	C	B x C	D	E				
1	1	1	1	1	1	1	1				
2	1	1	1	2	2	2	2				
3	1	2	2	1	2	1	2				
4	1	2	2	2	1	2	1				
5	2	1	2	1	1	2	2				
6	2	1	2	2	2	1	1				
7	2	2	1	1	2	2	1				
8	2	2	1	2	1	1	2				

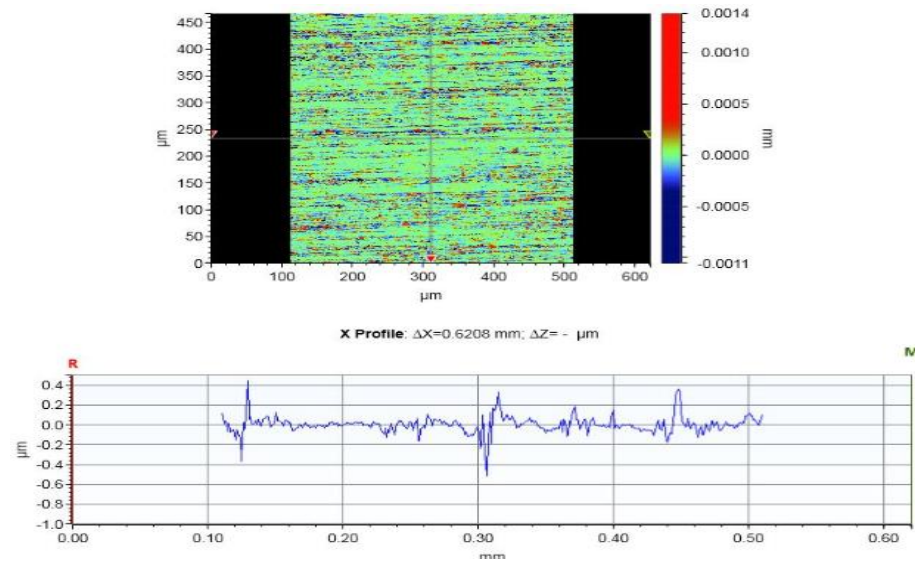
B-3a Surface Roughness measurements (with/without vibration) using The Bruker



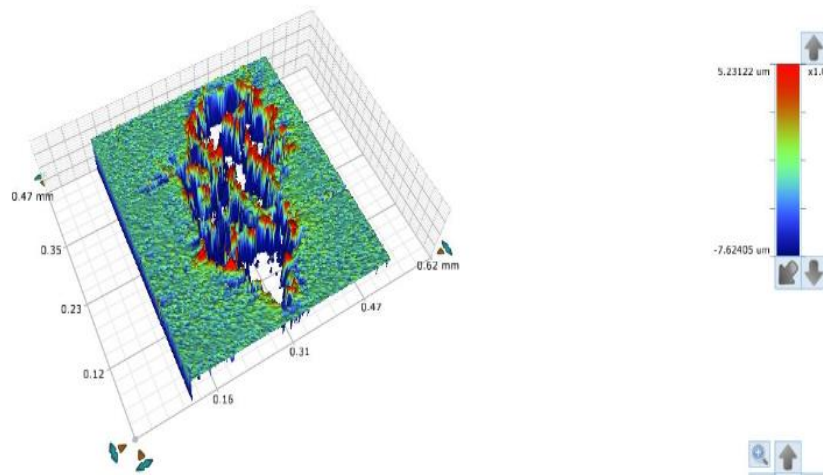
Ra: With vibration



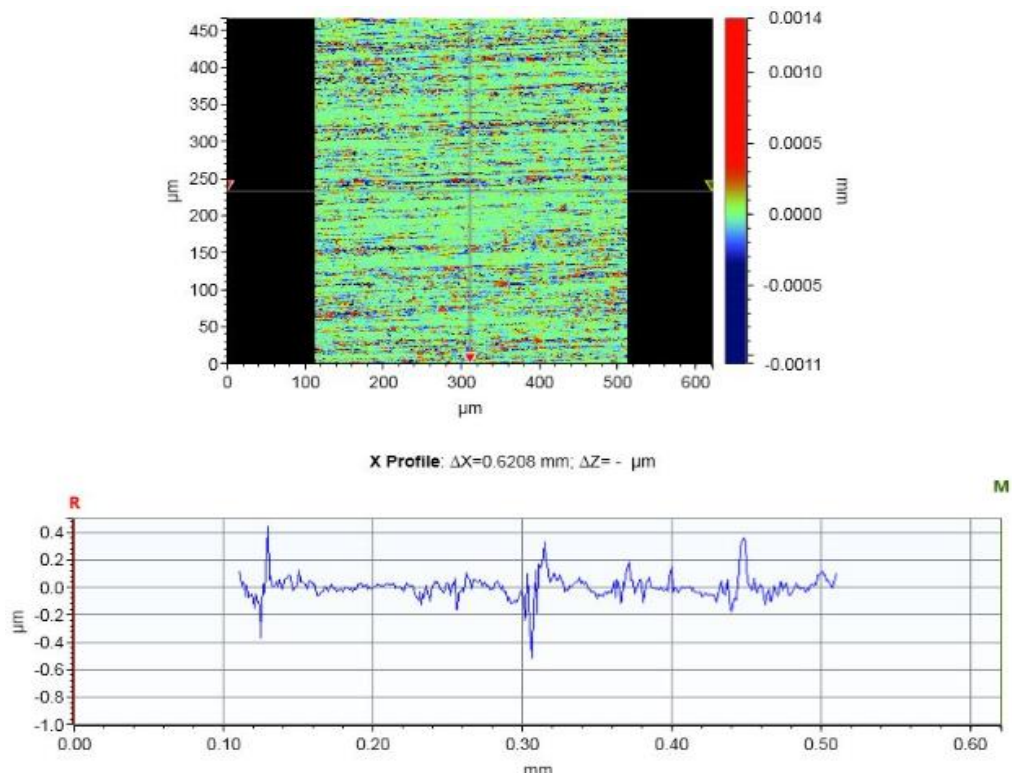
Ra: No Vibration



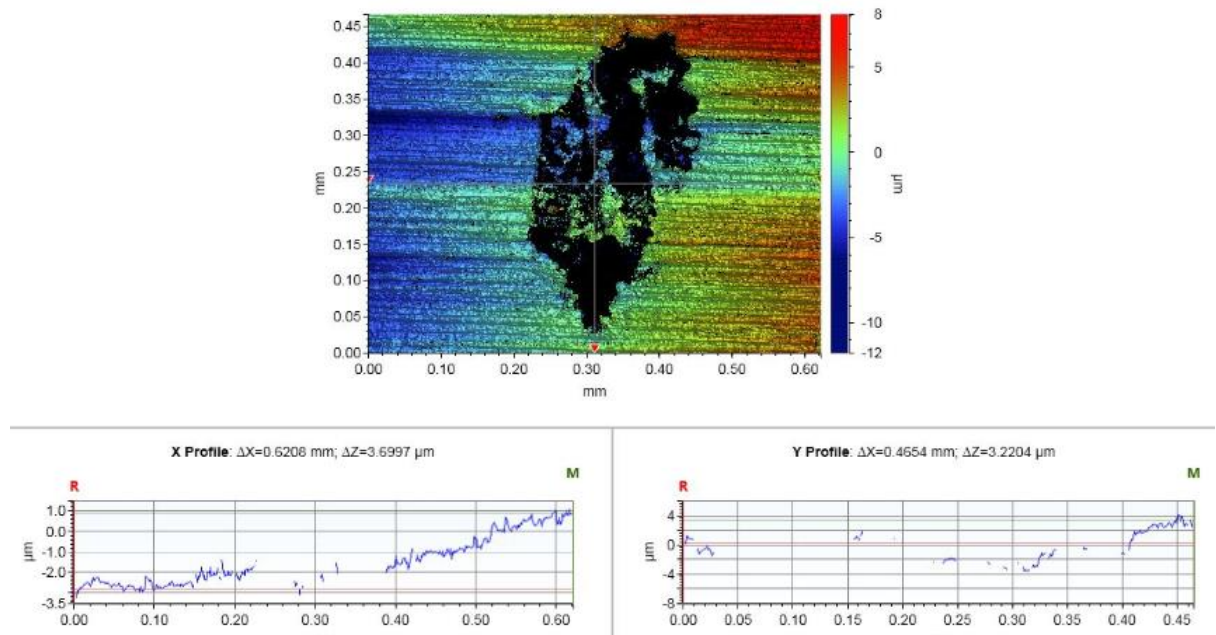
B-3b, Void, empty space due materials composition.



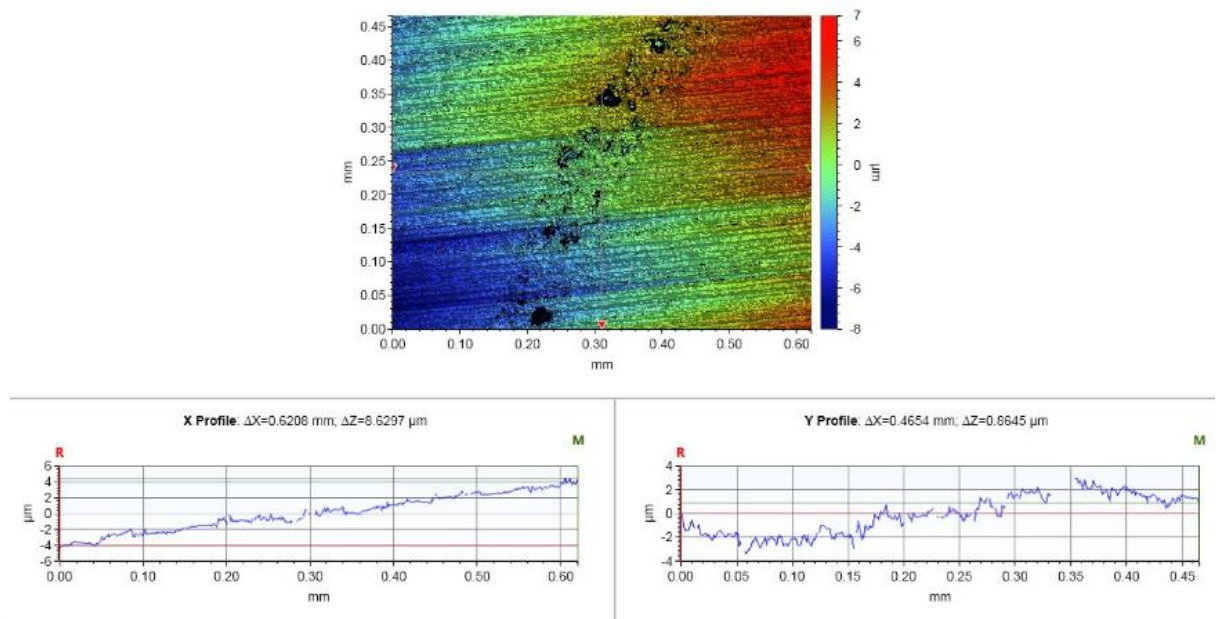
B-3c, Chatter phenomenon



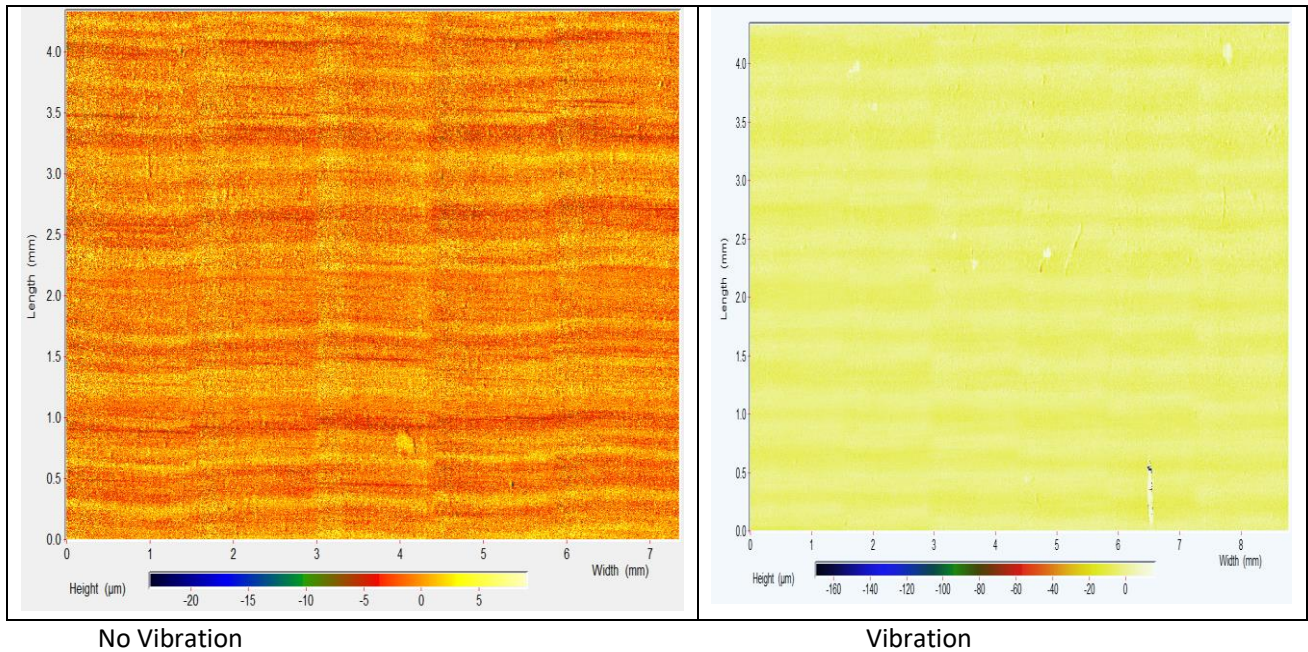
B-3d, Grinding wheel profile on the surface roughness when an void appears on material



B-3e, Titanium Surface roughness with crack on the material

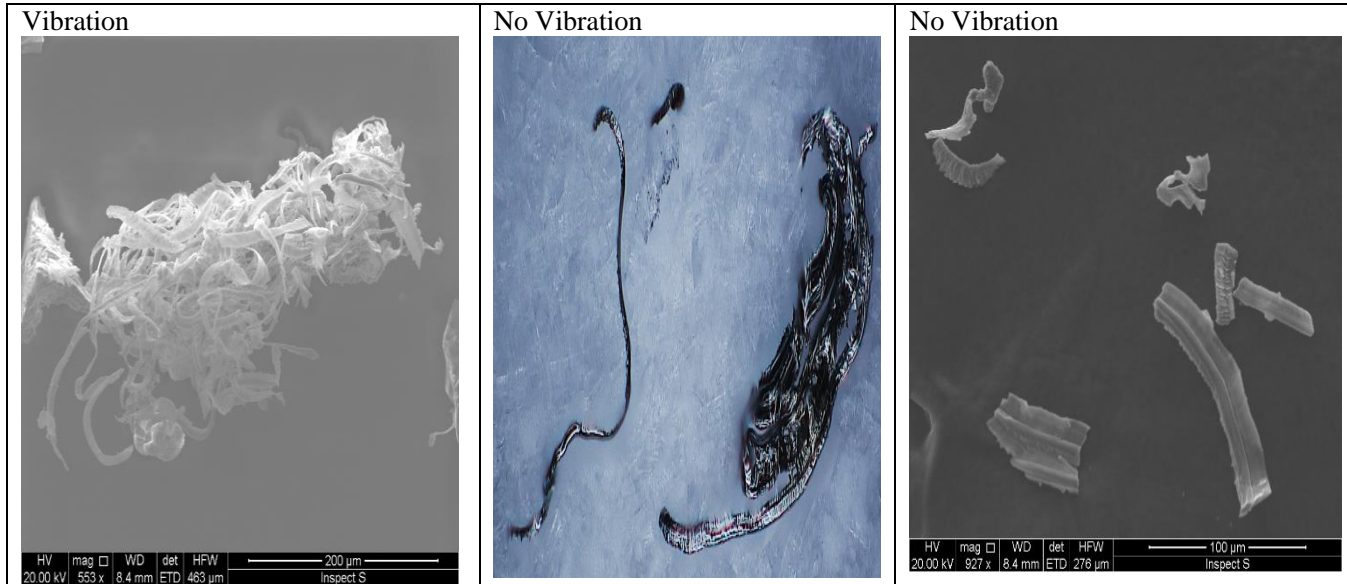


Titanium surface roughness when grinding without vibration/ with vibration Using (GFM)
Surface texture scan measurement machine



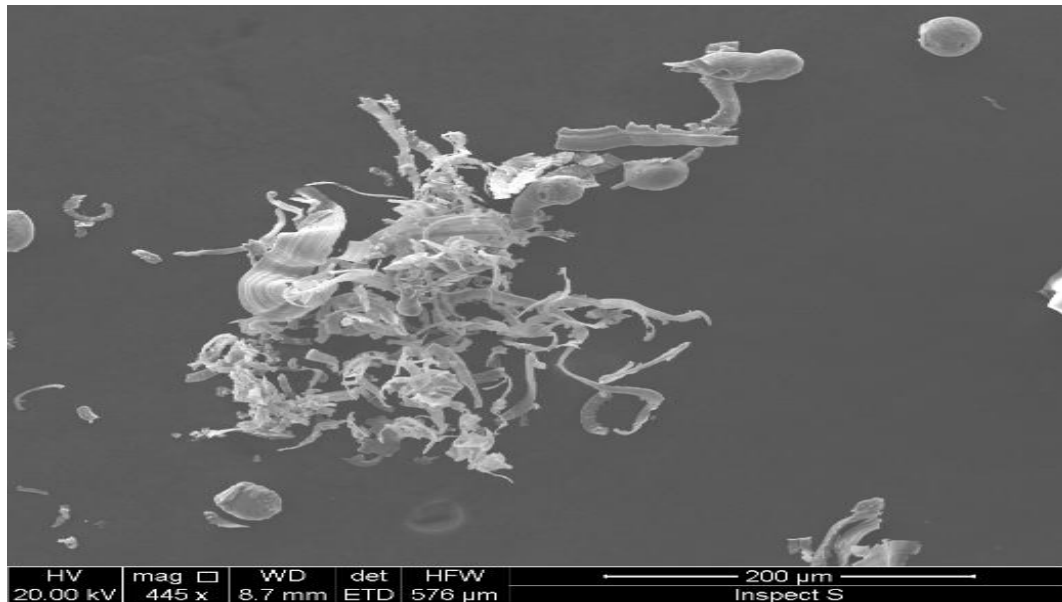
APPENDIX-C

C-1 (SEM) Chip length Images

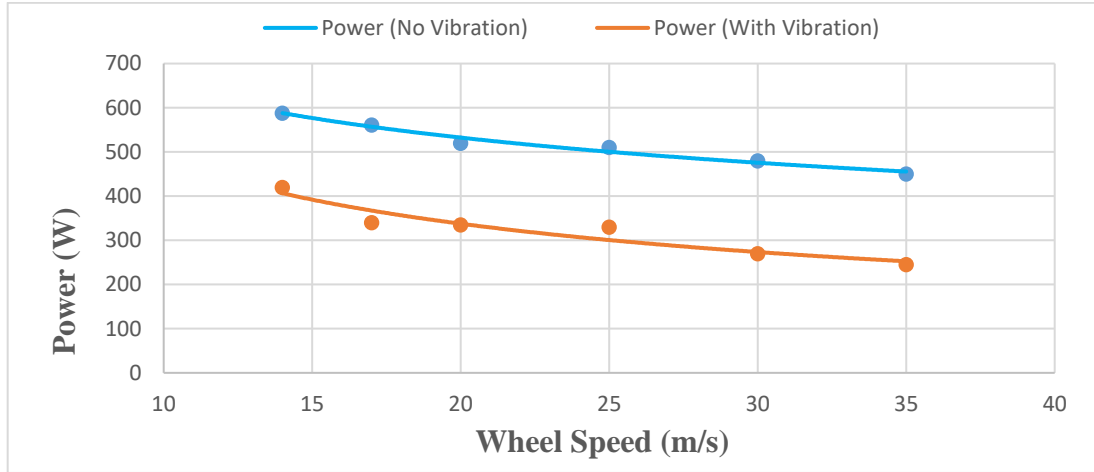


(SEM Images) chip formation

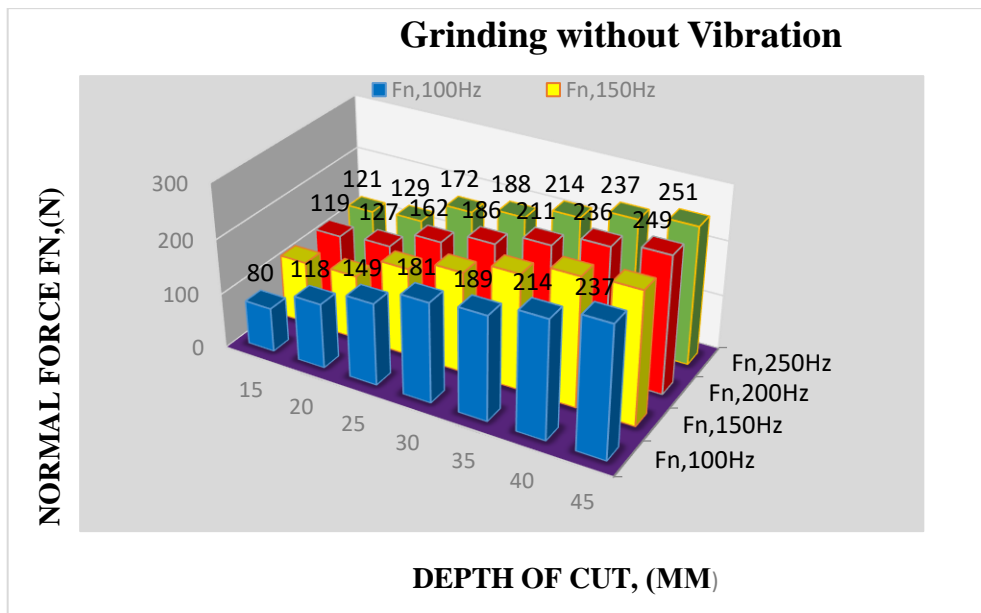
Vibration



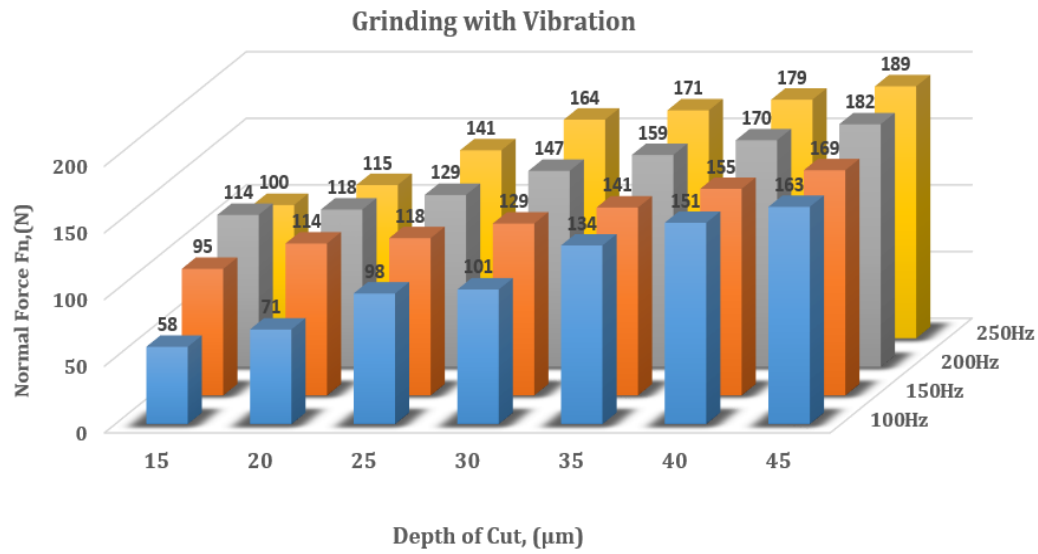
C-2 Power Consumption For (TiAl)Based on different wheel Speed



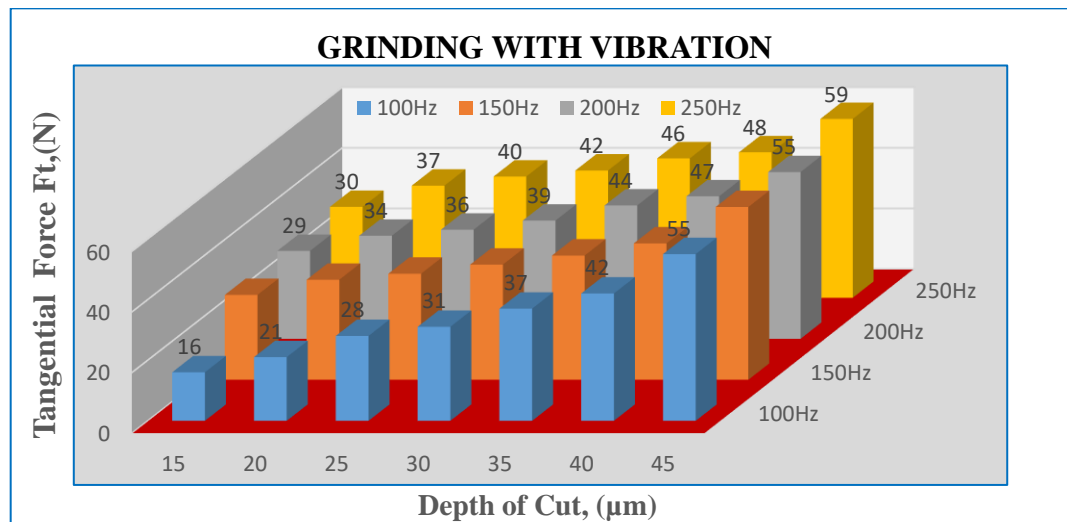
C-3, Cutting Forces based upon several frequencies from 100-250 Hz

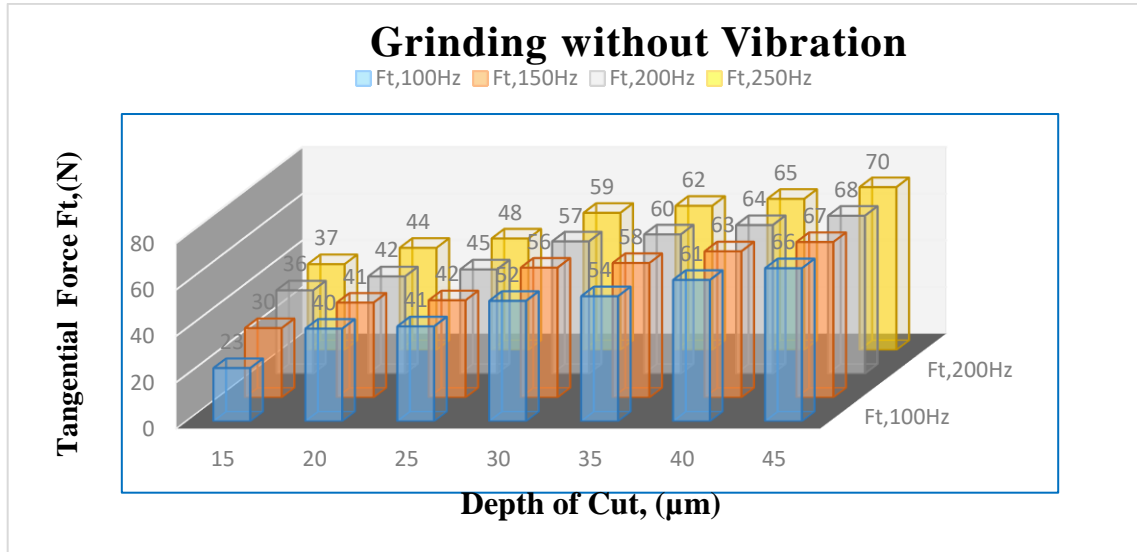


C-4, Grinding With Vibration at high frequencies up to 250Hz



C-5, The relationship between the normal forces and the applied depth of cut when grinding at different frequencies





C-6, Material removal rate for 2 aerospace materials

Dp	Nickel MRR, NoVb	Vb	Ti-6Al-4V MRR, No Vb	Vb
15	7	8.75	11	16
20	10.5	12.25	20	25
25	15.75	17.5	25	28
30	17.5	19.25	28	33

C-7, Ti-6Al-4V Force and power calculations at 17m/s grinding wheel speed

Applied Dp	Fn,No Vb	Fn,V b	Ft,NoV b	Ft,V b	ae,NoV b	ae,V b	P,Nv b	P,vb
15	34	25	19	11	7	10	323	187
20	56	46	31	23	9	14	527	391
25	70	55	40	30	14	16	680	510
30	77	70	43	40	16	19	731	680